

**DEVELOPING AND FIELD IMPLEMENTING AN ECO-
CRUISE CONTROL SYSTEM IN THE VICINITY OF
TRAFFIC SIGNALIZED INTERSECTIONS**

Final Report



TranLIVE

November 2016

DISCLAIMER

The contents of this report reflect the views of the authors, who are responsible for the facts and the accuracy of the information presented herein. This document is disseminated under the sponsorship of the Department of Transportation, University Transportation Centers Program, in the interest of information exchange. The U.S. Government assumes no liability for the contents or use thereof.

1. Report No.	2. Government Accession No.	3. Recipient's Catalog No.
4. Title and Subtitle Developing and Field Implementing an Eco-Cruise Control System in the Vicinity of Traffic Signalized Intersections		5. Report Date November 2016
		6. Performing Organization Code KLK900-SB-002
7. Author(s) Rakha H., Chen H., Almannaa M., El-Shawarby I. and Loulizi A.		8. Performing Organization Report No. NY17-02
9. Performing Organization Name and Address National Institute for Advanced Transportation Technology University of Idaho PO Box 440901; 115 Engineering Physics Building Moscow, ID 83844-0901		10. Work Unit No. (TRAIS)
		11. Contract or Grant No.
12. Sponsoring Agency Name and Address US Department of Transportation Research and Special Programs Administration 400 7th Street SW Washington, DC 20509-0001		13. Type of Report and Period Covered Final Report: 1/1/2012 – 12/31/2013
		14. Sponsoring Agency Code USDOT/RSPA/DIR-1
15. Supplementary Notes:		
16. Abstract The research develops Eco-CACC algorithms by considering a single intersection, multiple intersections, and field implementation for human drivers and automated vehicles. The INTEGRATION microscopic traffic assignment and simulation software is used to evaluate the performance of the proposed Eco-CACC algorithm by considering isolated intersection to assess its network-wide energy and environmental impacts. The analysis also demonstrates that the length of control segments, the SPaT plan, and the traffic demand levels significantly affect the algorithm performance. This research also develops Eco-CACC-MS algorithms to minimize fuel consumption for vehicles to pass multiple intersections. Simulation of the single-lane intersections proved that fuel consumption savings were greater at higher MPRs. The reductions in fuel consumption reached 7% for Eco-CACC-MS-Q and 4.2% for Eco-CACC-Q at 100% MPR. And, taking the vehicle queue into consideration, the Eco-CACC-MS-Q algorithm always performed better than Eco-CACC-O. In the two-lane intersection, due to lane-changing and passing behaviors, the proposed algorithm increased the total fuel consumption levels when the MPRs were less than 30%. Once the MPRs were larger than 30%, positive savings could be observed. In addition, the Eco-CACC-MS algorithm was implemented in a network with four consecutive intersections, and the fuel consumption savings were also observed to be as high as 7.7% for single-lane roads, and 4.8% for two-lane roads. Moreover, the Eco-CACC algorithm is implemented into an Eco-CACC system in the VTTI automated vehicle. In the Eco-CACC system, the computed speed profile can either be broadcasted as audio alert to the driver to manually control the vehicle, or be implemented into the automated vehicle (AV) to automatically control the vehicle. From an implementation standpoint the research addresses the challenges associated with communication latency, data errors, real-time computation, and ride smoothness. The system was tested in the Virginia Smart Road Connected Vehicle Test Bed. Four scenarios were tested for each participant under different combination of signal timing and road grade. The analyzed results demonstrate the benefits of the Eco-CACC system in assisting vehicle to drive smoothly in the vicinity of intersections and therefore reduce the fuel consumption levels. Compared to the uninformed drive, the longitudinally automated Eco-CACC system controlled vehicle resulted in savings in fuel consumption levels and travel times in the range of 37.8 and 9.3 percent, respectively.		
17. Key Words Eco-driving, eco-cooperative adaptive cruise control, optimize fuel consumption, queue impact, multiple		18. Distribution Statement Unrestricted; Document is available to the public through the National Technical Information Service; Springfield, VT.

intersections, field test, automated and connected vehicle			
19. Security Classif. (of this report) Unclassified	20. Security Classif. (of this page) Unclassified	21. No. of Pages #82	22. Price ...

Form DOT F 1700.7 (8-72)

Reproduction of completed page authorized

TABLE OF CONTENTS

EXECUTIVE SUMMARY 1
PROBLEM OVERVIEW 3
APPROACH AND METHODOLOGY 5
FINDINGS, CONCLUSIONS AND RECOMMENDATIONS..... 28
REFERENCES 79

EXECUTIVE SUMMARY

The research develops Eco-CACC algorithms by considering a single intersection, multiple intersections, and field implementation for human drivers and automated vehicles. In this research, the INTEGRATION microscopic traffic assignment and simulation software is used to evaluate the performance of a proposed Eco-CACC algorithm by considering isolated intersection to assess its network-wide energy and environmental impacts. A simulation sensitivity analysis demonstrates that as the CACC-equipped vehicle market penetrate rate increases the energy and environmental benefits also increase, and that the overall savings in fuel consumption are as high as 19% when the market penetration rate is 100%. On multi-lane roads, the algorithm may produce network-wide increases in the fuel consumption level when the market penetrate rate is less than 30%. The analysis also demonstrates that the length of control segments, the SPaT plan, and the traffic demand levels significantly affect the algorithm performance. The study further demonstrates that the algorithm may produce increases in fuel consumption levels when the network is over-saturated and thus further work is needed to enhance the algorithm for these conditions.

This research also develops Eco-CACC-MS algorithms to minimize fuel consumption for vehicles to pass multiple intersections. The algorithm accelerated or decelerated the equipped vehicles to a constant speed to cruise to the intersections so as to reduce their fuel consumption levels. In addition, the Eco-CACC-MS algorithm was evaluated with the INTEGRATION microscopic simulator. The simulation of the single-lane intersections proved that fuel consumption savings were greater at higher MPRs. The reductions in fuel consumption reached 7% for Eco-CACC-MS-Q and 4.2% for Eco-CACC-Q at 100% MPR. And, taking the vehicle queue into consideration, the Eco-CACC-MS-Q algorithm always performed better than Eco-CACC-O. In the two-lane intersection, due to lane-changing and passing behaviors, the proposed algorithm increased the total fuel consumption levels when the MPRs were less than 30%. Once the MPRs were larger than 30%, positive savings could be observed. In addition, the Eco-CACC-MS algorithm was implemented in a network with four consecutive intersections, and the fuel consumption savings were also observed to be as high as 7.7% for single-lane roads, and 4.8% for two-lane roads. The study also included a comprehensive sensitivity analysis of traffic demands, phase splits, offsets, and the distances between intersections. The analysis indicated that under the given offset of 75 seconds, the phase split of 50%, and the 1000-meter segment between the two intersections, loading vehicles at 700 vphpl resulted in the highest fuel consumption savings, at 13.5%. And, given the offset, the demand and the distance between intersections, with a larger percentage of the phase split, the savings from the proposed algorithm were smaller. In addition, when the offset was closer to the optimal offset, fuel consumption savings were smaller. Furthermore, the optimal distance between intersections exists to maximize the savings in fuel consumption.

The research develops an Eco-CACC system to compute the fuel-efficient speed profile in the vicinity of signalized intersections. The Eco-CACC algorithm is implemented into an Eco-CACC system in the VTTI automated vehicle. In the Eco-CACC system, the computed speed profile can either be broadcasted as audio alert to the driver to manually control the vehicle, or be implemented into the automated vehicle (AV) to automatically control the vehicle. From an algorithmic standpoint, the proposed algorithm addresses all

possible scenarios that a driver may encounter while approaching a signalized intersection. Additionally, from an implementation standpoint the research addresses the challenges associated with communication latency, data errors, real-time computation, and ride smoothness. The system was tested in the Virginia Smart Road Connected Vehicle Test Bed. Four scenarios were tested for each participant, including a base scenario of uninformed drive, a scenario that driver provided with a red indication countdown, a manual Eco-CACC scenario that driver follows an audio recommended speed profile, and finally an automated Eco-CACC scenario that vehicle uses longitudinally automated control to follow the speed profile. The field test includes 32 participants, and each participant conducted 64 trips to pass through a signalized intersection under different combination of signal timing and road grade. The analyzed results demonstrate the benefits of the Eco-CACC system in assisting vehicle to drive smoothly in the vicinity of intersections and therefore reduce the fuel consumption levels. Compared to the uninformed drive, the longitudinally automated Eco-CACC system controlled vehicle resulted in savings in fuel consumption levels and travel times in the range of 37.8 and 9.3 percent, respectively.

PROBLEM OVERVIEW

The United States is one of the prime consumers of petroleum in the world, burning more than 22 percent of the total petroleum refined on the planet; with its transportation sector consuming by itself nearly three-quarters of this product and is, consequently, ranked as the second largest carbon emitter in the country. The surface transportation sector is faced by three important challenges – availability of fuel to drive vehicles, emissions of greenhouse gases, and vehicular crashes. Therefore, it is important to reduce petroleum consumption and make surface transportation more safe, efficient and sustainable [1].

With the development of information and communication technology, connectivity between vehicles and between vehicles and transportation infrastructure was made possible. For instance, information of signal phasing and timing (SPaT) as well as, location and speed of vehicles could be easily transmitted and exploited for any application. The advanced communication power in connected vehicles ensures a very high update rate of the information, which enables researchers to develop connected transportation systems meeting safety, economy, and efficiency challenges [2]. Studies showed that vehicle fuel consumption levels in the vicinity of signalized intersections are dramatically increased due to vehicles' deceleration and acceleration [3, 4]. During the past decades, many studies have focused on changing traffic signal timings to optimize vehicles' delay and fuel levels [5, 6]. In recent years, researchers attempted to use connected vehicles and infrastructure technologies to develop eco-driving strategies that are more fuel-efficient. The concept of eco-driving is to provide, in real-time, recommendations to drivers so that vehicle maneuvers can be adjusted accordingly to reduce fuel consumption and emission levels [7-9].

One of such applications is the Eco-Cooperative Adaptive Cruise Control (Eco-CACC) which was developed to optimize individual vehicle fuel consumption by recommending a fuel-efficient trajectory using advanced information from surrounding vehicles and upcoming signalized intersections [10]. Various Eco-CACC algorithms were developed by researchers in recent years. Malakorn and Park proposed a cooperative adaptive cruise control system by using SPaT information to minimize absolute acceleration levels of vehicles and reduce fuel consumption level [11]. Kamalanathsharma and Rakha developed a dynamic programming based fuel-optimization strategy using recursive path-finding principles, and evaluated the developed strategy using an agent-based modeling approach [12]. Asadi and Vahidi proposed a schedule optimization algorithm to allocate “green-windows” for vehicles to pass through a series of consecutive signalized intersections [13]. Guan and Frey further extended the work in [13] to generate a brake-specific fuel consumption map which enables optimization of gear ratios, and dynamic programming is used to find the optimum solution [14].

Although many Eco-CACC algorithms were developed in the previous studies, the optimization for multiple intersections has not been considered to compare with the optimization for isolated intersections in a traffic network. Moreover, most of Eco-CACC algorithms are developed and tested in a traffic simulation environment where vehicles are forced to follow the recommended speed as calculated by the Eco-CACC algorithms. However, many problems that are not treated in simulation software need to be addressed in order to implement Eco-CACC systems in the field, such as communication latency, system malfunction, data collection error, driver perception/reaction delay, driver distraction resulting from following posted recommended speed, etc. Few studies attempted to

investigate the potentials of implementing Eco-CACC in the field. For instance, Barth and Xia developed a dynamic eco-driving system and conducted a field test on arterial roads [15-17]. However, vehicle fuel consumption is not explicitly considered in their algorithm objective function. Instead, their algorithm attempts to optimize vehicle acceleration/deceleration profiles to minimize the total tractive power demand and the idling time so that the fuel consumption levels are also reduced [17]. Munoz-Organero and Magana developed an expert system to reduce fuel consumption by calculating optimal deceleration patterns and minimizing the use of braking. The system was implemented on Android mobile devices and field-tested using five different vehicle brands and nine drivers [18]. However, fuel consumption is also not explicitly considered in their objective function. The algorithm provides the optimum solution for drivers to release the accelerator pedal and assumes it to result in a deduction of fuel consumption.

APPROACH AND METHODOLOGY

The Eco-CACC algorithms are developed in this project by considering a single intersection, multiple intersections and field implementation for human drivers and automated vehicles.

Eco-CACC Algorithms

The microscopic traffic simulator and the estimation of queue length at intersections are introduced first, since they are the foundations of developing Eco-CACC algorithms.

INTEGRATION Microscopic Traffic Simulator

This project implemented the proposed Eco-Cooperative Adaptive Cruise Control (Eco-CACC) system in the INTEGRATION microscopic traffic simulator, and then utilized the simulator to quantify the network-wide energy and environmental impacts of the system. This section makes a brief introduction of the INTEGRATION software, and then describes how the Eco-CACC algorithm was implemented in INTEGRATION.

The INTEGRATION model was first developed in the mid 1980's [19, 20] and is being continuously developed [21, 22]. It was conceived as an integrated simulation and traffic assignment model and performs traffic simulations by tracking the movement of individual vehicles every deci-second. This allows for detailed analysis of lane-changing movements and shock wave propagations. It also permits considerable flexibility in representing spatiotemporal variations in traffic conditions. In addition to estimating stops and delays, the model can also estimate the fuel consumed by individual vehicles, as well as the emissions [23]. Finally, the model also estimates the expected number of vehicle crashes using a time-based crash prediction model. The model tracks each vehicle from its origin until it exits the network at its destination.

The INTEGRATION model uses the Rakha-Pasumarthy-Adjerid (RPA) car-following model to model longitudinal vehicle motion [24-26]. The RPA model integrates a steady-state car-following model with a vehicle dynamics and a collision avoidance model to ensure that vehicle movements are consistent with vehicle dynamics and driver input. The steady-state model is the Van Aerde model [25, 27, 28], which describes the relationship between the traffic stream speed, flow and density (also known as the fundamental diagram), as illustrated in Figure 1.

$$\rho(x, t) = \frac{1}{c_1 + c_3 \cdot v(x, t) + \frac{c_2}{v_f - v(x, t)}} \quad (1a)$$

where $v(x, t)$ is the traffic stream space-mean-speed at location x and time t . The coefficients can be computed as

$$c_1 = \frac{v_f}{\rho_j v_c^2} (2v_c - v_f), \quad (1b)$$

$$c_2 = \frac{v_f}{\rho_j v_c^2} (v_f - v_c)^2 \quad (1c)$$

$$c_3 = \frac{1}{q_c} - \frac{v_f}{\rho_j v_c^2}, \quad (1d)$$

where v_f, ρ_j, q_c, v_c are the free-flow speed, jam density, roadway capacity, and speed-at-capacity, respectively. Figure 1 provides an example illustration of the fundamental diagram. Here, we also have the speed-density $v(x, t) = V(\rho(x, t))$ and flow-speed $q(x, t) = Q_v(v(x, t)) = \rho(x, t) \cdot v(x, t)$ relationships (Figure 1 (b) and (c)). Given (q_c, v_f, ρ_j, v_c) , the speed of the rarefaction wave generated by the green traffic signal indication can be estimated, and the time of the queue dissipation can also be estimated.

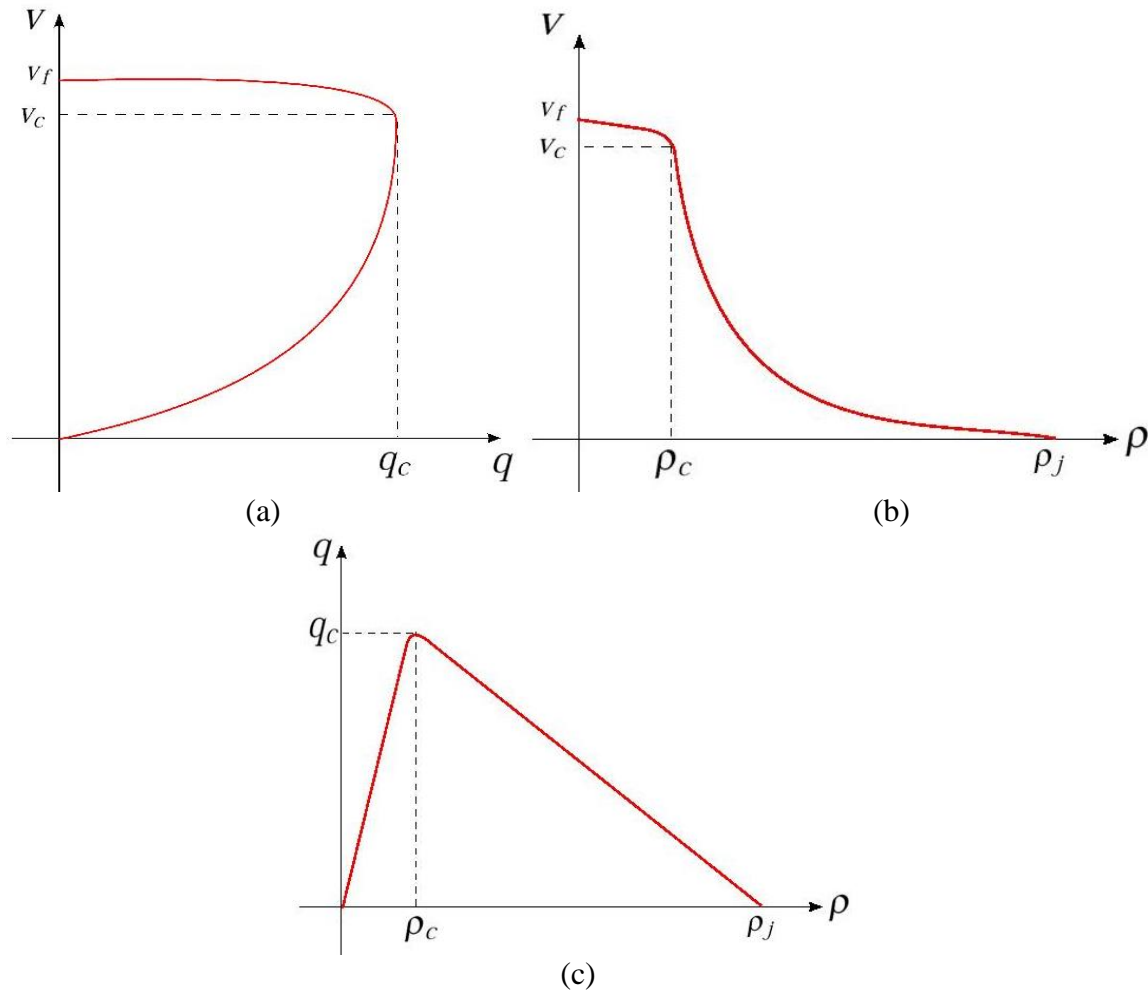


Figure 1: Sample Van Aerde fundamental diagram: (a) speed-flow, (b) speed-density, (c) flow-density

Moreover, the model computes the vehicle speed as the minimum of three speeds, namely: the maximum vehicle speed based on vehicle dynamics considering the driver throttle input, the desired speed based on the Van Aerde steady-state car-following model formulation [25], and the maximum vehicle speed that the vehicle can travel at ensuring that it does not collide with the vehicle ahead of it. In addition, the model is open-source, and allows users to add functions to realize various traffic and vehicle control strategies. In this study, we incorporate V2I communications to transmit two types of information to probe vehicles: (1) the SPaT information from the intersection controller, and (2) the queue

information, including its length and the time of dissipation, estimated by loop detectors installed at the beginning and the ending of the control segment upstream of the traffic signal. The Eco-CACC algorithms utilize this information to estimate the advisory speed limit. Subsequently, every deci-second, the probe vehicle receives an advisory speed limit, which controls the vehicle motion through the intersection. The actual speed of the vehicle at time t , $v(t)$, is determined by two values: (1) the advisory speed limit, $v_e(t)$ and (2) the speed computed by INTEGRATION, $v_I(t)$; *i. e.*, $v(t) = \min\{v_e(t), v_I(t)\}$. Hence, the influence of the Eco-CACC-Q algorithm on driving behavior of individual vehicles and its environmental benefits on the network performance can be assessed using the INTEGRATION software.

Queue Length Estimation at Intersections

This project attempts to develop an Eco-CACC algorithm that predicts vehicle queues upstream of signalized intersections to develop fuel-optimum vehicle trajectories in the vicinity of signalized intersections. In this project, a kinematic wave model is reviewed to describe traffic dynamics on a signalized road, and is used to predict the vehicle queue length.

The Lighthill-Whitham-Richard (LWR) is one traditional kinematic wave model that describes traffic dynamics on roads. Assume that $\{\rho(x, t), v(x, t), q(x, t)\}$ represent the density, speed, and flow at location x and time t , respectively then the LWR model gives

$$\frac{\partial \rho(x, t)}{\partial t} + \frac{\partial q(x, t)}{\partial x} = 0. \tag{2}$$

The model assumes that there exist a relationship between flow and density, *i. e.*, the fundamental diagram,

$$q(x, t) = Q(\rho(x, t)); \tag{3}$$

Figure 2 illustrates a general fundamental diagram. Generally, the flow is a concave function of the density.

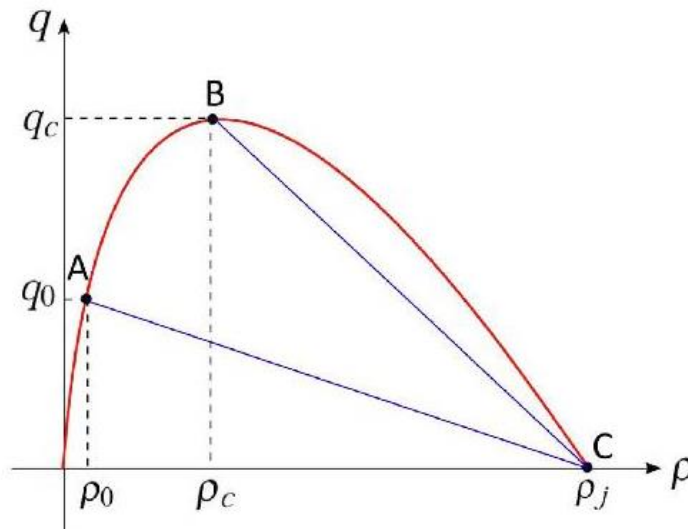


Figure 2: General fundamental diagram

With green and red indications, traffic signals generate various shock waves and rarefaction waves, which lead to significant variations in vehicular movements. Figure 3 shows the movements of a series of vehicles approaching and passing an intersection with traffic waves. If one vehicle arrives at the intersection when the traffic signal indication is green, it proceeds through the intersection without any delay; while it has to wait at the stop bar for a green indication when the traffic signal indication is red. The red signal indication generates a shock wave upstream of the intersection.

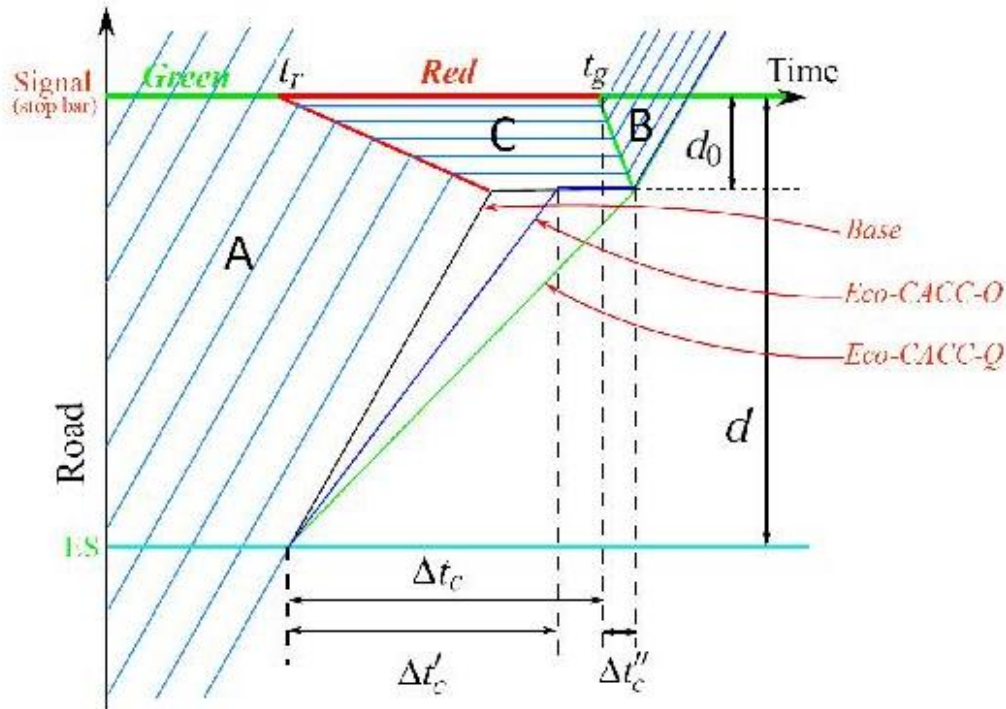


Figure 3: Vehicle trajectories at one intersection

Assume that the flow entering the intersection is q_0 , and during the green indication, the traffic state upstream of the intersection is A , as shown in Figure 2. Once the signal turns red, no vehicles can proceed through the intersection, i.e., within the queue the traffic stream is at the maximum road density, ρ_j , and the discharge rate is reduced to 0. The upstream state becomes C , and a shock wave is generated and propagates backward. The speed of the shock wave is determined by the states A and C as

$$v_{AC} = \frac{q_0}{\rho_0 - \rho_j} \quad (4)$$

Once the traffic signal turns green, the intersection starts to discharge vehicles at the saturation flow rate, i.e., q_c , in Figure 2. As a result, a rarefaction wave is formed to release the queue upstream of the intersection, and the downstream state becomes B . The speed of the rarefaction wave is computed as

$$v_{CB} = \frac{q_c}{\rho_c - \rho_j} \quad (5)$$

At time t , an Eco-CACC vehicle enters the control segment (travels a distance d from point ES to the traffic signal) with the speed v_0 ($v_0 = q_0/\rho_0$). Then, the tail location of the queue can be estimated as

$$d_0 = \begin{cases} \frac{v_{AC}}{v_0+v_{AC}} [d - v_0(t_r - t)] & \forall t \in \left[t_r - \frac{d}{v_0}, t_g + \frac{v_{AC}(t_g - t_r)}{v_{AC}+v_{BD}} \right] \\ 0 & otherwise \end{cases} \quad (6)$$

Here, t_r and t_g are the times that the traffic signal turns to a red and green indication, respectively. The stop duration of the vehicle ahead of the intersection is

$$t_{s,0} = \Delta t_c + \Delta t_c'' - \frac{d-d_0}{v_0}, \quad (7)$$

where $\Delta t = t_g - t_r$, and $\Delta t_c'' = \frac{d_0}{v_{CB}}$.

Note that if there are other Eco-CACC vehicles ahead, the propagation speed of the shock wave and the rarefaction wave cannot be estimated accurately using the fundamental diagram. Without vehicle-to-vehicle communication, the tail location cannot be identified exactly either. However, for the Eco-CACC vehicle, as it is controlled and does not pass any vehicles ahead, it considers all vehicles ahead as its queue. Hence, Eq(6) can still be applied to estimate the queue length with the assumption that all vehicles in the queue will stop at the traffic signal, which could result in an overestimation of the queue length.

In general, the speed of the rarefaction wave, v_{CB} , is greater than that of the shock wave, v_{AB} , as shown in Figure 2. As time progresses, the rarefaction wave will catch up with the shock wave and dissipate the queue. The traffic signal generates stop-and-go driving for individual vehicles, which increases fuel consumption levels significantly (see the base case in Figure 3). Consequently, controlling vehicle movements to ensure that they proceed through intersections smoothly without stopping is a critical factor in reducing vehicle fuel consumption levels.

Eco-CACC Algorithm at Independent Intersections

Eco-CACC Algorithm Considering Queue Effects

In this section, an Eco-CACC algorithm is developed to improve an algorithm developed earlier in [29] with the consideration of vehicle queues and to further minimize the fuel consumption of vehicles proceeding through intersections. The mechanism of vehicle control in the algorithm is described as follows. Once an Eco-CACC vehicle enters the segment between the point *ES* and the traffic signal, which is defined as the upstream control segment of length d , as shown in Figure 3, the following two actions will be applied.

1. If the Eco-CACC vehicle can pass through the intersection at its original speed, v_0 , without hitting the queue or the red indication, no control action will be applied to the vehicle, and the advisory speed limit is set as the free-flow speed, v_f .
2. If the vehicle cannot proceed through the intersection, we provide a lower speed limit, $v_c \leq v_0$, for the vehicle to approach the signal.

The basic criterion for estimating the advisory speed limit, v_c , is to reduce the stop duration while maintaining the average speed of the controlled vehicles without increasing their travel times. [29] has demonstrated that the most critical strategy to reduce fuel consumption levels is to prevent vehicles from coming to a complete stop at the stop bar.

However, without considering the impact of the queue, the strategy cannot prevent vehicle stops. Illustrated as the blue line (Eco-CACC-O) in Figure 3, the strategy proposed in [29] still forces vehicles to stop for the time $t_{s,1}$.

$$t_{s,1} = \Delta t_c - \Delta t'_c + \Delta t''_c, \quad (8)$$

where $\Delta t'_c = \frac{d-d_0}{v_2}$, and $v_2 = \frac{d}{\Delta t_c}$ is the advisory speed limit estimated by the Eco-CACC system without queue consideration (Eco-CACC-O). While considering the queue, the delay can be totally removed (see the green line (Eco-CACC-Q) in Figure 3).

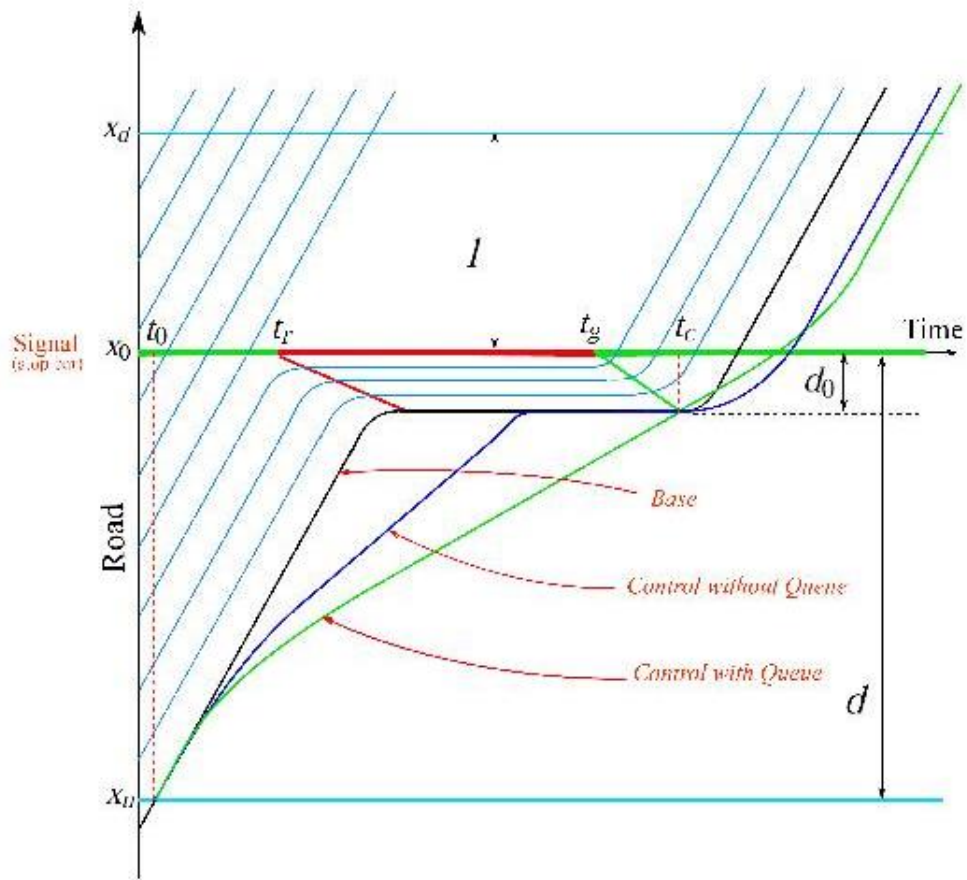
In Figure 3, vehicles are controlled assuming infinite acceleration/deceleration levels, which is not realistic. In this section, we develop an Eco-CACC algorithm considering queue effects (Eco-CACC-Q) to minimize vehicle fuel consumption levels while proceeding through an intersection with the consideration of realistic deceleration and acceleration levels, followed by an investigation of the impact of queue length on the algorithm performance.

Eco-CACC Algorithm at One Intersection

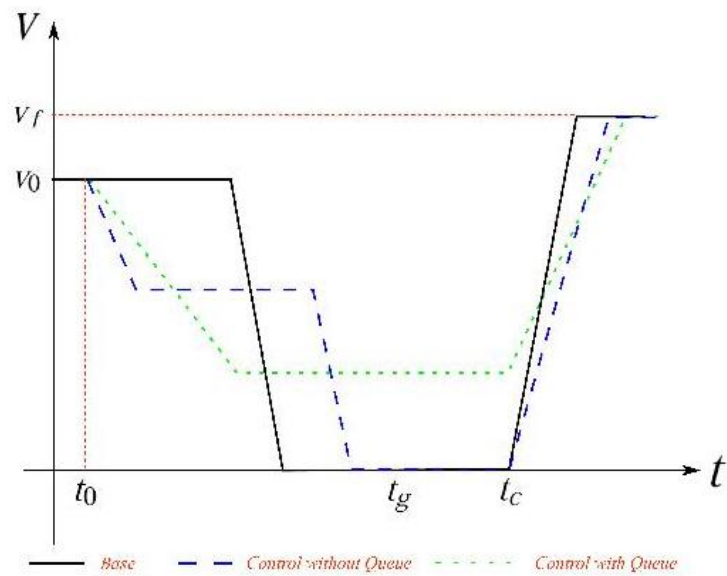
The Eco-CACC algorithms estimate time-dependent advisory speed limits considering realistic deceleration and acceleration levels to ensure that Eco-CACC vehicles decelerate to target speeds and cruise to the stop bar or the tail of the queue ahead of the intersection. Subsequently, once the queue is released, the probe vehicles accelerate to the free-flow speed at a constant throttle level. In that sense, the optimal deceleration and acceleration levels will be computed by the algorithms to minimize the total fuel consumed.

As shown in Figure 4(a), upstream of the intersection, the Eco-CACC-Q algorithm is activated for an Eco-CACC vehicle once it enters the control segment. Without control, the vehicle maintains its original speed v_0 until it stops at the end of the queue at the deceleration level, a_-^s . In the Eco-CACC algorithm without considering queue effects (Eco-CACC-O), the vehicle decelerates to a cruising speed, with which the vehicle cruises to the stop bar just when the signal turns green. While the queue forces the vehicle to stop at the queue tail at a deceleration level, a_-^s . Similarly, the Eco-CACC-Q algorithm reduces the speed of the probe vehicle at a constant deceleration level, however it allows the vehicle to arrive at the tail of the queue just when the queue is released, i.e., at $t = t_c$.

Downstream of the intersection, the algorithm should also allow the vehicle to accelerate back to the free-flow speed v_f at location x_d , where l is the length of the downstream control segment. Without control, the vehicle utilizes a constant acceleration level, a_+^s , to approach v_f . In the Eco-CACC-O and Eco-CACC-Q algorithms, optimal acceleration rates are applied for the vehicle to accelerate back to the free-flow speed at x_d . The acceleration levels are determined by the cruise speed and the distance x_d . The algorithms minimize the vehicle fuel consumption level by searching for the optimal combination of the upstream deceleration level, a_- , and the downstream acceleration level, a_+ .



(a)



(b)

Figure 4: Eco-CACC with deceleration and acceleration: (a) traffic dynamics at the intersection, (b) speed of the probe vehicle.

To develop Eco-CACC algorithms, the objective function is first defined in Eq(9). The algorithm is designed to minimize the total fuel consumed by Eco-CACC vehicles traversing the intersection.

$$\min_{a_-, a_+} \int_{t_0}^{t_0+T} F(v(t), v'(t)) dt, \quad (9a)$$

s.t.

$$\int_{t_0}^{t_0+T} v(t) dt = d + l, \quad (9b)$$

$$0 \leq a_- \leq a_-^{\hat{}}; \quad (9c)$$

$$0 \leq a_+ \leq a_+^{\hat{}}. \quad (9d)$$

$F(\cdot, \cdot)$ is a function of the speed $v(t)$ and acceleration $v'(t)$, defined by the VT-CPFM model [30], to estimate the fuel consumption rate based on vehicular speed and acceleration levels.

$$F(v(t), v'(t)) = \begin{cases} \alpha_0 + \alpha_1 P(t) + \alpha_2 P^2(t) & P(t) \geq 0 \\ \alpha_0 & P(t) < 0' \end{cases} \quad (10a)$$

Where $\{\alpha_0, \alpha_1, \alpha_2\}$ are the coefficients determined by vehicle types. $P(t)$ is the vehicle power at time t , and it is a function of speed and acceleration.

$$P(t) = \frac{R(t) + m \cdot v'(t) (1.04 + 0.0025 \xi^2(t))}{3600 \eta_d} \cdot v(t), \quad (10b)$$

$$R(t) = \frac{\rho_a}{25.02} C_D C_h A_f v^2(t) + 9.8066 m \cdot \frac{C_r}{1000} (c_1 v(t) + c_2) + 9.8066 m G(t). \quad (10c)$$

Here, $R(t)$ is the resistance force of the vehicle, and $\xi(t)$ is the gear ratio, and $G(t)$ is the road grade at time t . $m, \rho_a, \eta_d, C_D, C_h, A_f$ represent the vehicle mass, the density of the air, the vehicle drag coefficient, the correction factor of altitude, and the vehicle front area, respectively. C_r, c_1, c_2 are rolling resistance parameters that vary as a function of the road surface type, road condition, and vehicle tire type.

In Eq(9), $v(t)$ is the advisory speed limit of Eco-CACC vehicles traveling in the vicinity of the intersection at time t , computed using Eq(11) and Eq(12) for the Eco-CACC-O and Eco-CACC-Q algorithms, respectively. T is the time duration that the probe vehicle travels the upstream and downstream control segments. In the Eco-CACC-O algorithm the duration is defined as $T = T_n$; while, it is defined as $T = T_q$ for the Eco-CACC-Q algorithm. For *Eco-CACC-O*, $v(t)$ can be computed as

$$v(t) = \begin{cases} v_0 - a_-(t - t_0) & t \in [t_0, t_0 + \delta t_{n,1}) \\ v_{n,t} & t \in [t_0 + \delta t_{n,1}, t_0 + \delta t_{n,1} + \delta t_{n,2}) \\ v_{n,t} - a_-^{\hat{}}(t - t_0 - \delta t_{n,1}) & t \in [t_0 + \delta t_{n,1} + \delta t_{n,2}, t_0 + \delta t_{n,1} + \delta t_{n,2} + \delta t_{n,3}) \\ 0 & t \in [t_0 + \delta t_{n,1} + \delta t_{n,2} + \delta t_{n,3}, t_c) \\ v_{n,t} + a_+(t - t_c) & t \in [t_c, t_c + \delta t_{n,4}) \\ v_f & t \in [t_c + \delta t_{n,4}, t_0 + T_n] \end{cases} \quad (11a)$$

Here, $v_{n,t}$ is defined as the algorithm cruise speed without considering the queue effects. The speed profile is shown as the blue dashed line in Figure 4(b). Furthermore, given the values of a_- and a_+ , the variables, $(T_n, v_{n,t}, \delta t_{n,1}, \delta t_{n,2}, \delta t_{n,3}, \delta t_{n,4})$ can be estimated using Eq(11) (b - g).

$$\delta t_{n,1} = \frac{v_0 - v_{n,t}}{a_-}, \quad (11b)$$

$$v_0 \cdot \delta t_{n,1} - \frac{1}{2} a_- \delta t_{n,1}^2 + v_{n,t} \delta t_{n,2} + v_{n,t} \delta t_{n,3} + \frac{1}{2} a_+ \delta t_{n,3}^2 = d - d_0, \quad (11c)$$

$$v_0 \cdot \delta t_{n,1} - \frac{1}{2} a_- \delta t_{n,1}^2 + v_{n,t} \delta t_{n,2} + v_{n,t}(t_g - t_0 - \delta t_{n,1}) = d, \quad (11d)$$

$$\delta t_{n,3} = \frac{(v_{n,t})}{a_+}, \quad (11e)$$

$$\delta t_{n,4} = \frac{v_f}{a_+}, \quad (11f)$$

$$\frac{1}{2} a_+ \delta t_{n,4}^2 + v_f \cdot (t_0 + T_n - t_c - \delta t_{n,4}) = l + d_0. \quad (11g)$$

For *Eco-CACC-Q*, there is

$$v(t) = \begin{cases} v_0 - a_-(t - t_0) & t \in [t_0, t_0 + \delta t_{q,1}) \\ v_{q,t} & t \in [t_0 + \delta t_{q,1}, t_c) \\ v_{q,t} + a_+(t - t_c) & t \in [t_c, t_c + \delta t_{q,2}) \\ v_f & t \in [t_c + \delta t_{q,2}, t_0 + T_q] \end{cases}. \quad (12a)$$

Here, $v_{q,t}$ is the cruise speed of the algorithm with queue. The speed profile is illustrated as the green dotted line in Figure 4(b). And, given the values of a_- and a_+ , the variables, $(T_q, v_{q,t}, \delta t_{q,1}, \delta t_{q,2})$ can be estimated by Eq(12) (b - e).

$$\delta t_{q,1} = \frac{v_0 - v_{q,t}}{a_-}, \quad (12b)$$

$$v_0 \cdot \delta t_{q,1} - \frac{1}{2} a_- \delta t_{q,1}^2 + v_{q,t} (t_c - t_0 - \delta t_{q,1}) = d - d_0, \quad (12c)$$

$$\delta t_{q,2} = \frac{v_f - v_{q,t}}{a_+}, \quad (12d)$$

$$v_t \cdot \delta t_{q,1} + \frac{1}{2} a_+ \delta t_{q,2}^2 + v_f \cdot (t_0 + T_q - t_c - \delta t_{q,2}) = l + d_0. \quad (12e)$$

Given the road traffic condition, including the queue length, start and end times of each phase, and the approaching speed of the probe vehicles, the speed profile is a function of a_- and a_+ (see Eq(11) and Eq(12)). Since the fuel consumption rate is determined by the speed profile, there exist the optimal deceleration and acceleration rates to minimize the fuel consumption rate. The *Eco-CACC* algorithms search for the optimal values within appropriate ranges (Eq(10c) and (10d)).

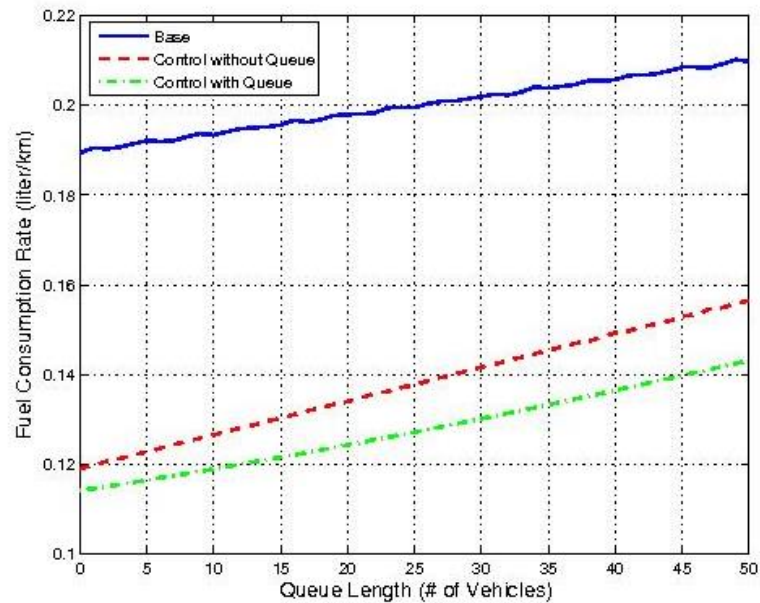
The details of the *Eco-CACC-Q* algorithm are described below.

1. For a probe vehicle k , once it enters the segment $[x_u, x_d]$, where x_u and x_d are the start and end points of the control region, the algorithm is activated.

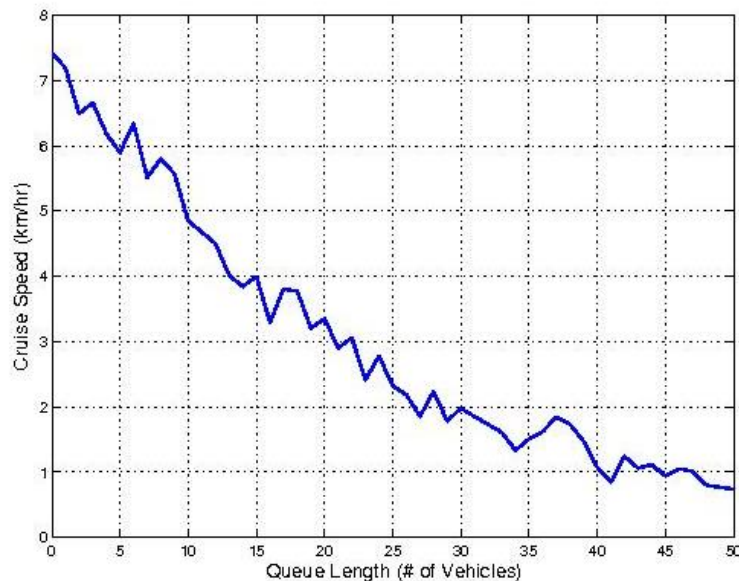
2. Upstream of the intersection
 - a. The algorithm provides an advisory speed limit to the probe vehicles for the following two scenarios; otherwise, the free-flow speed is used as the advisory limit.
 - i. The current signal indicator is green, but the traffic signal will turn red when the vehicle arrives at the stop bar if it travels at its current speed.
 - ii. The current signal indicator is red and will continue to be red when the vehicle arrives at the stop bar while traveling at its current speed.
 - b. Once either of the above scenarios occurs, we predict the queue length ahead of the Eco-CACC vehicle, and estimate the release time of the queue, t_c , based on the speed of the rarefaction wave (see Eq(6)).
 - c. The algorithm estimates the optimal upstream deceleration level and the downstream acceleration level using Eq(9) and Eq(12) to minimize the vehicle fuel consumption, and provides an advisory speed limit to the Eco-CACC vehicle at the next time step $t + \Delta t$, where Δt is the speed update interval.
3. Downstream of the intersection, the algorithm searches for the optimal acceleration level based on its current speed to minimize the fuel consumption to reach the free-flow speed v_f at location x_d .
4. Once the Eco-CACC vehicle arrives at x_d , the Eco-CACC-Q algorithm is deactivated.

Impact of Queue Length

The impact of the queue length on the Eco-CACC-Q algorithm performance is investigated in this section. We apply an ideal simplistic example to analyze the impact of the queue length on the algorithm performance. Assume that the lengths of the controlled segments upstream and downstream of the intersection are $d = 500$ m, and $l = 200$ m, respectively. The Eco-CACC vehicle arrives at location x_u at $t_0 = 0$ s with an initial speed $v_0 = 72$ km/h, and the signal turns green at $t_g = 60$ s. Moreover, the free-flow speed, the roadway saturation flow rate, the jam density, and the density-at-capacity are $v_f = 72$ km/h, $q_c = 1600$ vph, $\rho_j = 160$ veh/km, and $\rho_c = 20$ veh/km, respectively. Here, we assume that the Eco-CACC vehicle is a 2011 Honda Civic or similar; and the values of the parameters in the VT-CPFM model are calibrated in [30].



(a)



(b)

Figure 5: Impact of queue length: (a) fuel consumption level, (b) Eco-CACC algorithm recommended speed

Figure 5 illustrates the impact of queue length on the total fuel consumed and the cruise speed. Generally, with the longer queue length, the advisory cruise speed is smaller. This is true, as a longer queue indicates the cruise distance is shorter, and the queue dissipation time is longer. Here, it is not exactly true that the advisory cruise speed is smaller for a longer queue (see the fluctuation in the curve in Figure 5 (b)), as the upstream deceleration and

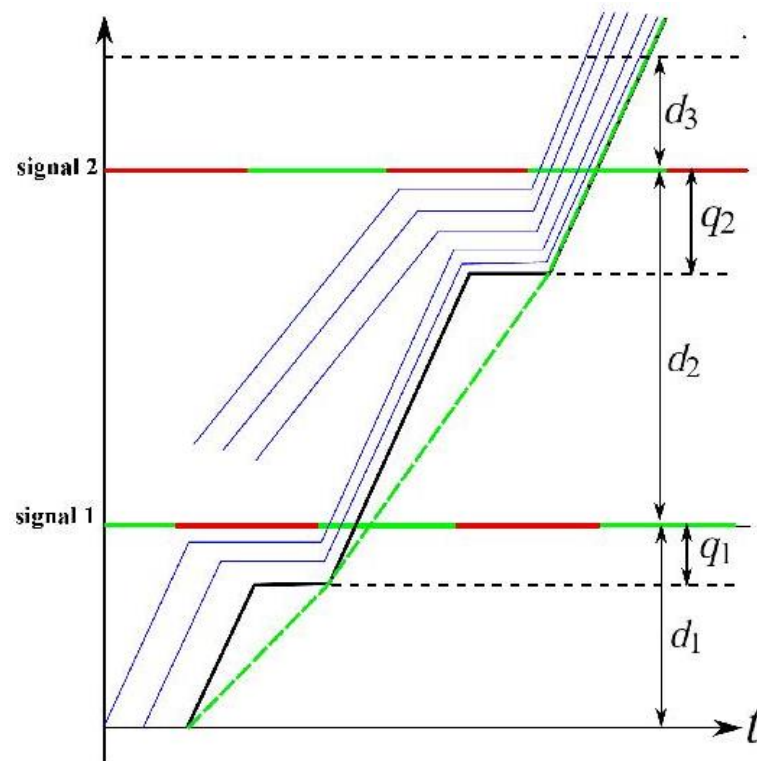
downstream acceleration levels should be optimized to reduce the fuel consumption of Eco-CACC vehicles. Furthermore, a larger deceleration results in larger cruise speeds. Both acceleration and deceleration levels vary with queue lengths, and the cruise speed oscillates, as shown in Figure 5 (b).

Moreover, both the Eco-CACC algorithms significantly reduce the fuel consumption of the Eco-CACC vehicles. The Eco-CACC-O algorithm reduces the fuel consumption by as high as 25% while the Eco-CACC-Q algorithm reduces the fuel consumption by 32%. Comparing the two algorithms, the Eco-CACC-Q algorithm produces fuel consumption levels that are 10% lower. Furthermore, with longer queues, the cruise speed is smaller, which can be derived from Eq(12). At the same time, the fuel consumption is larger. This finding demonstrates that the Eco-CACC-Q algorithm can further improve the fuel efficiency of Eco-CACC vehicles.

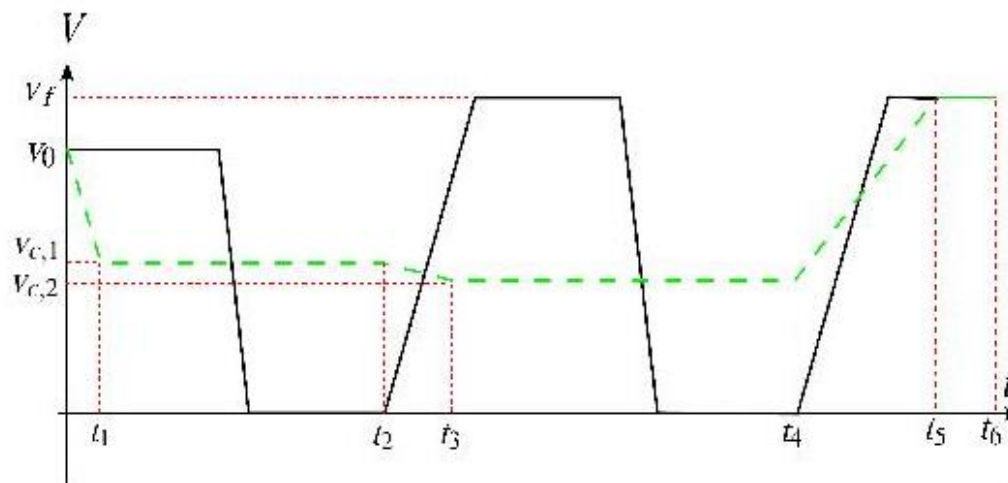
Eco-CACC Algorithm at Multiple Intersections

The Eco-CACC algorithm proposed above utilizes SPaT data obtained via V2I communications to compute a fuel-optimized vehicle trajectory in the vicinity of one signalized intersection. The trajectory is optimized by computing an advisory speed limit using the Eco-CACC algorithm, which takes the vehicle queue ahead of the intersection into consideration. However, the trajectory is only optimized for one intersection. When it comes to multiple intersections, the trajectory may not work effectively on minimizing fuel consumption. In this section, the algorithm is extended for multiple intersections.

Figure 6(a) shows the trajectories of vehicles passing two consecutive intersections. The solid black line represents the trajectory of one vehicle experiencing two red lights without control (assume that the vehicle has infinite acceleration/deceleration rates). The vehicle is stopped ahead of both intersections by the red lights and the vehicle queues. Applying the Eco-CACC algorithm for multiple intersections (Eco-CACC-MS), the vehicle cruises to each intersection with a constant speed (see the dashed green line in Figure 6(a)). However, the assumption that the acceleration/deceleration rates of the equipped vehicle are infinite is not realistic. Figure 6(b) compares the speed profiles of the vehicle with (green line) and without (black line) control considering both acceleration and deceleration durations. Without control, the vehicle has to stop completely at the first intersection. Between the two intersections, the vehicle first accelerates to the speed limit and then decelerates to 0 again. The stop-and-go behaviors and the long idling time waste a great deal of energy. However, with control, the vehicle decelerates to a speed, $v_{c,1}$, and cruises to the first intersection. Between the two intersections, it decelerates or accelerates from $v_{c,1}$ to $v_{c,2}$, and cruises to the second intersection. Here, $v_{c,1}$ and $v_{c,2}$ are the cruise speeds to the first and second intersection, respectively. Once the queue at the second intersection is released, the vehicle accelerates to the speed limit. Compared to the base case without control, both the trajectory and the speed profile with Eco-CACC-MS are much smoother.



(a)



(b)

Figure 6: Dynamics of the equipped vehicle at two intersections: (a) trajectories, (b) speed profiles.

The objective of developing the Eco-CACC-MS algorithm is to minimize the vehicle fuel consumption level in the vicinity of the two intersections. In addition to the shape of the vehicle speed shown in Figure 6(b), the algorithm determines the optimum upstream

acceleration/deceleration levels of the controlled speed profile in Figure 6(b). The mathematical formulation of the algorithm can be cast as

$$\min_{a_1, a_2, a_3} \int_0^{t_6} F(v(t), v'(t)) dt, \quad (13a)$$

s.t.

$$v(a_1, a_2, a_3) = \begin{cases} v_0 + a_1 t & 0 < t \leq t_1 \\ v_{c,1} & t_1 < t \leq t_2 \\ v_{c,1} + a_2(t - t_2) & t_2 < t \leq t_3 \\ v_{c,2} & t_3 < t \leq t_4 \\ v_{c,2} + a_3(t - t_4) & t_4 < t \leq t_5 \\ v_f & t_5 < t \leq t_6 \end{cases}; \quad (13b)$$

$$v_{c,1} = v_0 + a_1 \cdot t_1; \quad (13c)$$

$$v_0 \cdot t_1 + \frac{1}{2} a_1 t_1^2 + v_{c,1} (t_2 - t_1) = d_1 - q_1; \quad (13d)$$

$$t_2 = t_{g,1} + \frac{q_1}{w_1}; \quad (13e)$$

$$v_{c,2} = v_{c,1} + a_2 \cdot (t_3 - t_2); \quad (13f)$$

$$v_{c,1}(t_3 - t_2) + \frac{1}{2} a_2 (t_3 - t_2)^2 + v_{c,2} (t_4 - t_3) = d_2 + q_1 - q_2; \quad (13g)$$

$$t_4 = t_{g,2} + \frac{q_2}{w_2}; \quad (13h)$$

$$v_{c,2} + a_3 (t_5 - t_4) = v_f; \quad (13i)$$

$$v_{c,2}(t_5 - t_4) + \frac{1}{2} a_3 (t_5 - t_4)^2 + v_f (t_6 - t_5) = d_3 + q_2; \quad (13j)$$

$$a_-^s \leq a_1 \leq a_+^s; \quad (13k)$$

$$a_-^s \leq a_2 \leq a_+^s; \quad (13l)$$

$$0 \leq a_3 \leq a_+^s; \quad (13m)$$

where

- $F(v(t), v'(t))$: the vehicle fuel consumption rate at any instant t computed using the Virginia Tech Comprehensive Power-based Fuel Consumption Model (VT-CPFM);
- $v(t)$: the advisory speed limit for the equipped vehicle at time t ;
- a_k : the acceleration/deceleration rates for the advisory speed limit, $k=1,2,3$;
- v_0 : the speed of the vehicle when it enters the upstream control segment of the first intersection;
- v_f : the road speed limit;
- d_1 : the length of the upstream control segment of the first intersection;

- d_2 : the distance between the two intersections;
- d_3 : the length of the downstream control segment of the second intersection;
- $t_{g,1}$: the time instant that the indicator of the first signal turns to green;
- $t_{g,2}$: the time instant that the indicator of the second signal turns to green;
- t_k : the time instant defined in \reff(signal)(b), $k=1,2,\dots,6$;
- $v_{c,1}$: the cruise speed to the first intersection;
- $v_{c,2}$: the cruise speed to the second intersection;
- q_1 : the queue length at the first immediate downstream intersection;
- q_2 : the queue length at the second immediate downstream intersection;
- w_1 : the queue dispersion speed at the first immediate downstream intersection;
- w_2 : the queue dispersion speed at the second immediate downstream intersection;
- a_-^s : the saturation deceleration level;
- a_+^s : the saturation acceleration level.

Eq(13) demonstrates that given the traffic state, including queue lengths, the start and end times of the indicators of the two intersections and the approaching speed of the controlled vehicles, the speed profile varies as a function of (a_1, a_2, a_3) . Eq(13) (c-e) defines that the equipped vehicle decelerates to $v_{c,1}$ and passes the first intersection just when the queue is released. Eq(13) (f-h) determines that the vehicle passes the second intersection when the queue is released. Eq(13) (i-j) shows how the vehicle recovers its speed back up to the speed limit. The Eco-CACC-MS algorithm searches for the three acceleration levels to minimize the fuel consumption of the controlled vehicle over the entire control section. The flow chart of the Eco-CACC-MS algorithm is illustrated in Figure 7, and the details of the algorithm, including how it is extended to N consecutive intersections (labeled as $1, 2, \dots, N$ from upstream to downstream), is described below.

1. When an equipped vehicle k that enters the upstream control segment of the first intersection--i.e., the distance between the vehicle and the stop line of the intersection 1 (the first upstream intersection) is less than d_1 , the Eco-CACC-MS algorithm is activated.
2. Upstream of the intersection 1 or the section between the intersection $i - 1$ and $i = 2, 3, \dots, N$.

The algorithm estimates the optimal trajectory for the equipped vehicle to pass intersections based on the SPaT and vehicle queue information. The algorithm categorizes the traffic condition into three scenarios, and controls the vehicle differently.

- a. If the equipped vehicle can pass its immediate downstream intersection, i , with its current speed v_0 or speed limit v_f without complete stops caused by either the red indicator or the vehicle queue, the algorithm does not control the movements of the equipped vehicle, and the vehicle will only apply the road speed limit to pass the intersection.
- b. If the equipped vehicle is stopped by the red indicator or the queue at its immediate downstream intersection, i , but it can pass the second intersection, $i + 1$, without stops, or $i = N$, the Eco-CACC algorithm of a single intersection proposed in the aforementioned section is applied to the equipped vehicle with the SPaT and the queue information of the intersection i . The

optimal trajectory is estimated for the equipped vehicle to pass the intersection.

- c. If the equipped vehicle is stopped by the red indicators or the queues at the two immediate downstream intersections, i and $i + 1$, the optimization problem described in Eq(13) is applied to find the optimal trajectory for the vehicle to pass the two intersections. The function estimates three optimal acceleration/deceleration rates (a_1^* , a_2^* , a_3^*) of the trajectory for the equipped vehicle to minimize the total fuel consumption to pass two intersections.
3. Downstream of the intersection N, the algorithm computes the fuel-optimum acceleration level from its current speed to the speed limit v_f over the distance d_3 .
4. Once the equipped vehicle passes the intersection N, and its distance to the intersection is larger than d_3 , the Eco-CACC-MS algorithm is deactivated.

The Eco-CACC-MS algorithm described above applies vehicle queue information in the estimation of the optimal trajectory (We call the algorithm Eco-CACC-MS-Q.). However, if there is not sufficient information from V2I communications to estimate vehicle queues, the algorithm can be simplified by only using SPaT information. For that case, we developed the Eco-CACC-MS algorithm without the consideration of queue (This algorithm is Eco-CACC-MS-O.), where the queue lengths are all assumed as 0, i.e., $q_1 = q_2 = 0$ in Eq(13).

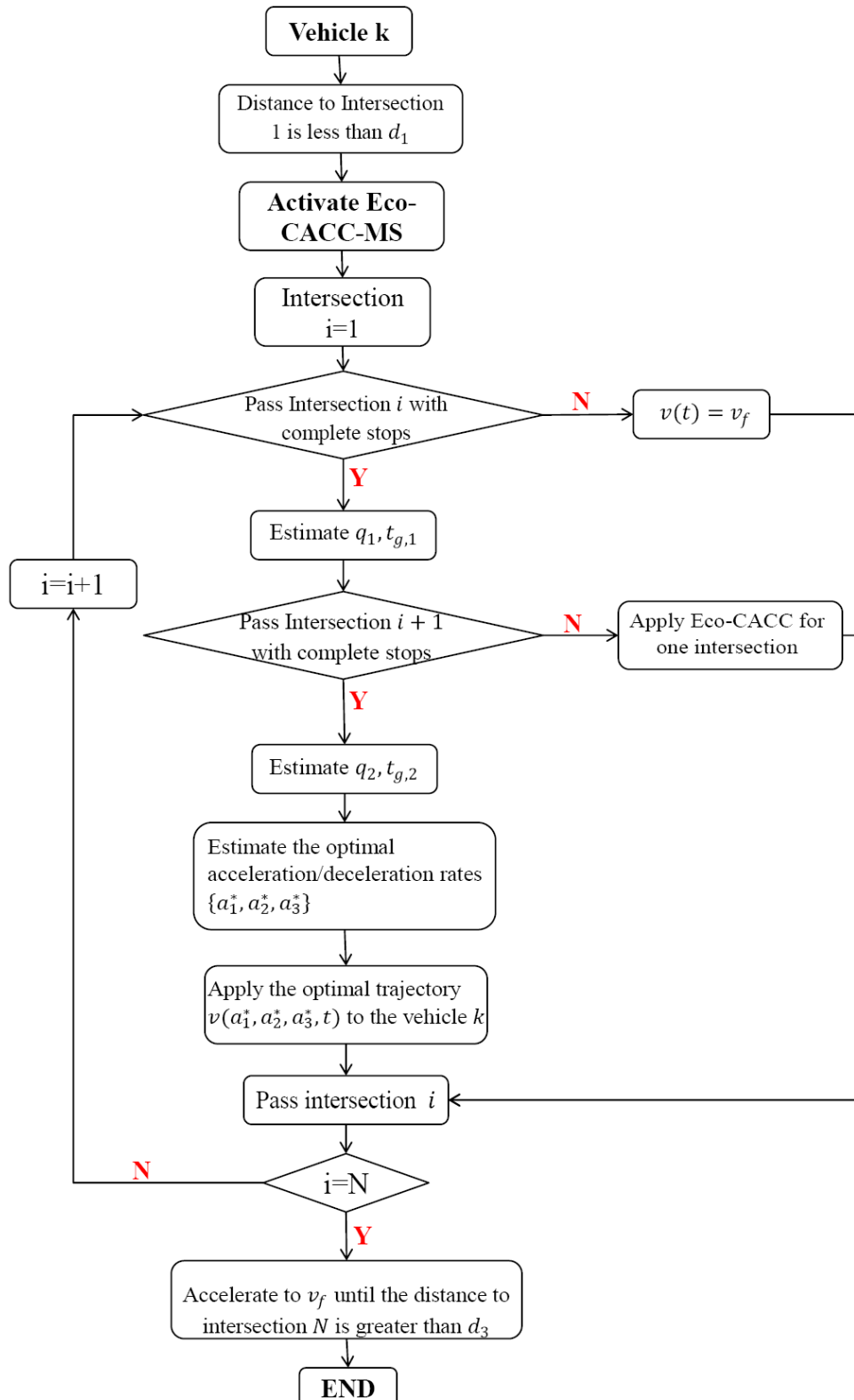


Figure 7: Flow chart of the Eco-CACC-MS algorithm

Field Implementation of Eco-CACC Systems

The Eco-CACC algorithms for field implementation are developed in this section by considering different driving mode (manually and automated drive) and challenges associated with communication latency, data errors, real-time computation, and ride smoothness.

Definitions and Assumptions

Given that both upstream and downstream vehicle speed profiles are considered in the Eco-CACC algorithm, a control region in the vicinity of signalized intersections should be defined. Considering the communication range of Dedicated Short Range Communications (DSRC), Eco-CACC algorithm is activated at a distance of d_{up} upstream of the intersection to a distance of d_{down} downstream of the intersection. It is to note here that the distance is calculated from the vehicle location to the intersection stop line. The value of d_{down} is defined to ensure that the vehicle has enough downstream distance to accelerate from zero speed to the limit speed at a low throttle level (e.g. 0.3). This ensures that all computations are made along a fixed distance of travel.

The Eco-CACC algorithm described in this report computes the optimum vehicle speed profile starting from upstream to downstream of a signalized intersection, by incorporating vehicle dynamics and fuel consumption models. It should be noted that the impacts from neighboring vehicles such as car-following and/or lane-changing behavior are not considered in the algorithm tested in this paper. However, the impact of these factors was tested in a traffic simulation environment [1, 12, 29, 31-33]. As such, the tested algorithm treats eco-speed control under light traffic conditions. The developed Eco-CACC algorithm could be refined for more complicated traffic conditions by considering the calculated optimum speed profile as the variable speed limit as demonstrated in [29]. Consequently, a general solution of ECO-CACC can be achieved by constraining the vehicle speed by the variable speed limit produced by the algorithm as well as other common traffic flow constraints such as car following model, gap acceptance, collision avoidance, etc.

When a vehicle is approaching a signalized intersection, the vehicle may accelerate, decelerate, or cruise (keep its current speed) depending on its speed, distance to the intersection, signal timing, etc. Considering that the vehicle may or may not need to decelerate when approaching the traffic signal, two cases are considered to develop the Eco-CACC strategies:

- Case 1: vehicle is able to pass the intersection on green phase without deceleration (either keeping a constant speed, or accelerating to a higher speed and then keeping that speed).
- Case 2: vehicle needs to decelerate to a lower speed, and then keep that speed to pass the intersection on green phase.

The above two cases describe the vehicle's optimum trajectory in order to minimize fuel consumption while traversing the intersection. After the vehicle passes the stop line, the vehicle tries to reach the speed limit, which describes the vehicle's maneuver downstream of the intersection. More details of optimum speed profiles during various situations have been discussed in [1, 15]. Figure 8 demonstrates the optimum speed profile when vehicle passes a signalized intersection, and the Eco-CACC algorithm helps to find the best acceleration and deceleration levels. The sample speed profiles (initial speed u_1 and u_2) for case 1 are

highlighted in blue, and the sample speed profile (initial speed u_3) for case 2 is represented in maroon. The road speed limit is denoted as u_f . Note that the samples of case 1 and 2 in Figure 8 happens at the red phase when vehicle passes the upstream distance d_{up} . The same classification of case 1 and 2 also exist for the situation of green phase. Considering the simplicity to explain the proposed ECO-CACC algorithm, the initial red phase is assumed for the following sections.

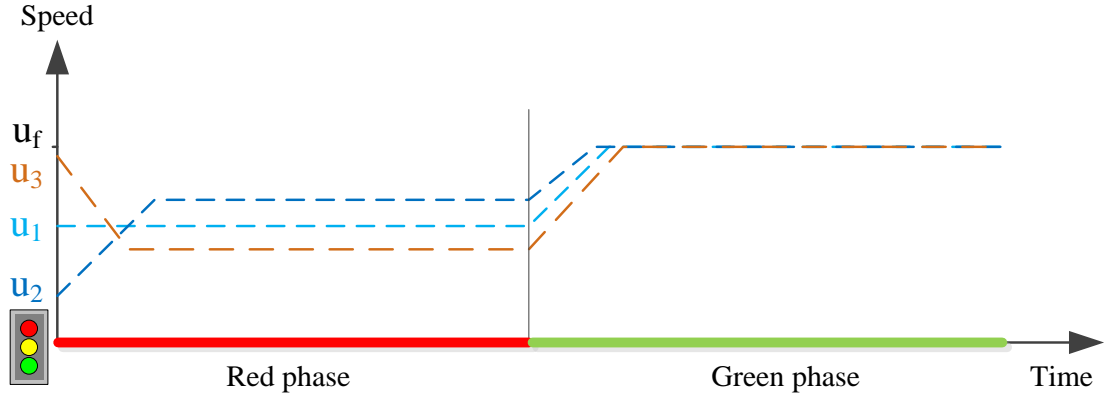


Figure 8: Samples of optimum speed profile when vehicle approaches a signalized intersection.

Fuel Consumption and Vehicle Dynamics Models

In the proposed ECO-CACC algorithm, the deceleration is assumed constant for case 2. In case 1, the vehicle acceleration follows the vehicle dynamics model developed in [34]. In this model, the acceleration value depends on vehicle speed and throttle level. Given that the throttle level is typically around 0.6 as obtained from field studies [1], a constant throttle level of 0.6 is assumed in the vehicle dynamic model to simplify the calculations in the Eco-CACC algorithm for case 1. In case 2, the throttle level ranges between 0.4 to 0.8, and the optimum throttle level can be located by the minimum fuel consumption level. The vehicle dynamics model is summarized by the following Equations.

$$v(t + Dt) = v(t) + 3.6 \frac{F(t) - R(t)}{m} Dt \tag{14}$$

$$F = \min \left\{ \frac{\beta}{\eta_d} 3600 f_p b h_d \frac{P}{v}, m_{ta} g \frac{\ddot{\theta}}{\theta} \right\} \tag{15}$$

$$R = \frac{r}{25.92} C_d C_h A_f v^2 + m g \frac{c_{r0}}{1000} (c_{r1} v + c_{r2}) + m g G \tag{16}$$

where F is the vehicle tractive effort; R represents the resultant of the resistance forces, including aerodynamic, rolling and grade resistance forces; f_p is the driver throttle input [0,1] (unitless); β is the gear reduction factor (unitless), and this factor is set to 1.0 for light-duty vehicles; η_d is the driveline efficiency (unitless); P is the vehicle power (kW); m_{ta} is the mass of the vehicle on the tractive axle (kg); g is the gravitational acceleration (9.8067

m/s²); μ is the coefficient of road adhesion (unitless); ρ is the air density at sea level and a temperature of 15°C (1.2256 kg/m³); C_d is the vehicle drag coefficient (unitless), typically 0.30; C_h is the altitude correction factor (unitless); A_f is the vehicle frontal area (m²); c_{r0} is rolling resistance constant (unitless); c_{r1} is the rolling resistance constant (h/km); c_{r2} is the rolling resistance constant (unitless); m is the total vehicle mass (kg); and G is the roadway grade at instant time t (unitless).

A fuel consumption model is needed in the ECO-CACC algorithm to calculate fuel consumption using vehicle speed data. The VT-CPFM-1 was selected due to its simplicity, accuracy and ease of calibration [30]. The selected fuel model utilizes instantaneous power as an input variable and can be easily calibrated using publicly available fuel economy data (e.g., Environmental Protection Agency [EPA]-published city and highway gas mileage). Thus, the calibration of model parameters does not require gathering any vehicle-specific data. The VT-CPFM-1 is formulated as presented by

$$FC(t) = \begin{cases} \alpha_0 + \alpha_1 P(t) + \alpha_2 P(t)^3 & P(t) \geq 0 \\ \alpha_0 & P(t) < 0. \end{cases} \quad (17)$$

$$P(t) = \left(\frac{R(t) + 1.04ma(t)}{3600\eta_d} \right) v(t). \quad (18)$$

Where α_0 , α_1 and α_2 are the model parameters that can be calibrated for a particular vehicle, and the details of calibration steps can be found in [30]; $P(t)$ is the instantaneous total power (kW); $a(t)$ is the acceleration at instant t , which can be calculated by consecutive time speed values; $v(t)$ is the velocity at instant t and $R(t)$ is the resistance force on the vehicle as given by Equation (16).

Eco-CACC Algorithm for Field Implementation

Given that vehicles behave differently for the two cases described above, the ECO-CACC algorithms are developed separately for cases 1 and 2 [35, 36].

Case 1:

The vehicle can pass the intersection during a green indication without decelerating. In order to have the maximum average speed to save fuel consumption, the cruise speed during red phase is defined as shown by Equation (19). If u_c is equal to vehicle's initial speed $u(t_0)$, then the vehicle can proceed at a constant speed upstream of the intersection. Otherwise, the vehicle should accelerate to u_c by following the vehicle dynamics model presented by Equations (14) to (16). Thereafter, when the signal turns green, the vehicle needs to follow the vehicle dynamics model and accelerate from cruise speed u_c to the speed limit u_f until the vehicle travels a distance d_{down} downstream of the intersection. Thus, the optimum speed profile is the profile that minimizes the fuel consumption from upstream d_{up} to downstream d_{down} .

$$u_c = \min \left(\frac{d_{up}}{t_r}, u_f \right). \quad (19)$$

Case 2:

Upstream of the intersection, the vehicle needs to slow down with a deceleration level a , then cruises at a speed u_c to pass the intersection when the signal just turns into green. Downstream of the intersection, the vehicle should accelerate from u_c to u_f , and then cruises at u_f . Since the deceleration level upstream of the intersection and the throttle level f_p downstream of the intersection are the only unknown variables for this case, the optimum speed profile can be calculated by solving the optimization problem described below. The vehicle's speed profile for case 2, is illustrated as blow.

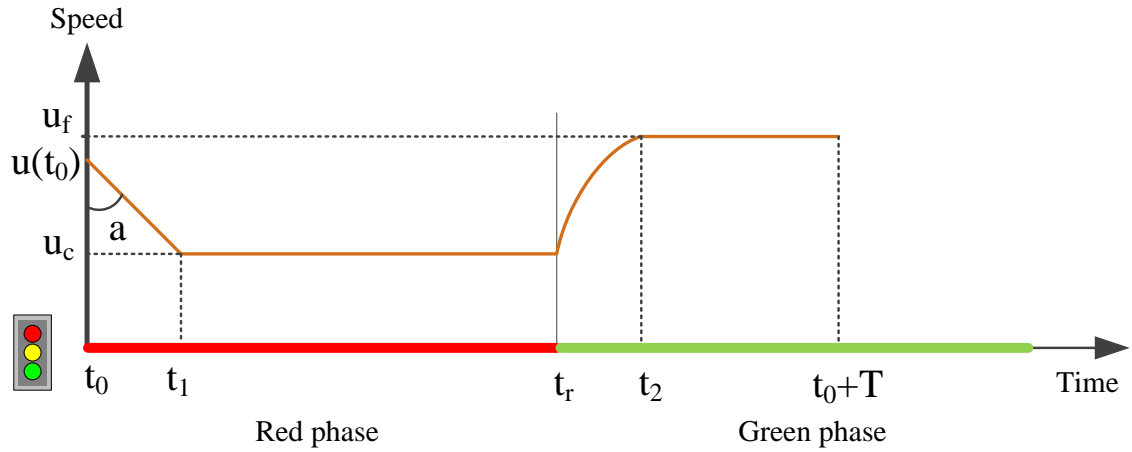


Figure 9: Optimum speed profile.

Assume a vehicle arrives d_{up} at time t_0 and passes d_{down} at time t_0+T , the cruise speed during red phase is u_c , the objection function is the total fuel consumption level given by:

$$\min \int_{t_0}^{t_0+T} FC(u(t)) \cdot dt \quad (20)$$

where $FC(*)$ denotes the calculated fuel consumption at instant t (Equation (17)) with vehicle speed $u(t)$. The constraints can be constructed by the relationships between speed, acceleration, deceleration, and distance as shown below:

s.t.

$$u(t) : \begin{cases} u(t) = u(t_0) - at; & t_0 \leq t \leq t_1 \\ u(t) = u_c; & t_1 < t \leq t_r \\ u(t + \Delta t) = u(t) + 3.6 \frac{F(f_p) - R(u(t))}{m} \Delta t; & t_r < t \leq t_2 \\ u(t) = u_f; & t_2 < t \leq t_0 + T \end{cases} \quad (21)$$

$$\begin{aligned}
u(t_0) - \frac{1}{2}at^2 + u_c(t_r - t_1) &= d_{up} \\
u_c &= u(t_0) - a(t_1 - t_0) \\
\int_{t_r}^{t_2} u(t)dt + u_f(t_0 + T - t_2) &= d_{down} \\
u(t_2) &= u_f \\
0 < a &\leq 5.9 \\
0.4 \leq f_p &\leq 0.8 \\
u_c &> 0
\end{aligned} \tag{22}$$

In Equation 8, the functions $F(*)$ and $R(*)$ represent the vehicle tractive effort and resistance force as computed by Equations (15) and (16), respectively. According to the relationships in Equations (21) and (22), the deceleration a and throttle level f_p are the only unknown variables. It is to note that the maximum deceleration level is limited to 5.9 m/s^2 (comfortable deceleration threshold felt by a driver). In addition, the throttle level is set to range from 0.4 to 0.8, given that the optimum throttle level is usually around 0.6 [1]. Dynamic programming (DP) is used to solve the problem by listing all the combinations of deceleration and throttle values and calculating the corresponding fuel consumption levels; the minimum calculated fuel gives the optimum parameters [1, 14].

Implementation of an Eco-Cooperative Adaptive Speed Control System

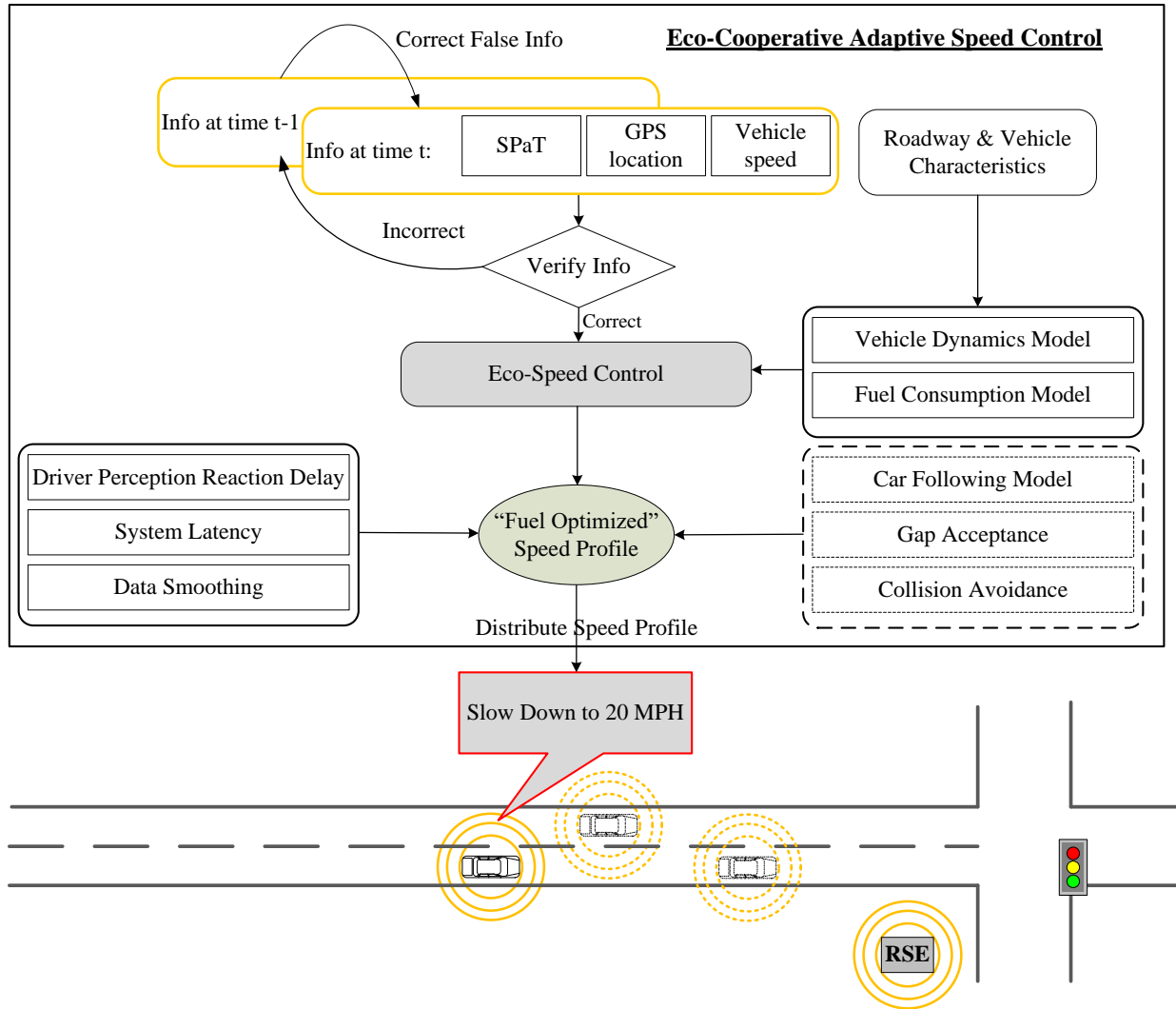


Figure 10: Illustration of the Eco-CACC system.

Theoretically, the ECS algorithm provides a “fuel optimized” speed profile at any instant time t , when vehicle is driving within the range of Eco-Speed Control (from d_{up} to d_{down}). The speed profile include all the speed values at each time interval Δt , which covers vehicle’s target speeds from its current location to the downstream location d_{down} . Practically, the driver can only follow one target speed value at instant time t , and then follow another target speed after a certain time interval Δt^* . The value of Δt^* was set equal to be 2 seconds during the field test described in this paper.

Considering the practical situation, Figure 10 provides an illustration showing the implementation of ECO-CACC algorithm into an Eco-CACC System. When the vehicle enters the ECO-CACC range at the intersection, the vehicle receives SPaT information from roadside equipment (RSE). At the same time, the vehicle onboard unit collects vehicle speed and GPS location data. Those data are the input information for Eco-Speed Control. Note that all the input information should be verified to avoid false information because of device

malfunction or measurement error. Any false information can be updated using the information from the previous time interval. Other than these time-dependent data, some constant data for the roadway and vehicle characteristics are also needed for the ECO-CACC, since they are used in the vehicle dynamics and fuel consumption models. Using the developed ECO-CACC algorithm from the previous section, the “fuel optimized” speed profile can be obtained. If there is no surrounding vehicles on the road (condition of the test described in this paper), constraints such as driver perception/reaction delay, system latency and data smoothing are only considered to extract the target speed from the speed profile. Otherwise, the impacts of other vehicles should also be considered, which means more constraints including car following model, gap acceptance, collision avoidance, etc. Eventually, the speed profile can be computed and distributed to the vehicle control system. In the developed Eco-CACC system, the computed speed profile can either be broadcasted as audio alert to the driver to manually control the vehicle, or be implemented into the automated vehicle (AV) to automatically control the vehicle [36, 37]. The performance of the Eco-CACC system will be validated in the field test of this study.

FINDINGS, CONCLUSIONS AND RECOMMENDATIONS

This section includes the findings of evaluating Eco-CACC algorithms at a single intersection and multiple intersections under simulation environment, and the field test of Eco-CACC systems.

Simulation Evaluation at a Single Intersection

The Eco-CACC algorithm at single intersections is evaluated for different intersection configurations, as illustrated in Figure 11. We start with a single approach intersection (see Figure 11) with an upstream segment of length d and a downstream segment of length l . One- and two-lane roads are simulated using INTEGRATION to evaluate the Eco-CACC-Q algorithm performance.

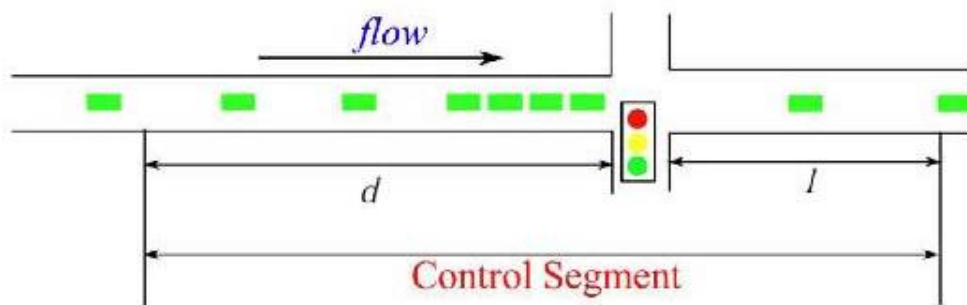


Figure 11: Intersection Configuration

Performance on Single-lane Roads

The first example considers one single-lane intersection, where both the upstream and downstream roads have only one lane. This configuration ensures that all vehicles do not pass their leaders and that the Eco-CACC-Q algorithm is not affected by lane-changing behavior. In the simulation, the free-flow speed, the jam density, the saturation flow rate, and

the speed-at-capacity are set as $v_f = 80$ km/h, $\rho_j = 160$ veh/km, $q_c = 1600$ vph, and $v_c = 60$ km/h, respectively. For the SPaT plan of the intersection, we set the green, amber, and red durations as 40 seconds, 4 seconds, and 40 seconds, respectively.

Assume that a constant demand of $q = 500$ vph is loaded to the intersection for one hour, and 20 % of the vehicles act as Eco-CACC vehicles with equipped with wireless communication devices to receive the SPaT and vehicle queue information, i.e., approximately 100 CVs are loaded on the network. Here, we assume that all vehicles are the type 1 vehicle defined in VT-CPFM model. The length of the control segments upstream and downstream of the intersection are assumed to be $d = 500$ meters and $l = 200$ meters, respectively. All CVs apply both the Eco-CACC-O and Eco-CACC-Q algorithms, and the advisory speed limits are updated every second. Here, we assume that the CACC system implements these speed recommendations without any intervention from the driver.

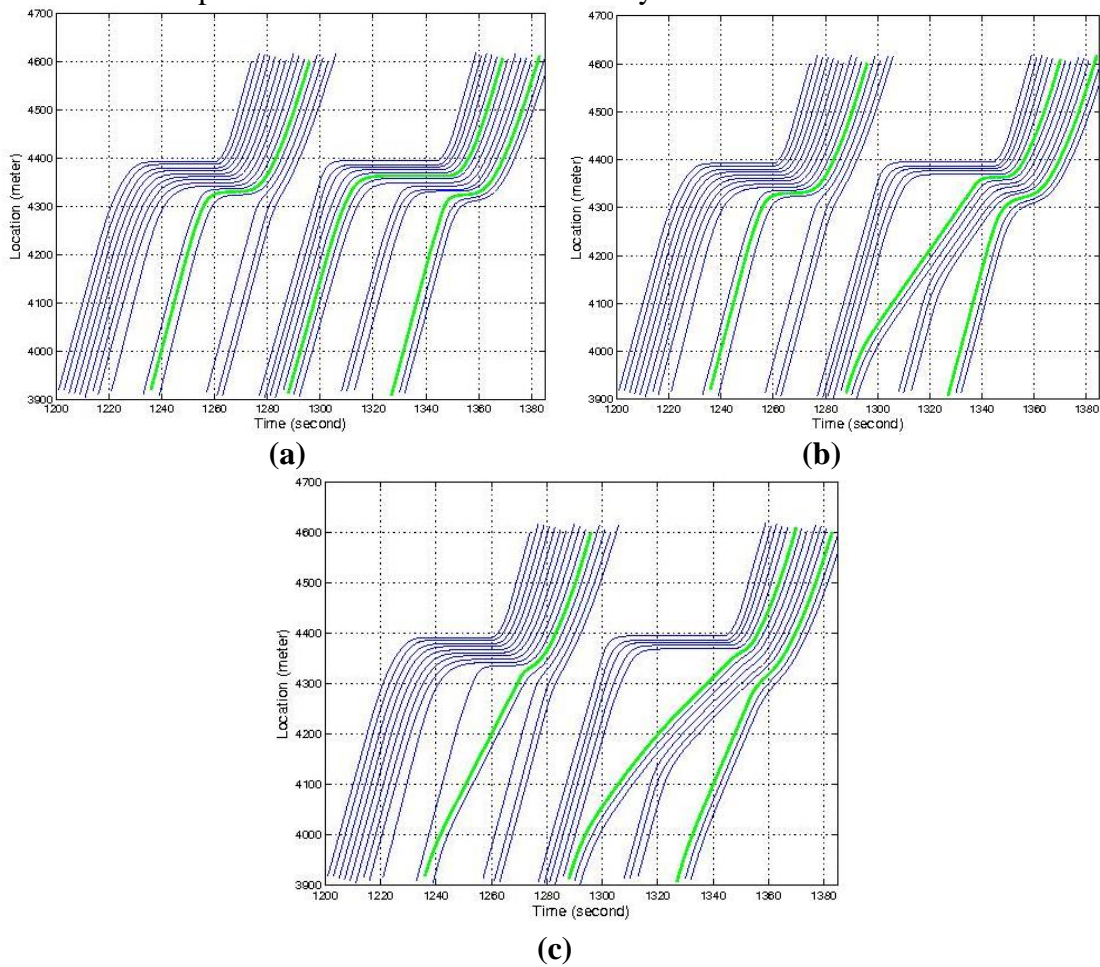


Figure 12: Vehicle trajectories around a single-lane intersection: (a) base case, (b) Eco-CACC without queue, (c) Eco-CACC with queue

Figure 12 illustrates the trajectories of all vehicles before and after applying the Eco-CACC algorithms at the intersection over two cycles, where the signal is located at $x = 4400$ meters. In Figure 12(a), without control, the Eco-CACC vehicles just follow their leaders, and they come to a complete stop ahead of the traffic signal waiting for the green

indication to release the queue. Figure 12(b) shows the trajectories after applying the Eco-CACC-O algorithm. As can be seen from the second Eco-CACC vehicle in the figure, the vehicle slows down to approach the traffic signal and catches the green light. Because of the vehicle queue, the vehicle has to stop ahead of the intersection to wait for the release of the queue. While in Figure 12(c), the Eco-CACC-Q algorithm ensures that the vehicle is able to cruise to the intersection and catch the tail of the queue just when it is released, so that the vehicle can avoid coming to a complete stop upstream of the intersection.

Note that in Figure 12 (b), the first and the third Eco-CACC vehicles are not controlled by the Eco-CACC algorithms. The reason is that the Eco-CACC-O algorithm estimates that the vehicles will proceed through the intersection at their current speed. However, due to the impact of the vehicle queues, the vehicles have to wait for the release of the queue. Hence, they still experience complete stops. The Eco-CACC-Q algorithm solves this problem. Consequently, we observe these two vehicles are controlled in Figure 12 (c) and do not stop at the signal.

Figure 13 compare the speed profiles of the second probe vehicle for the three different scenarios, respectively. The speed profiles computed by the Eco-CACC algorithms are much smoother than the base case, and the Eco-CACC-Q algorithm generates the smoothest trajectory (The standard deviations of the speed profiles from the base case, Eco-CACC-O, and Eco-CACC-Q are 29.7 km/h, 17.2 km/h, and 15.3 km/h, respectively.) Moreover, for the Eco-CACC-O algorithm, the probe vehicle cruises at a speed of 28 km/h, and stops for approximately 8 seconds (for the base case, it stops for approximately 30 seconds.) While being controlled by the Eco-CACC-Q algorithm, the vehicle cruises at 20 km/h, and does not stop upstream of the traffic signal. Furthermore, the fuel consumption generated by the probe vehicles are 0.125 l/km for the base case, 0.116 l/km for Eco-CACC-O, and 0.111 l/km for Eco-CACC-Q, respectively. In summary, the Eco-CACC-Q algorithm is the most efficient control strategy, with reductions in fuel consumption levels as high as 11.4 %; and compared with Eco-CACC-O, it reduces fuel consumption levels by approximately 4.5 %.

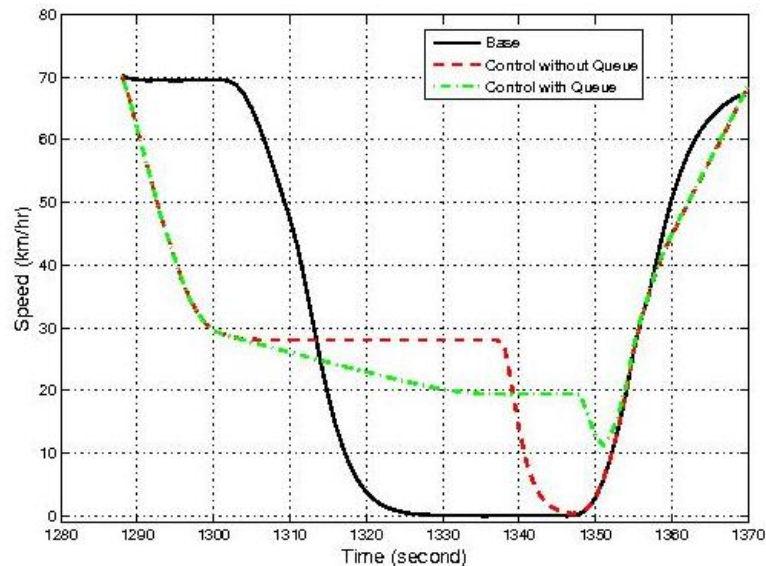


Figure 13: Speed profiles of the second probe vehicle in the single-lane intersection

Besides the probe CVs, both Eco-CACC algorithms smooth the behavior of non-CVs given that they are governed by car-following rules and thus would have to follow the behavior of their lead vehicle (it should be noted that the approaches are single lanes). This means the algorithm is able to reduce the overall fuel consumption at the signalized intersection. The example above demonstrates that the algorithm without queue consideration and with queue consideration reduces the fuel consumption level by approximately 8.4 % and 10.4 %, respectively.

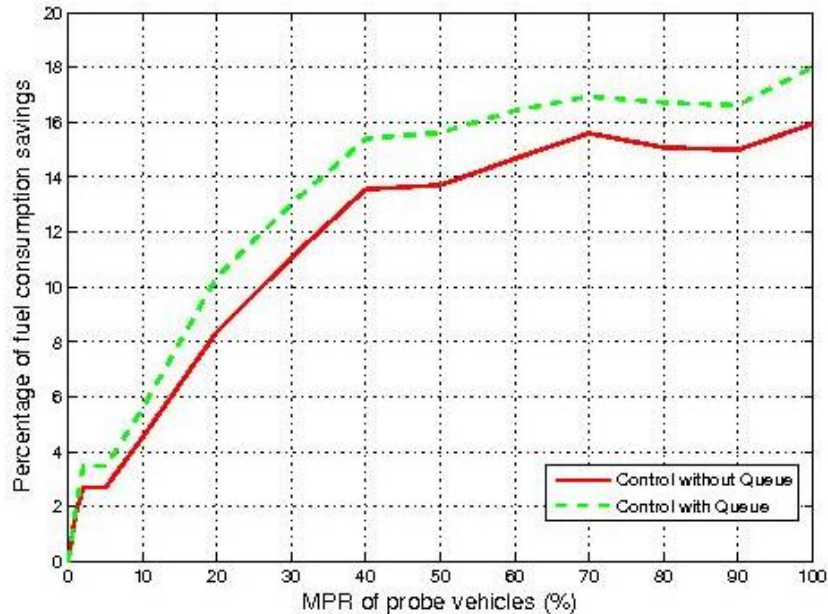


Figure 14: Savings of fuel consumption rate for different MPRs on a single-lane intersection

In addition, we investigate the impact of market penetration rates (MPRs) on the Eco-CACC algorithm performance. The settings of the simulation are the same as the example above, except that the MPR varies from 0 to 100 %. Figure 14 shows the savings in the average fuel consumption derived from the algorithm with and without queue consideration. With higher MPRs, the fuel savings are higher. If all vehicles are controlled by the algorithm, the fuel consumption is reduced by approximately 15.9 % for Eco-CACC-O, and 18.0 % for Eco-CACC-Q. Thus, the algorithm considering the queue produces additional fuel savings.

Performance on Multi-lane Roads

In this subsection, a simulation for a more realistic intersection layout, namely a multi-lane intersection where the roads upstream and downstream of the intersection have more than a single lane, is considered. To simplify the simulation, we simulate a two-lane intersection. The scenario is designed to quantify the benefits of the algorithm for different MPRs with realistic network topologies. The settings of the roads, the signal phasing and timing plan, the vehicle type, and the Eco-CACC algorithm are the same as the simulation configuration that was described in the previous subsection. In that sense, the lane-based fundamental diagram remains the same. The demand entering the intersection is set as $q = 500$ vph/lane, i.e., 1000

vph. Vehicles are loaded to the network for approximately one hour. We assume 20 % of vehicles are CVs that receive SPaT and vehicle queue information.

Figure 15 illustrates the vehicle trajectories for vehicles on the left lane before and after applying the Eco-CACC algorithm over two cycle lengths, where the signal is located at $x = 4400$ meters. Without control, the probe vehicles in Figure 15 (a) only follow their leaders. In Figure 15(b), the probe vehicles are controlled by the Eco-CACC-O algorithm, and thus cannot avoid incurring a complete stop. In Figure 15(c), the probe vehicles are controlled by the Eco-CACC-Q algorithm to allow the vehicles to proceed through the intersection without incurring a stop.

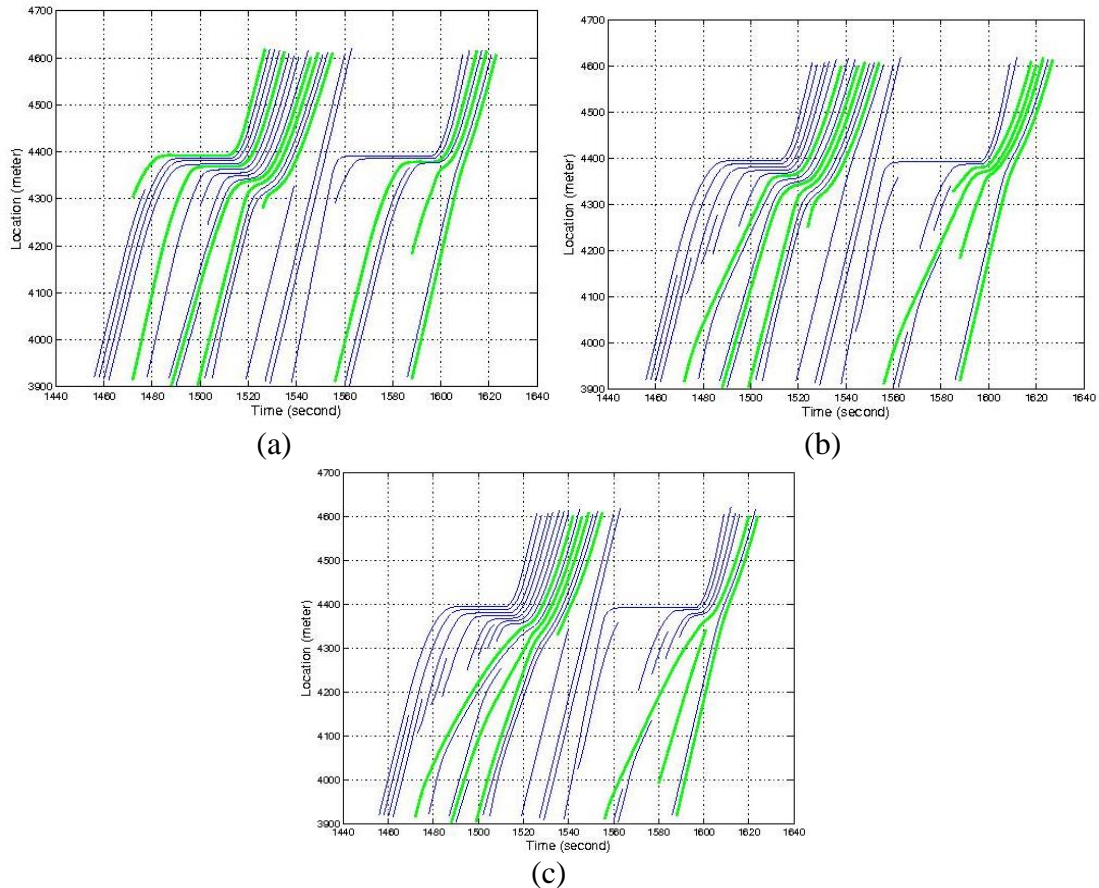


Figure 15: Vehicle trajectories around the intersection: (a) base case, (b) Eco-CACC without queue, (c) Eco-CACC with queue

Figure 16 compares the speed profiles of the first CV (the second one in Figure 15 (a)) for the three scenarios, respectively. It demonstrates that the Eco-CACC-Q algorithm generates the smoothest speed profile (the standard deviations of the speed from the base case, Eco-CACC-O, and Eco-CACC-Q are 31.9 km/h, 19.2 km/h, 16.5 km/h, respectively). For the Eco-CACC-O algorithm, the CV cruises at a speed of 40 km/h, and experiences a stop of approximately 6 seconds (for the base case, it stops for approximately 17 seconds). While when the Eco-CACC-O algorithm is used, the vehicle cruises at 20 km/h, and does not stop upstream of the traffic signal. Due to lane-changing behavior, the queue length changes over time and thus the recommended cruise speed also changes over time. The fuel

consumption rates generated by the probe vehicles are 0.125 l/km for the base case, 0.107 l/km for Eco-CACC-O, and 0.101 l/km for Eco-CACC-Q, respectively. In summary, the Eco-CACC-Q algorithm provides the most efficient control, with reductions in fuel consumption levels for CVs as high as 19.2 %; and compared with Eco-CACC-O, it reduces fuel consumption levels by approximately 5.6 %.

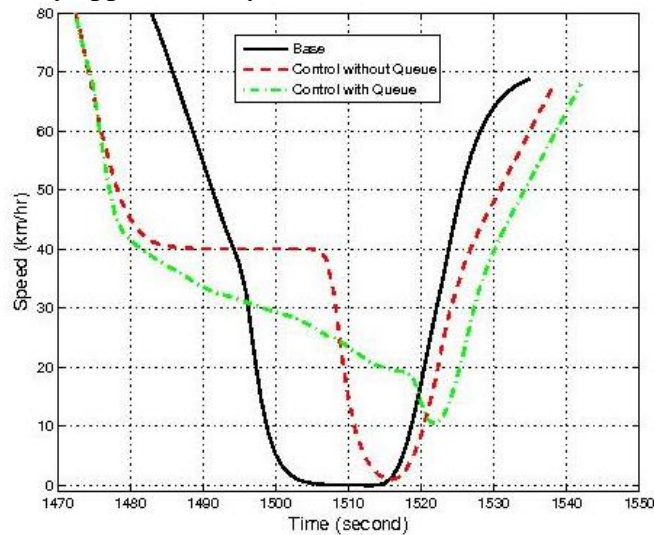


Figure 16: Speed profiles of the second probe vehicle in the two-lane intersection

Unlike the example in the previous subsection, both roads have two lanes. Consequently, as the CVs are controlled and travel at a lower speed compared to the surrounding traffic, non-CVs make lane changes to cut into the gaps ahead of the CVs (see Figure 15). The overall average speed of the CVs is further reduced, i.e., they take longer time to reach the same position downstream of the intersection (see Figure 16). Moreover, another drawback of the algorithm is that the intense lane changing behavior, which cause frequent accelerations and traffic oscillations, result in high fuel consumption levels for low MPRs. In that sense, the overall fuel consumption may increase. Below MPRs of 20 %, both the Eco-CACC-O and Eco-CACC-Q algorithm result in an increase in the fuel consumption level by approximately 5 %.

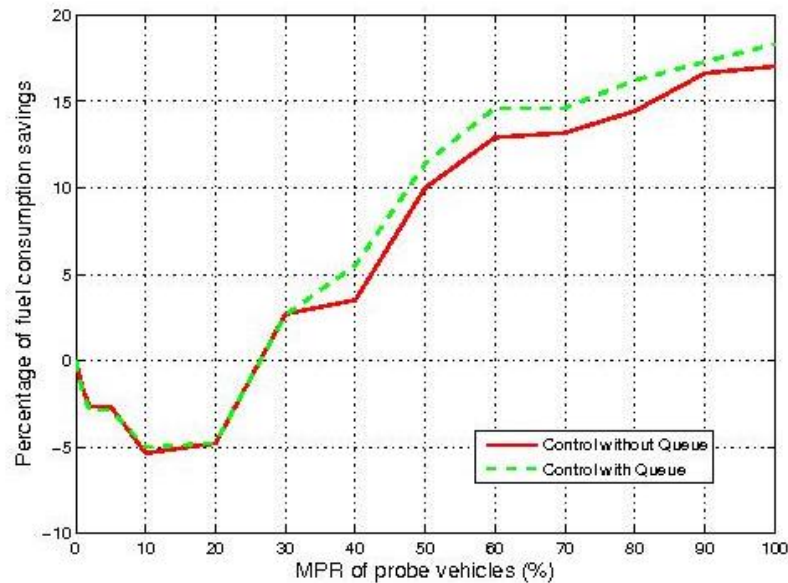


Figure 17: Savings of fuel consumption rate for different MPRs on a multi-lane intersection

Moreover, we investigate the impact of MPRs on the Eco-CACC algorithm performance. The settings of the simulation are the same as the example above, except that the MPR varies from 0 to 100 %. Figure 17 shows the savings in the average fuel consumption rate for all vehicles for the two algorithms. For lower MPRs, both algorithms have a negative impact on the overall fuel consumption rate. This is caused by the intense lane changes around the controlled vehicles. Once the MPR is greater than 30 %, the number of Eco-CACC vehicles is large enough to prevent the non-Eco-CACC vehicles from cutting in and thus reduce the lane change intensity. Hence, the Eco-CACC algorithms generate fuel consumption savings at higher MPRs. These savings increase as the MPR increases. If all vehicles are Eco-CACC vehicles, the fuel consumption rate is reduced by approximately 17.0 % for Eco-CACC-O, and 18.3 % for Eco-CACC-Q demonstrating the benefits of the Eco-CACC-Q system.

Sensitivity Analysis

This section describes the results of a sensitivity analysis of the proposed algorithm. The sensitivity analysis considers the impact of the market penetration rate (MPR) of Eco-CACC-Q equipped vehicles, the number of lanes of the controlled segments, the timing plan of the traffic signal, the length of the control segments, and the traffic demand levels. Subsequently, the limitations of the algorithm are analyzed and discussed.

As a starting point, a simple intersection defined in Figure 11 is simulated. Vehicles are only loaded from one origin and exit at one destination, i.e., only one-direction of through traffic is simulated. For the SPaT plan, the cycle length is set at $C = 84$ seconds, and the green and amber durations are 40 and 2 seconds, respectively. For all case studies below, we assume that the speed limits of all roads are $v_f = 50$ mph and the saturation flow rates are all $q_c = 1600$ vphr/lane (vphpl). The INTEGRATION simulation software is used to model the movements of individual vehicles including the control of CACC-equipped vehicles.

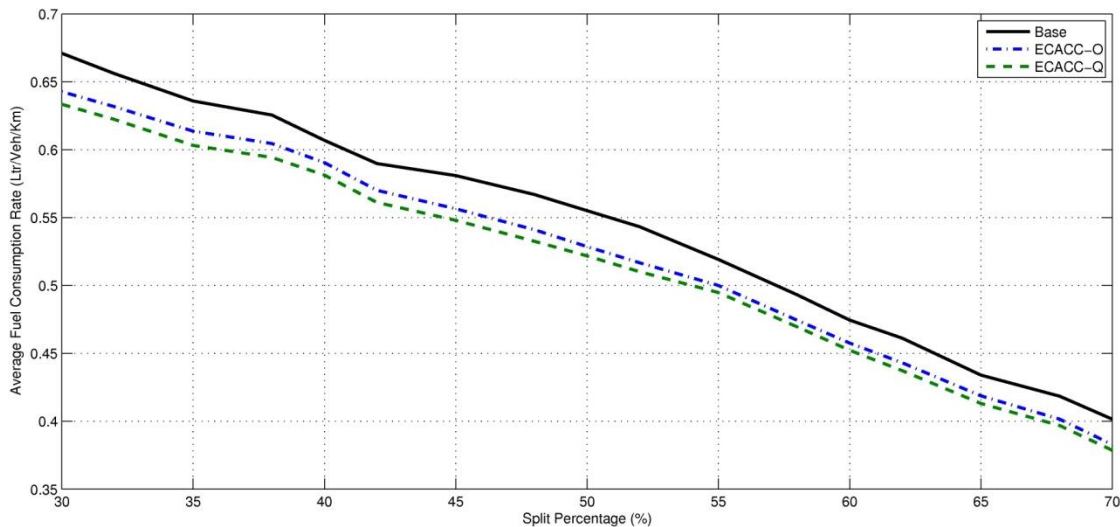
Table 1 shows the settings of the Eco-CACC-Q algorithm. Under these settings, once a probe vehicle arrives within $d = 500$ meters of the signalized intersection, the Eco-CACC-Q algorithm is activated, and the controlled vehicle receives a desired speed based from the algorithm that is updated every second. The vehicle continues to receive an updated desired speed until it travels a distance $l = 200$ meters downstream of the traffic signal to ensure that the vehicle acceleration is optimized.

Table 1: Settings of the Eco-CACC-Q algorithm

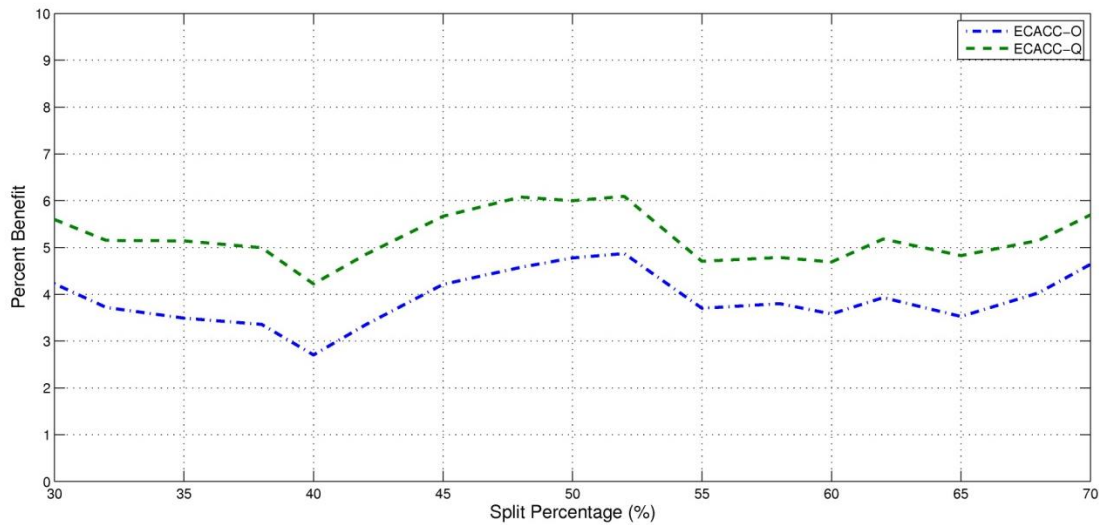
Parameters	Values
Length of the upstream control segment, d (meter)	500
Length of the downstream control segment, l (meter)	200
Maximum deceleration level, a_{-}^s , (m/s^2)	3
Maximum acceleration level, a_{+}^s , (m/s^2)	2

Sensitivity to Phase Splits

The SPaT plan determines the split of each phase, and the performance of the intersection is highly related to the split. As the proposed Eco-CACC algorithms utilize the SPaT information to compute the optimum trajectories of CACC-equipped vehicles, the impact of the phase split has to be carefully examined. In this subsection, a sensitivity analysis of the phase split is studied.



(a)



(b)

Figure 18: Impact of phase length on: (a) average fuel consumption, (b) savings in fuel consumption

The single-lane intersection is simulated in this subsection using the same link characteristics and Eco-CACC algorithm settings. Vehicles were loaded at a rate of 300 vph, but only 20% of the vehicles were controlled. The phase split varied from 30% to 70% along the main road. Figure 18(a) compares the average fuel consumption rates of each vehicle from the base case without control, Eco-CACC-O, and Eco-CACC-Q for different phase splits. The results demonstrate that for longer phase lengths, vehicles have a higher probability to pass the intersection without experiencing the red indication, i.e., they are less likely to be stopped by the signal. Hence, they can travel smoothly to their destination with less fuel consumption. Regarding the savings in the fuel consumption, Figure 18(b) shows that the phase length does not affect the algorithm performance with differences not exceeding 1%. Moreover, the comparison between Eco-CACC-Q and Eco-CACC-O also verifies the benefits of considering the vehicle queue. For all phase lengths, Eco-CACC-Q produces the lowest fuel consumption with savings in the range of 1-2% higher than that for Eco-CACC-O control.

Control Segment Length

The length of the control segment, especially the upstream segment length, d is expected to have a significant impact on the algorithm performance. In this subsection, we conduct a sensitivity analysis on the impact of d on the algorithm performance for the single-lane and two-lane intersections.

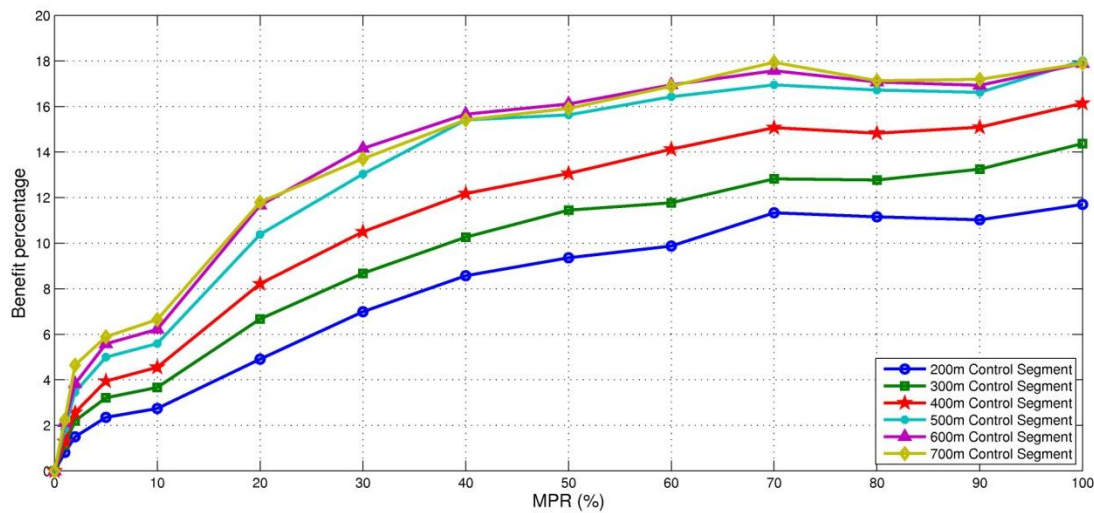


Figure 19: Impact of control length on the fuel savings at a single-lane intersection

First, the single-lane intersection is simulated using the same link characteristics and SPaT plan. Vehicles are loaded at a rate of 500 vph. The settings for the Eco-CACC-Q algorithm in Table 1 are kept the same, except the upstream control segment length, d , varies from 200 to 700 meters. Note that, this range is selected based on the effective distance of the Dedicated Short-Range Communication (DSRC) Technology, which is implemented to construct communications between probe vehicles and signals. [38] indicated that the effective distance of the technology varies from 10 meters to 1 km. Given that the control length cannot be very short. Hence, a range of [200, 700] meters is arbitrarily selected. Figure 19 compares the fuel savings for different control lengths for various MPRs. With higher MPRs, the savings for different d 's are larger. Moreover, comparing different d 's, we find that the longer control length results in larger savings. At an $MPR = 100\%$, 700-meter control segment reduces fuel consumption by as high as 18%, while for a 200-meter segment savings in fuel consumption are approximately 12%. The observation is reasonable as the longer length allows the CACC vehicles to receive SPaT information earlier, and they have longer time to control their movements. In addition, Figure 19 shows that when the control length is longer than 500 meters the savings do not improve. The study demonstrates that a 500-meter segment is sufficiently long to provide the desired benefits.

In the second example, the two-lane intersection is simulated. Similar to the example above, the link characteristics and the settings of the Eco-CACC-Q algorithm are kept the same with only changes in the upstream control segment. Vehicles are loaded at a rate of 500 vph. Figure 20 compares the fuel consumption savings for different control lengths for different MPRs. Similarly, for low MPRs ($<30\%$), the algorithm produces negative effects on fuel consumption levels due to intense lane changing around the controlled vehicles. With a longer control length, regular vehicles are able to pass more controlled vehicles, and thus the frequency of lane changes is higher. Consequently, as the control length increases, the algorithm results in increased overall fuel consumption levels. While, for high MPRs ($\geq 30\%$), the controlled vehicles are able to force the regular vehicles to follow them given that the regular vehicles have less opportunities to maneuver around them. Hence, the benefits of the algorithm are similar to those for the single-lane intersection. The

fuel savings are similar when the length is longer than 500 meters. At MPR=100%, the 500-meter control segment can reduce fuel consumption by as high as 18%, while for the 200-meter segment the fuel savings are only 11%.

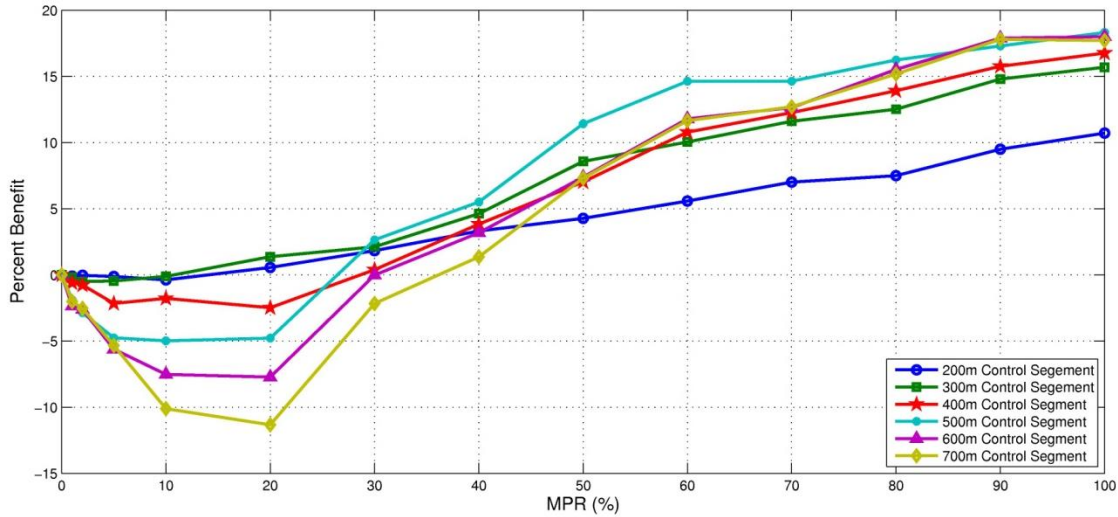


Figure 20: Fuel consumption savings for two-lane intersection for different control lengths

Traffic Demand Level

In the evaluation of the Eco-CACC-Q algorithm, the impact of demand levels should be carefully studied, as they are directly related to the number of probe vehicles controlled and the performance of the network. This subsection deals with the sensitivity of demands on the energy and environmental benefits of the algorithm under a single-lane and a multi-lane intersection.

The first example simulates the single-lane intersection using the same link characteristics in the previous section, the SPaT plan, and the Eco-CACC-Q algorithm settings. However, the demand level varies from 300 to 700 vph. Figure 21 illustrates the savings in fuel consumption as a function of the demand level. The results indicate that for the given settings of control length and phase split, the algorithm can obtain the highest savings in fuel consumption for a specific demand as a function of the MPR. In this example, loading vehicles at a rate of 500 vph can achieve the lowest fuel consumption, i.e., the greatest saving.

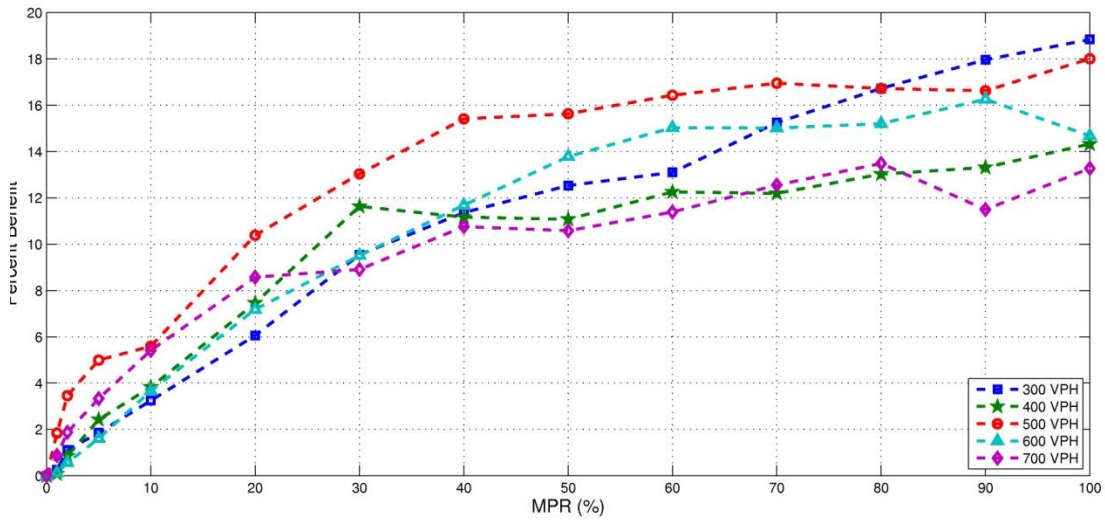


Figure 21: Fuel consumption savings for single-lane intersection for different demand levels

The second example entails modeling the two-lane intersection. The link and Eco-CACC-Q algorithm parameters are kept the same, however the demand varies from 300 to 700 vphpl. Figure 22 illustrates the savings in fuel consumption. For lower MPRs the algorithm produces negative fuel consumption impacts. With higher demands, the algorithm generates more fuel consumption, and needs a larger MPR to obtain positive benefits. This is intuitively correct, as larger demands result in more vehicles traveling simultaneously on the control segment. Hence, more regular vehicles produce increases in lane changes, and it is more difficult for the controlled vehicles force the regular vehicles to follow them. In the case of high MPRs (>50%), the conclusion is similar to the first example. Loading vehicles at the rate of 600 vph can achieve the lowest fuel consumption level.

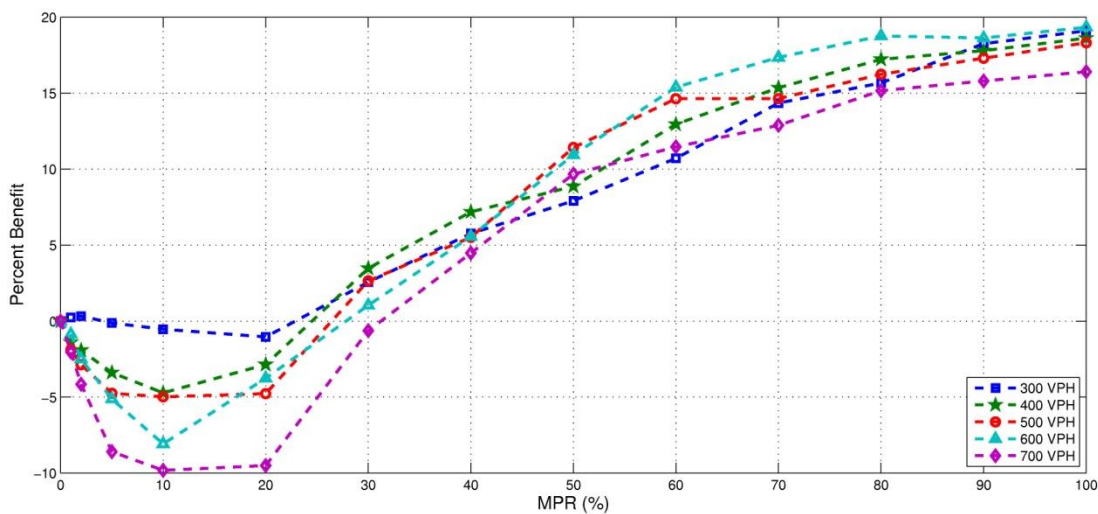


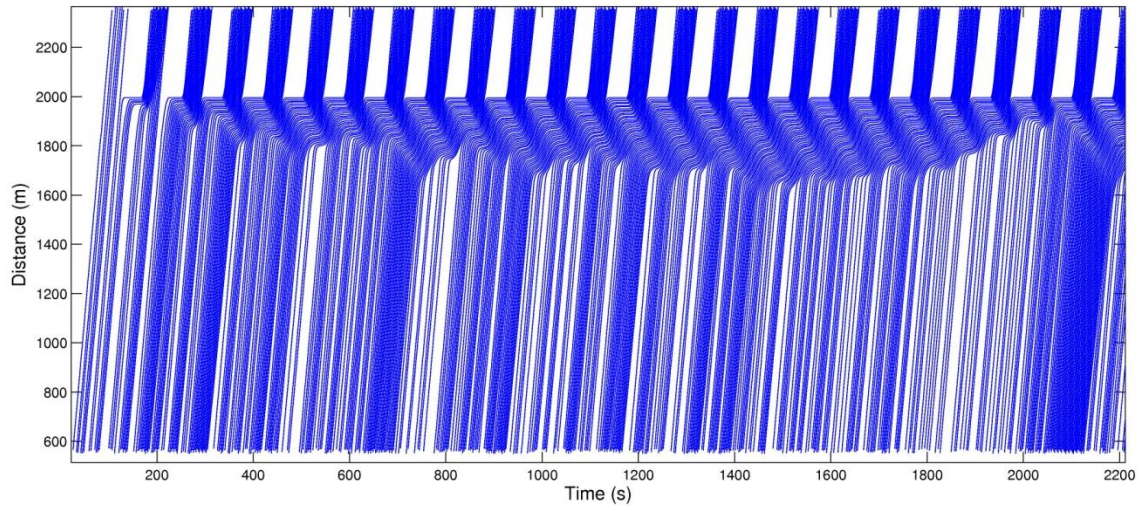
Figure 22: Fuel consumption savings for a two-lane intersection for different demand levels

Algorithm Shortcomings

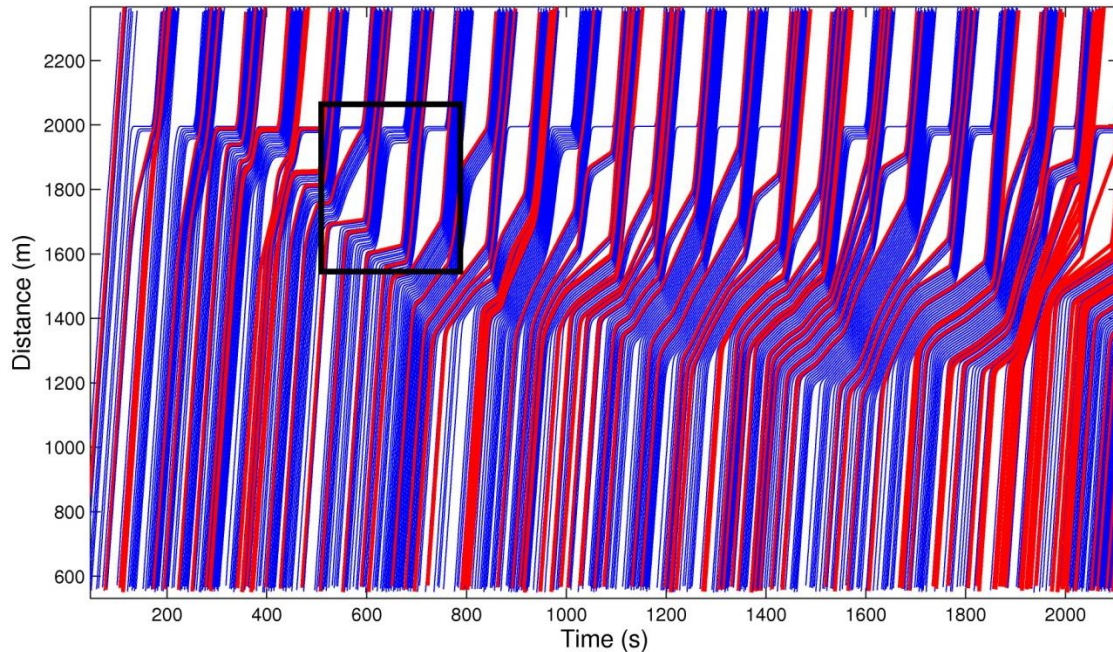
In the development of the Eco-CACC-Q algorithm, one critical assumption is that the studied network should not be over-saturated; otherwise, the estimation of queue length is not accurate. In that sense, the advisory speed limits cannot control the behavior of probe vehicles appropriately to minimize their fuel consumption levels. In this subsection, we simulate the single-lane intersection to demonstrate this limitation.

The link parameters, the SPaT plan, and the Eco-CACC-Q algorithm parameters are kept the same in the simulation runs. Vehicles are loaded at a rate of 800 vph, which is greater than the actual capacity of the control segment, and thus results in over-saturated delay. Figure 23 shows the vehicular trajectories around the intersection before and after applying the Eco-CACC-Q algorithm, where the signal is located at $x = 2000$ meters. From Figure 23(a), the queues upstream of the signal are very long, and some vehicles in queue have to wait for two or three cycles to proceed through the intersection. This demonstrates that they experience more than one stop-and-go maneuver. Figure 23(b) shows the trajectories of all vehicles when 20% of them are CACC-equipped. Clearly, we see once the queue is not dissipated by the next green interval, the algorithm fails at providing appropriate desired speeds to the controlled vehicles.

There are two major causes of the problem. First, when the road is over-saturated, the queue might not be dissipated during a single green indication. Subsequently, in the next cycle, the unreleased queue is not formed at the stop bar, located at position x_s ; instead, it rolls between the intersection and the starting point of the control segment, x_u . Thus, the queue estimation method based on the kinematic wave model cannot update the queue length correctly based on the instantaneous traffic information collected by the loop detectors. Unless historical road conditions are provided, the estimation cannot be accurate. Second, the algorithm assumes that controlled vehicles only perform deceleration upstream of the traffic signal, and they enter the segment with a high speed (such as the road speed limit). But, the rolling queue generates several stop-and-go waves on the control segment, which prevents the probe vehicles from maintaining the recommended speed estimated by the algorithm. When they enter the rolling queue ahead, they will slow down and maintain a low speed even there is a large gap ahead (see black box in Figure 23(b)). These two causes can be eliminated when vehicle-to-vehicle communication is introduced. With the assistance of the technology, the queue length can be updated in real-time, and the stop-and-go behavior can be identified. The algorithm would also need to be updated to reflect that fact that the vehicle will stop multiple times



(a)



(b)

Figure 23: Vehicular Trajectories under an over-saturated intersection: (a) base, (b) Eco-CACC-Q

Eco-CACC at one general intersection

In the aforementioned sections, only one approach to an intersection is simulated. In reality, vehicles can pass through the intersection from typically four approaches (see Figure 24). In this section, a comprehensive simulation analysis is conducted considering a four-legged intersection to examine the environmental benefits of the Eco-CACC-Q algorithm.

Figure 24 illustrates the configuration of the simulated intersection. In the network, vehicles are loaded from four origins 1,2,3,4, and travel to the remaining three destinations,

5,6,7,8. The speed limits of all roads are $v_f = 50$ mph, and their capacities are all $q_c = 1600$ vph. The length of the upstream control segment for the major roads (1 and 3 to the signal) is set at 500 meters, and for the minor roads (2 and 4 to the signal) at 300 meters. All downstream control segments are set to 200 meters. The deceleration and acceleration rates are 3 m/s^2 and 2 m/s^2 , respectively.

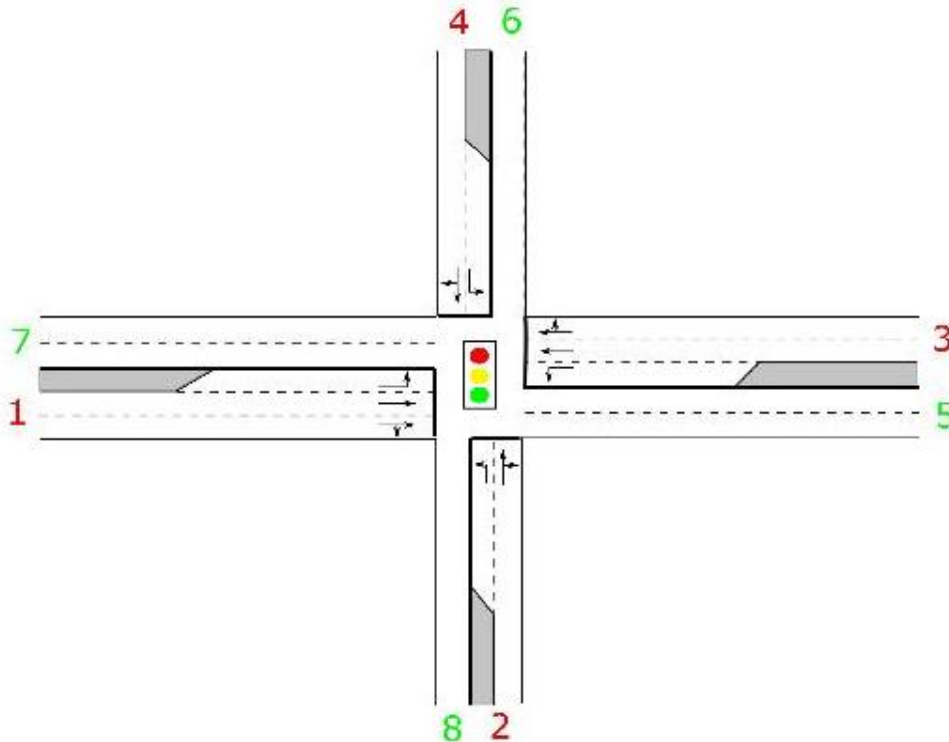


Figure 24: Configuration of a four-legged intersection

Table 2 shows the simulation settings, the OD demand, and SPaT plan used in the simulation (To simplify the simulation, the right-turn demands are ignored). As demonstrated in Table 2, the through traffic on the major roads is as high as 1000 vph, and on the minor roads the left-turn volumes are higher than the through volumes. **Figure 25** illustrates the savings in fuel consumption of all vehicles traveling through the intersection. As the through traffic on the major road is very high, the benefits of the algorithm should mainly be determined by the CACC-equipped vehicles, and the results are similar to the example of the two-lane intersection. As was the case earlier, for lower MPRs (<25%), the algorithm results in an increase in the overall fuel consumption level. As long as the MPR is greater than 25%, the algorithm imparts positive benefits to the network. Once all vehicles are equipped, the fuel consumption level can be reduced by as as much as 12.5%.

Table 2: Simulation setting of the four-legged intersection

Origin	Destination	Movement	Demand (vph)	Green+Amber:Cycle (second)
1	5	Through	1000	72:113
1	6	Left	150	12:113

2	6	Through	50	12:113
2	7	Left	150	17:113
3	7	Through	1000	72:113
3	8	Left	150	12:113
4	8	Through	50	12:113
4	5	Left	150	15:113

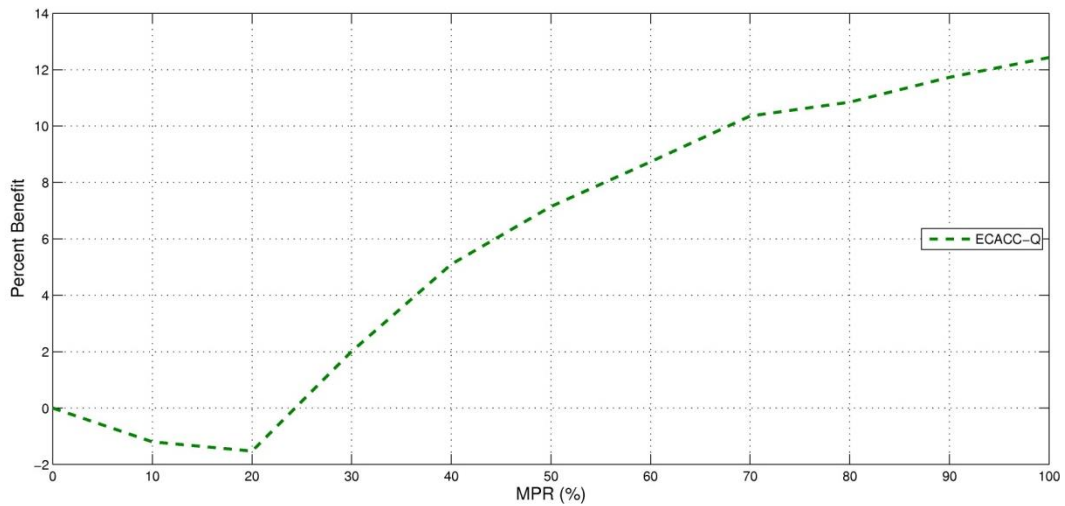


Figure 25: Savings in fuel consumption at a four-legged intersection

Simulation Evaluation at Multiple Intersections

This section evaluates the benefits of the proposed Eco-CACC-MS algorithm with INTEGRATION. The proposed algorithm is implemented at networks with two and four intersections to test its impacts on individual vehicle dynamics, to estimate its benefits on vehicle energy, and to check its feasibility in large networks.

Impact on Equipped Vehicles

As a starting point, a simple network of two intersections defined in Figure 25 is simulated. The simulation is conducted from one-way movement where vehicles are loaded from one origin to one destination only. In the experiment, the speed limits are 80 km/hr, and the road capacities without considering intersections, i.e., non-interrupted capacities, are $q_c = 1600$ vphpl for all links.

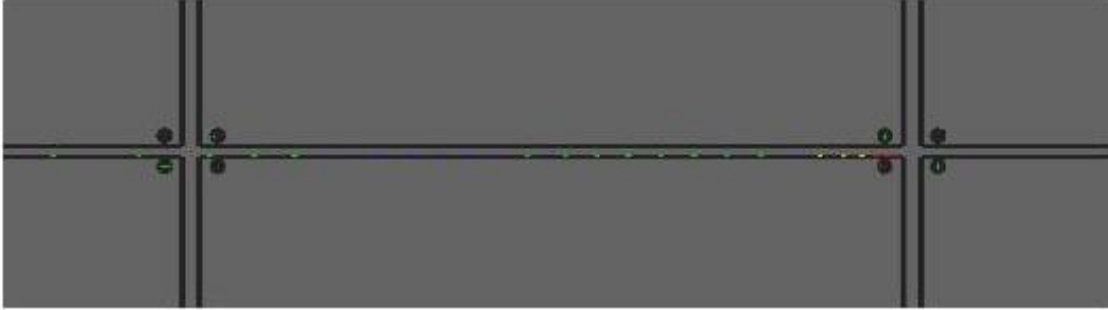
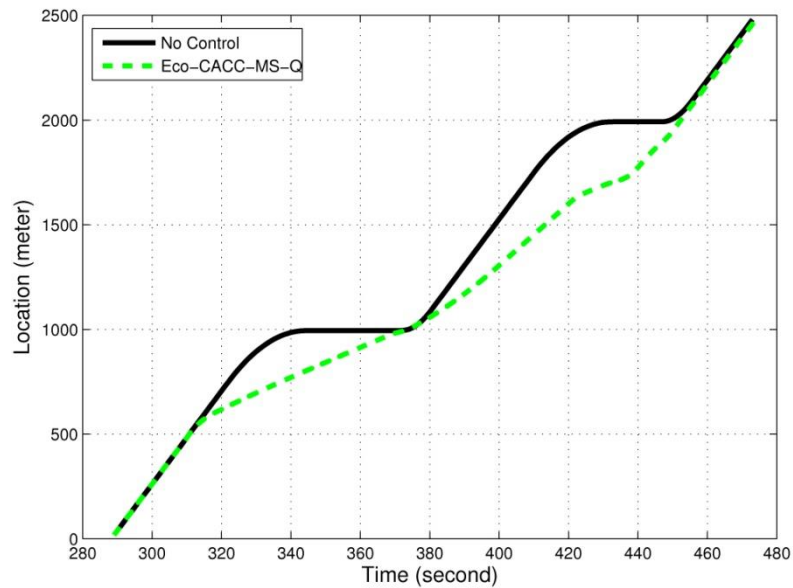


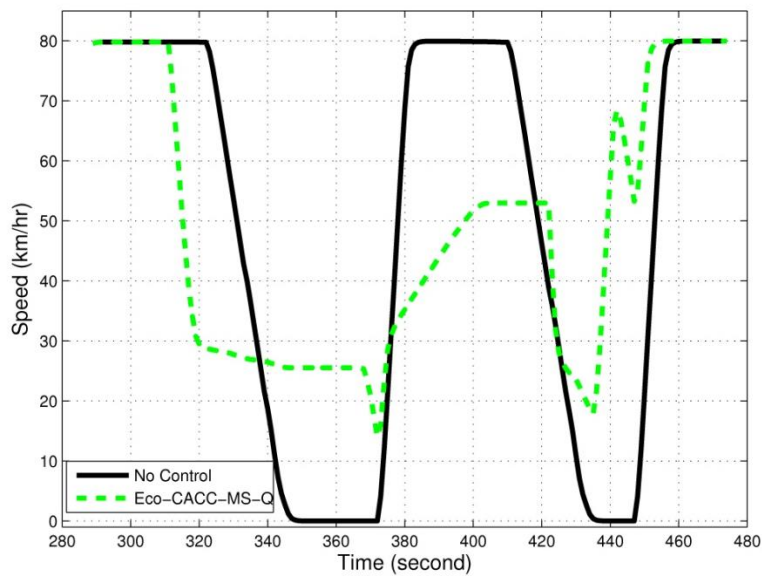
Figure 26: Configuration of two consecutive intersections

Assume that the distance between the two intersections in **Figure 26** is $d_2 = 1000$ meters, the upstream control segment length of the first intersection is $d_1 = 500$ meters, and the downstream control segment length of the second intersection is $d_3 = 200$ meters. The number of lanes of all links is set as one. In the first simulation, vehicles are only loaded from east (left end) to west (right end) at the rate of 600 vphpl, and 10% of them are equipped with the Eco-CACC-MS-Q algorithm (with the consideration of queues). For the SPaT information, the cycle lengths of both signals are 120 seconds, and the durations of the green and the amber indicators of the through traffic for the first and second signals are all 65 and 2 seconds, respectively. The offset of the second signal with respect to the first one is 75 seconds. In this network, the optimal offset of the second signal is 45 seconds. While, to check the benefits of the Eco-CACC-MS-Q algorithm, we try to set the offset to make the equipped vehicles experiencing two stops. The 75-second offset gives a high probability for us to observe two stops for one equipped vehicle. The equipped vehicles receive advisory speed limits from the algorithm, which is updated every second.

Figure 27(a) compares the trajectories of one equipped vehicle before and after applying the Eco-CACC-MS-Q algorithm. Compared to the trajectory without control, the trajectory (location between 500 meters and 2200 meters) is much smoother when the algorithm is applied. Figure 27(b) compares the speed profiles of the vehicle before and after applying the algorithm. Similar to Figure 6(b), the equipped vehicle slows down and cruises to the first intersection with a smaller speed, and passes the intersection without stops. Between the first and second intersections, it accelerates to another cruise speed with a moderate rate and passes the second intersection without stops. The standard deviations of the speed profiles before and after applying the algorithm are 34.2 km/hr and 22.1 km/hr, respectively, i.e., the speed oscillation is reduced as high as 30%. In addition, the fuel consumption levels before and after applying the algorithm are 0.146 liter/km and 0.113 liter/km, indicating that the algorithm reduces fuel consumption by about 22.5%.



(a)



(b)

Figure 27: Comparison of vehicle movements before and after applying the Eco-CACC-MS-Q algorithm

Note that in Figure 27(b), after applying the algorithm, the equipped vehicle's speed still drops ahead of the signals and fluctuates a lot, even though the vehicle does not experiencing complete stops. This fluctuation is caused by the estimation of the vehicle queue lengths, q_1 and q_2 , and the queue dispersion speeds, w_1 and w_2 . In the Eco-CACC-MS-Q algorithm, these variables are estimated with the kinematic wave model using road properties, including road capacity, jam density, and critical density. However, in the microscopic simulations, due to the randomness of vehicle dynamics, the estimation cannot be accurate. Hence, the advisory speed limits calculated by the Eco-CACC-MS-Q algorithm

cannot perfectly smooth the movements of equipped vehicles, and the oscillations occur when they travel through the intersections. In the future, with the help of vehicle-to-vehicle communications, queue lengths and queue dispersion speed can be monitored in real time. Then, the estimation of the advisory speed limits will be accurate, and the oscillation can be mitigated.

Eco-CACC-MS Algorithm at Two Intersections

In this section, we evaluate the benefit of the proposed algorithm on the network-wide fuel consumption levels, and compare the algorithms with and without the consideration of vehicle queues (Eco-CACC-MS-Q and Eco-CACC-MS-O) under different MPRs of the equipped vehicles. In addition, the algorithms are compared with Eco-CACC-Q and Eco-CACC-O for independent intersections.

The network settings in the aforementioned section are also applied in this section. For the multiple intersection control algorithms (Eco-CACC-MS-Q and Eco-CACC-MS-O), the equipped vehicles are under control once they are within 500 meters ahead of the first intersection and within 200 meters after the second intersection for the Eco-CACC-MS algorithms. For the single intersection control algorithms (Eco-CACC-Q and Eco-CACC-O), the equipped vehicles are under control once they are within 500 meters before each intersection and 200 meters after each intersection. This simulation was done with a single-lane network, which prevents lane changing or vehicle over-passing behaviors. The demand for the network is still 600 vphpl, and the SPaT plans of the two intersections in the previous intersection are also applied. The offset of the second signal is set as 0 seconds. To better evaluate performance, the algorithms are tested under different MPRs; only a portion of the vehicles are equipped, while the rest drive normally using car-following models. Figure 28 demonstrates the overall network-wide energy savings of the Eco-CACC and Eco-CACC-MS algorithms considering different MPRs. The figure illustrates that higher MPRs lead to greater savings in all control systems. At 100% MPR, the fuel consumption is reduced about 7% with Eco-CACC-MS-Q and 4.2% with Eco-CACC-Q. In the simulations, the movements of the equipped vehicles are smoothed by the proposed algorithm, and at the same time due to the car-following behaviors, the trajectories of some non-equipped vehicles are also smoothed, which further reduces the network-wide fuel consumption levels. Figure 28 also demonstrates that even without the consideration of vehicle queues, the Eco-CACC-MS-O and Eco-CACC-O algorithms can still produce larger fuel savings as MPRs increase. However, the savings are smaller than those that take queues into consideration. Specifically, without considering queues, the fuel consumption rate is reduced from 7% to 6.1% for the multiple intersection control and from 4.2% to 3.9% for the single intersection control.

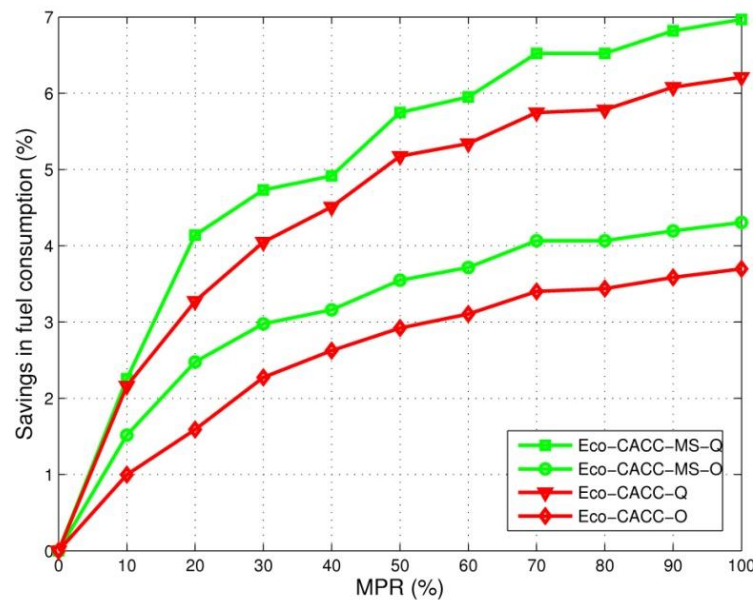


Figure 28: Savings in fuel consumption at the single-lane network under different MPRs

In the simulation of the single-lane intersections above, lane changing and over-passing behaviors are not allowed; while in reality, links with two or more lanes are common. Accordingly, the impacts of lane changing and vehicle over-passing need to be considered. In the second example, the same settings used in the previous simulation are applied to the same network with two-lane links. Figure 29 compares the fuel consumption savings of Eco-CACC-Q, Eco-CACC-O, Eco-CACC-MS-Q, and Eco-CACC-MS-Q algorithms under different MPRs. Unlike the single-lane network, the savings in fuel consumption are not always observed in the two-lane scenarios, especially when the MPR is less than 30%. When MPRs are less than 30%, all algorithms increase the overall fuel consumption levels. The negative impact of the lower MPRs is a result of the lane changing and over-passing of non-equipped vehicles. As the algorithms only control the equipped vehicles, which are traveling at lower speeds than the non-equipped vehicles, larger gaps will be generated ahead of them. The non-equipped vehicles, traveling at higher speeds, then have a greater likelihood of changing lanes and cutting into the gaps ahead of the equipped vehicles, increasing their speed oscillations and the fuel consumption level for the whole network. With 30% MPRs and above, the number of equipped vehicles increases, making it increasingly possible for equipped vehicles to travel side-by-side for the whole link, preventing lane changing and over-passing movements, and increasing fuel consumption savings. All algorithms provide positive savings with MPRs higher than 30%. At 100% MPR, fuel consumption is reduced by about 6.5% for the Eco-CACC-MS-Q, 5.8% for Eco-CACC-MS-O, 4.2% for Eco-CACC-Q and, and 3.2% for Eco-CACC-O. Similar to the single-lane example, the algorithms taking queue effects into consideration always result in better performance for the network with two-lane links.

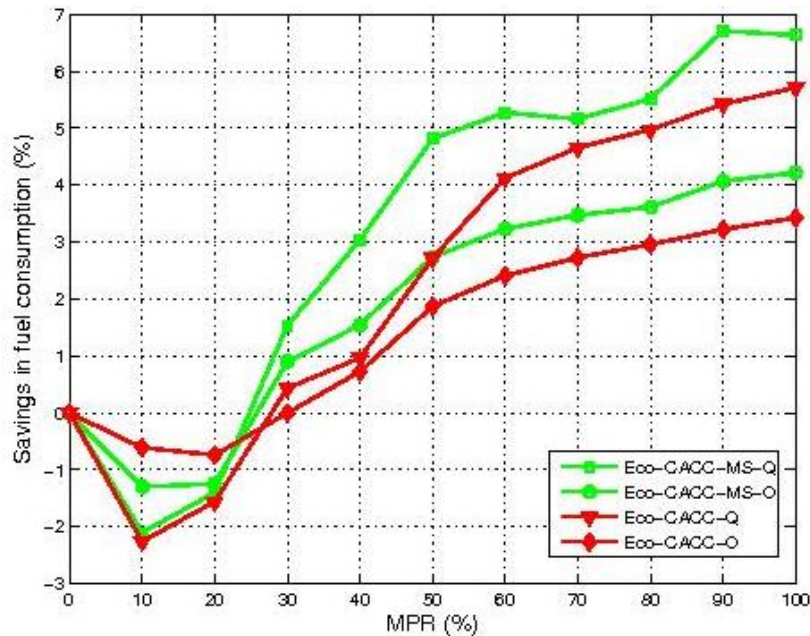


Figure 29: Savings in fuel consumption at the two-lane network under different MPRs
Eco-CACC-MS Algorithm at Four Intersections

In addition to two-intersection networks, the Eco-CACC-MS-Q algorithm is also applied to a larger network with more than two intersections. The network in Figure 30(a), which has four consecutive intersections, is simulated. Assume that the distance between any two consecutive intersections is 600 meters. The demand from the west to east is constant at 600 vph. For the SPaT plan, the cycle lengths and phase splits of all intersections are 120 seconds and 50%, respectively, and the offsets of all signals are set as 0. Figure 30(b) illustrates the fuel consumption savings from the Eco-CACC-Q and Eco-CACC-MS-Q algorithms under different MPRs in single-lane and two-lane networks. For the single-lane network, both algorithms have positive benefits to fuel consumption at different MPRs, and higher MPRs result in greater savings for both algorithms. At 100% MPR, fuel consumption is reduced by 7.7% with Eco-CACC-MS-Q, and by 6.2% with the Eco-CACC-Q algorithm. The savings come from both equipped vehicles with the optimal trajectories and non-equipped vehicles following them with car-following models. For the two-lane network, negative effects of the algorithms are still observed when the MPR is low (<15% for Eco-CACC-Q and <25% for Eco-CACC-MS-Q). When the MPR is larger than 30%, positive savings in fuel consumption can be obtained for both algorithms and the savings from the multiple intersection control is higher than the single intersection control (even though the different is not quite large). At 100% MPR, both algorithms can reduce the fuel consumption as high as 4.8%. The two simulations also verify the effectiveness of the proposed algorithm on networks with multiple intersections.



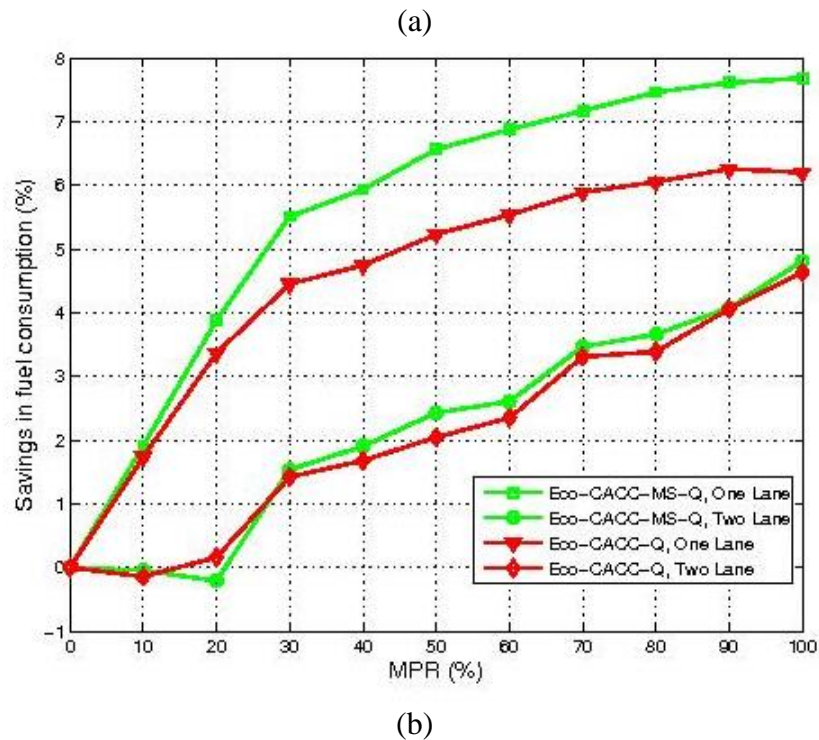


Figure 30: Eco-CACC-MS at four intersections: (a) configuration, (b) savings

Sensitivity Analysis

This section makes a comprehensive sensitivity analysis of variables applied in the proposed Eco-CACC algorithms, including traffic demand levels, phase splits, offsets between two consecutive signals, and distances between intersections. In addition, the impact of over-saturated traffic on the algorithm is assessed. Moreover, the Eco-CACC-Q and the Eco-CACC-MS-Q algorithms are compared to examine the advantage of the multiple intersection control. To complete the analysis, the network in \reff(simsig) with two intersections is simulations, and link properties, including the road speed limits, the road capacities, the jam densities, and the density at capacity, are the same to previous examples.

Demand Levels

On arterial roads, vehicle demands are directly related to queue lengths ahead of signals and the number of the equipped vehicles in the network, and they play an important role on evaluating the performance of the intersections and assessing the benefits of the Eco-CACC algorithms. In this section, we examine the fuel efficiency of the Eco-CACC-MS-Q and Eco-CACC-Q algorithms under different demand levels. The signal settings of the two intersections are the same to the previous intersection. Here, the 75-second offset is also applied to observed obvious different between the single and multiple intersection control strategies. In addition, we assume that all vehicles are equipped (i.e., the MPR is 100%), and the demand varies from 100 to 700 vphpl for both algorithms.

Figure 31 illustrates the fuel consumption savings of both algorithms as a function of the demand. The results show that under the given settings of the signal plans and the offset, positive savings in fuel consumption can be observed for all demand levels. In addition, for

the Eco-CACC-MS-Q algorithm, the demand at 400 vphpl results in the best savings for the whole network, about 13.5%. Demands from 400 vphpl to 700 vphpl result in savings of 7% for the Eco-CACC-Q algorithm. The savings are a result of the increase in the number of equipped vehicles in the network. However, this simulation only considers demands below the saturated flow (800 vphpl). The implementation of the algorithm in the over-saturated network will be different, and the details will be analyzed in the rest of this report.

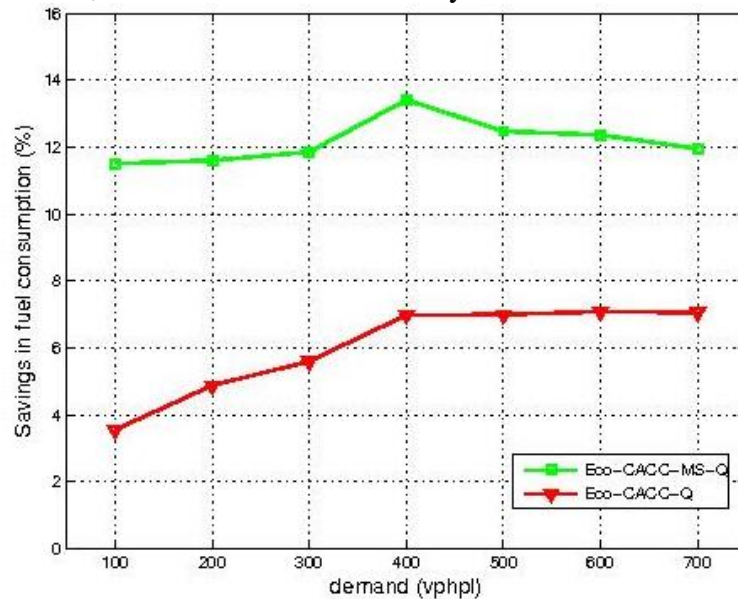


Figure 31: Saving in fuel consumption under different traffic demand levels

Phase Splits

In this study, both Eco-CACC-MS-Q and Eco-CACC-Q algorithms utilized the SPaT information to compute the optimal trajectories for the equipped vehicles, which indicates the phase splits are highly related to the effectiveness of the algorithms. In this subsection, the impact of the phase splits to the overall network performance is investigated. The simulation settings are the same as those used in the example in the previous section. The demand is constant as 600 vphpl, and the phase split (i.e., the ratio of the total duration of the green and amber indicator to the cycle length) ranges from 35% to 75% for the major road (through traffic from west to east) respect to the total cycle length of 120 seconds.

Figure 32 illustrates the fuel consumption savings of both algorithms as a function of the phase split. The figure indicates that with higher phase splits, the savings in fuel consumption will be smaller. With a 35% green split for the major road, the savings reach up to 13.8% for the Eco-CACC-MS-Q and 7.2% for Eco-CACC-Q. This results are intuitively correct. With higher phase splits, the equipped vehicles have less chance of stopping at the signals, resulting in lower fuel consumption savings, as less vehicles have to stop. Consequently, it only needs to control the behaviors of less vehicles at higher phase splits. In addition, the benefits of the proposed algorithms come from the control of the stopped vehicles. In that sense, the savings of fuel consumption will be smaller.

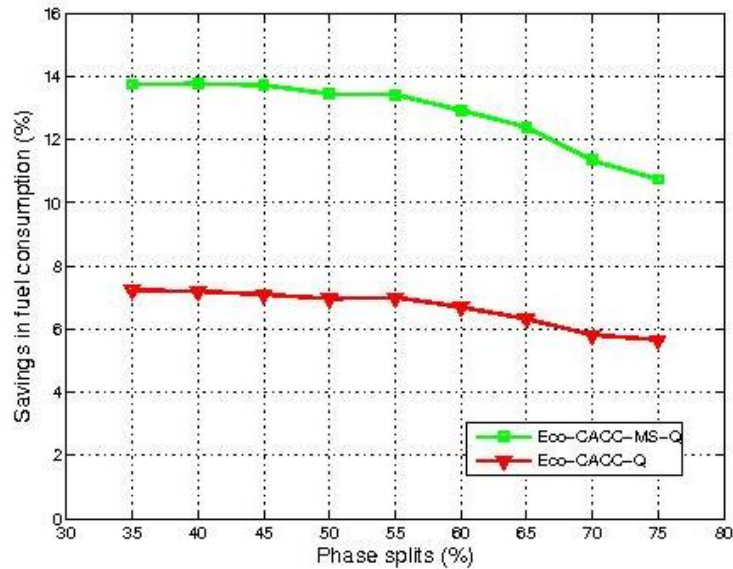


Figure 32: Saving in fuel consumption under different phase splits

Signal Offsets

The offset is important to coordinate multiple intersections and to improve the performance of the whole network. And, the fluctuations of vehicles' movements through multiple intersections are directly related to the offset. This section investigates the impact of offsets on the performance of the proposed algorithms. The simulation settings are still the same to the example in the previous section, except that the phase split is constant at 55%, and the second signal offset with respect to the first varies from 0 to 120 seconds. In this simulation, the distance between the two intersections is 1000 meters, which can be traveled by equipped vehicles within 45 seconds at the free-flow speed, i.e., the optimal offset of the second signal is about 45-50 seconds (with consideration of lost time).

Figure 33 illustrates the fuel consumption savings of both Eco-CACC-MS-Q and Eco-CACC-Q algorithms as a function of the offset. Results indicate that when the offset is closer to the optimal value, the savings of fuel consumption obtained from both algorithms will be smaller. At the optimal offset, the Eco-CACC-MS-Q provides the lowest saving of 2.8%, and the Eco-CACC-Q 2.5%. The highest savings of fuel consumption can be observed at 13.0% with 100-second offset for Eco-CACC-MS-Q, and 7.3% with 65-second offset for Eco-CACC-Q. This result is valid, as the savings of the algorithms are observed if the equipped vehicles have to stop at both intersections. At the optimal offset, most vehicles only need to stop at the first signal, which results in the least savings for both algorithms.

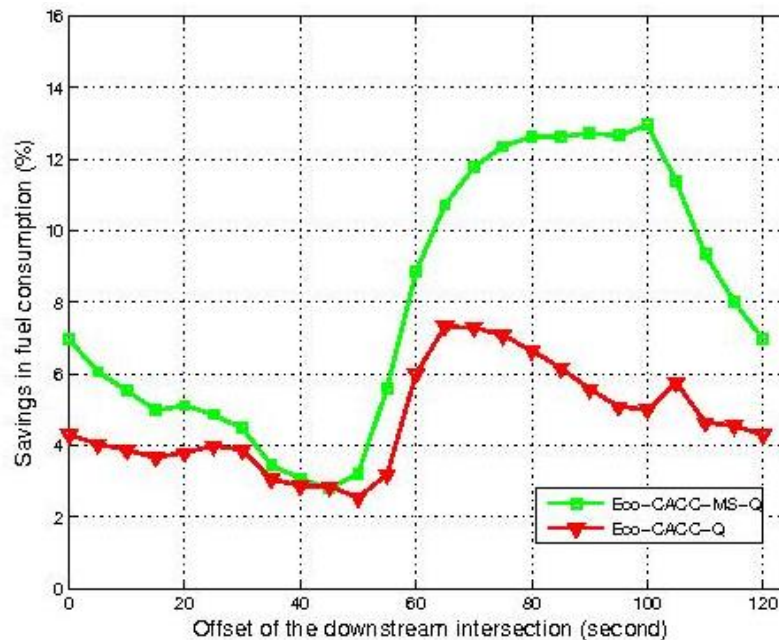


Figure 33: Savings in fuel consumption under different offsets

Distance between intersections

Distance between intersections is another variable affecting the benefits of the proposed algorithm. In this section, the impact of the distance between the intersections is evaluated. The simulation settings are the same to the previous section, except that the offset is constant as 75 seconds, and the distance between the two intersections ranges between 200 and 1000 meters.

Figure 34 shows the fuel consumption savings for both Eco-CACC-MS-Q and Eco-CACC-Q algorithms as a function of the distance between intersections. Results indicate that under the given signal plans and the demand level, 700 meters is the optimal distance between intersections for both algorithms. The Eco-CACC-MS-Q algorithm provides fuel consumption savings of 13.1% for the 700-meters distance between intersections, and the Eco-CACC-Q algorithm provides 7.2% savings.

The pattern from the Eco-CACC-MS-Q algorithm is determined by the following two factors. (1) With a longer distance between intersections, equipped vehicles can be controlled for a longer time, allowing the algorithms to provide more fuel-efficient trajectories. However, (2) the longer distance makes the prediction of the queue lengths and queue dispersion times at the downstream intersection less accurately, which reduces the effectiveness of the algorithm. Hence, there exists an optimal value for the distance when the Eco-CACC-MS-Q algorithm is applied. In addition, with the Eco-CACC-Q algorithm, the two intersections are controlled independently. When the distance is large enough, the two intersections can be considered to be isolated to each other. Hence, the benefit from the single intersection control will keep constant.

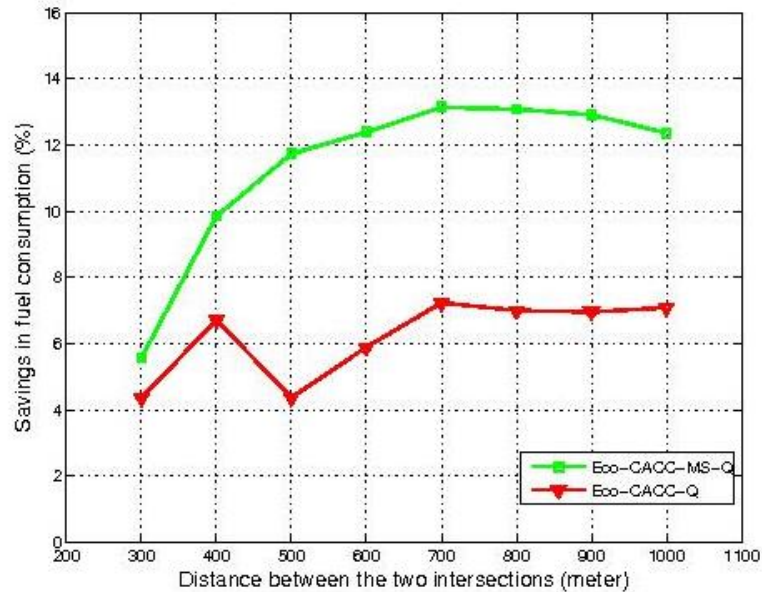


Figure 34: Savings in fuel consumption under different distances between intersections

Algorithm Shortcomings: Over-Saturated Demands

In the development of the Eco-CACC-MS-Q algorithms, one critical assumption is that the network is not over-saturated, and vehicle queues can be released during one cycle. Once the network is over-saturated, rolling queues are generated upstream of the intersections. Then, the queue estimation in Eq(6) cannot determine the queue length and the dispersion time accurately. Consequently, the advisory speed limits are not optimized for the equipped vehicles to pass the intersections. The previous section has showed that the Eco-CACC-Q algorithm for independent intersections was unable to obtain positive savings under over-saturated demands. In this section, we investigate the impact of over-saturated demands on the Eco-CACC-MS-Q algorithm.

The example of two intersections is applied. The simulation settings maintain the same, except that the demand increases to 1000 vphpl, which is greater than the capacity of the controlled segment. Figure 35 compares the trajectories of all vehicles before and after applying the Eco-CACC-MS-Q algorithm. In Figure 35(a), most vehicles experience stops at both intersections, and generally the queues at the first intersection cannot be released in one cycle. Figure 35(b) shows the trajectories with 10% equipped vehicles. As shown within the black box in the figure, the algorithm fails to provide the optimum speed limits for the equipped vehicles to pass the intersection without stops. The rolling queues caused by the over-saturated demand generate traffic fluctuations and complete stops for the equipped vehicles, reducing the benefits of the algorithm dramatically. However, as the inflow to the second intersection is gated by the first one, over-saturation is averted, and fuel consumption savings can still be observed at the second intersection using the proposed algorithm. In the simulation, a 10% MPR actually reduces fuel consumption by about 2.7%. This implies that compared with Eco-CACC-Q, the Eco-CACC-MS-Q algorithm is more efficient at providing fuel consumption savings under over-saturated demands.

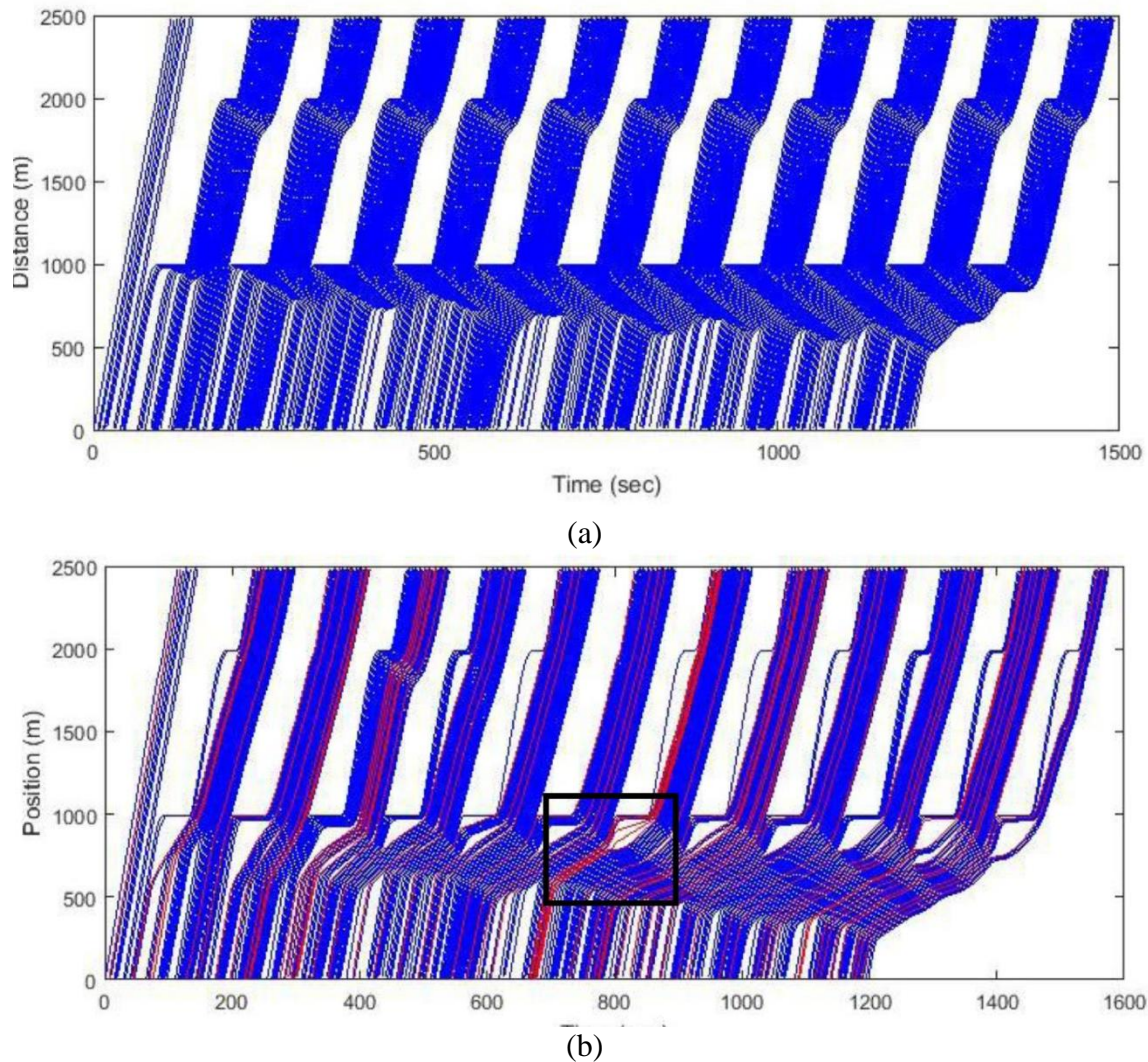


Figure 35: Vehicle trajectories under over-saturated demands: (a) No control, (b) Eco-CACC-MS-Q

Field Evaluation

Test Environment Setup

The facility on the Virginia Smart Road Connected Vehicle Test Bed was used to test the benefits of the proposed Eco-CACC system. The Virginia Smart Road is a 3.5 km (2.2 miles) stretch of road with turn-around loops at either end. The layout of the test road is illustrated in Figure 36. The road in the vicinity of the signalized intersection is a two-lane highway (one-lane for each direction). The four-way signalized intersection is located in the center of the figure. The road vertical grades for the downhill and uphill direction are approximately 3percent. The stop lines for both directions are marked by red color on the center of the figure. The Eco-CACC is activated when the testing vehicle is at 250 meters upstream of the stop bar and is deactivated when the testing vehicle is at 180 meters downstream of the stop line. Thus, the values of d_{up} and d_{down} are 250 and 180 meters, respectively. The speed limit

of the testing facility is 40 mph. In order to have a fair comparison across different runs, vehicle should drive at 40 mph by entering and leaving the range of the system. Thus, two cones were placed at the 250 meters upstream (the first cone) and 180 meters downstream (the second cone) of the intersection for each direction, so totally there are four cones. And drivers were asked to drive at 40 mph to pass the cones.

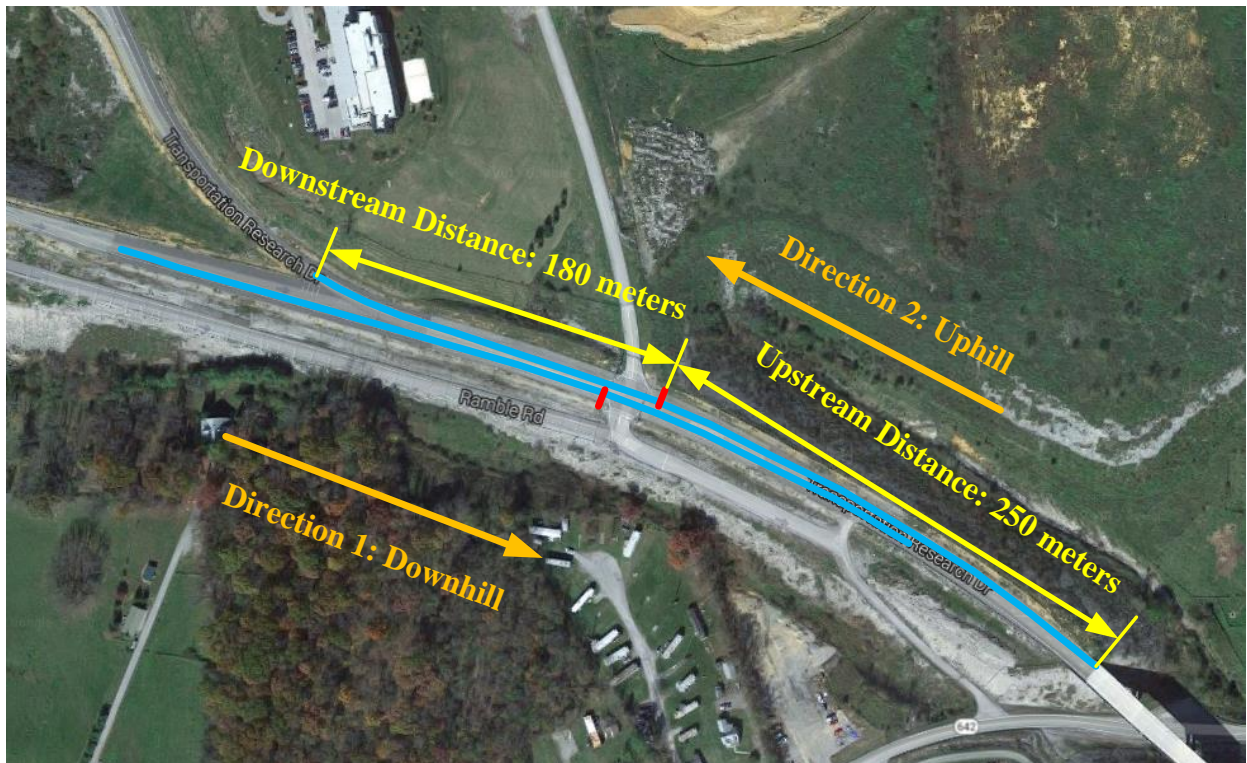


Figure 36: Layout of the test road.

In order to test the Eco-CACC system in response to different signal timings, four different values for this variable are selected for the test. This variable is named hereafter as “red phase offset”, which represents the remaining red light time when vehicle enters the test area by passing the first cone. And the selected values for the testing are 10, 15, 20 and 25 seconds. When the testing vehicle is far away and moving towards the signalized intersection, the signal phase is red. Then, the red phase offset is triggered when the testing vehicle arrives at a distance d_{up} upstream of the intersection, which means that the remaining time for the red phase is the randomly preset value (either 10, 15, 20 or 25 seconds). The green phase is chosen as 25 seconds, which is long enough for the vehicle to pass the downstream distance d_{down} , even for the case when the testing vehicle encounters a complete stop on the stop line.

Four scenarios are included in the field test, which includes a base case of uninformed drive, a driver provided with a red indication countdown, a driver provided with an audio recommended target speed and finally a longitudinally-automated ECO-CACC system.

Scenario 1 (S1): Uninformed drive.

Driver approaches the intersection in an uninformed manner, and driver needs to control the vehicle speed at 40 mi/h when passing the first to the second cones.

Scenario 2 (S2): Informed drive by providing “time to next signal indication change” to the driver.

The driver can use the information to adjust the vehicle speed to pass the intersection, and driver needs to control the vehicle speed at a 40 mi/h when passing the first and second cones.

Scenario 3 (S3): Informed drive by providing a “target speed” to the driver, the target speed is calculated by the proposed Eco-CACC algorithm. (Manual Eco-CACC System)

The driver needs to control vehicle speed at 40 mi/h when passing the first cone. Then audio information with the target speed is activated and the driver attempts to control vehicle speed by following the target speed to his/her best effort.

Scenario 4 (S4): Automated drive mode, in which the vehicle automatically controls the gas and brake levels by following the target speed calculated by the proposed algorithm. (Automated Eco-CACC System)

The driver needs to maintain the vehicle speed at 40 mph when passing the first cone. Then the driver will hear an audio alert “Engage” to indicate the automated control is activated. When the vehicle passes the second cone, the driver will hear an audio alert of “Dismiss” to indicate the automated control is deactivated. Note that the driver needs to control the steering wheel all the time.

The VTTI automated vehicle was used for the testing. It is a 2014 Cadillac SRX and is equipped with a vehicle onboard unit for V2V and V2I communication. The manufacturer specifications for this vehicle were used to calibrate the fuel consumption model (Equation (17)); the calibration procedure can be found in [30]. Note that this is an automated vehicle, and the vehicle can drive automatically by following the optimum speed profile produced by the developed ECO-CACC algorithm. This automated drive mode was tested in Scenario 4 during the field test. Two options for communicating the target speed were designed in the test vehicle: Monitor display as shown in Figure 37 and an audio system. Many studies have shown that drivers can be highly distracted by visual display in their natural driving environment [39, 40], and therefore the audio system was selected in scenarios 2 and 3 for this study. The Eco-CACC algorithm was coded in C/C++ to the Eco-CACC system in the test vehicle. The optimum speed profile and target speed are calculated every 0.1 second (10 hertz) to ensure the system can be used for real-time applications. In the scenario 2 and 3, since the average driver perception/reaction time is approximately 1.5 seconds and the latency in the communication system is around 0.5 seconds, the sound system was set to provide audio information to the driver at 2-second intervals. In the scenario 4, the automated Eco-CACC system follows the target speed by every 0.1 second.



Figure 37: Test vehicle and equipment.

The field test includes 32 participants, and each participant conducted 64 trips to pass through the signalized intersection under different combination of signal timing and road grade. The pre-defined signal timing table is presented in Table 3, we can see that each

scenario includes 16 runs and Each participant randomly repeated two times each of the four red phase offset values for each direction. It should be pointed out that only the data from d_{up} and d_{down} are extracted during each trip. Eventually, 2048 trips were collected to analyze the system performance under different scenarios.

Table 3: Pre-defined Signal Timing Table.

Run Index	Scenario 1 (second)	Scenario 2 (second)	Scenario 3 (second)	Scenario 4 (second)	Direction
1	25	15	15	25	uphill
2	25	25	25	20	downhill
3	10	25	25	20	uphill
4	15	25	10	20	downhill
5	15	10	25	25	uphill
6	10	20	15	15	downhill
7	25	25	15	15	uphill
8	25	10	20	10	downhill
9	10	15	10	15	uphill
10	20	20	15	15	downhill
11	15	20	20	20	uphill
12	15	15	20	10	downhill
13	20	20	20	10	uphill
14	10	10	10	25	downhill
15	20	10	10	10	uphill
16	20	15	25	25	downhill

Field Test Results

The instantaneous fuel consumption, vehicle speed and location were collected during each trip to calculate the total fuel consumption level and the total travel time. Table 4 presents the average fuel consumption levels of four scenarios under different combination of trip direction and red phase offset value. For the same trip direction and red phase offset value, the fuel consumption level keeps reducing from scenario 1 to 4, and scenario 4 always consumes the least fuel level. The above mentioned findings can be easily observed in Figure 38. Moreover, the results of trip travel times in Figure 39 also have the similar trends as fuel consumption results. For the same trip direction and red phase offset value, the average trip travel time keeps reducing from scenario 1 to 4, and scenario 4 generally produces the least travel time. We also find that both of fuel consumption and travel time increase when red light offset increases, since longer red signal timing results in slower average vehicle speed and longer travel time for the vehicle to pass the signalized intersection. Considering the average road grade values are -3 degrees for downhill direction and 3 degrees for uphill direction, the trip for uphill direction consumes much higher fuel level compared to the trip for downhill direction. According to the test results in Table 5, the uphill trips consume averagely more than 50% of fuel than downhill trips in the same scenario.

Table 4: Average Fuel Consumption.

Direction	Red phase offset (second)	Scenario 1 (liter)	Scenario 2 (liter)	Scenario 3 (liter)	Scenario 4 (liter)
Downhill	10	0.034	0.020	0.020	0.019
	15	0.063	0.042	0.034	0.029
	20	0.070	0.070	0.053	0.040
	25	0.078	0.075	0.065	0.047
Uphill	10	0.077	0.055	0.053	0.053
	15	0.104	0.085	0.079	0.062
	20	0.116	0.103	0.091	0.085
	25	0.125	0.112	0.101	0.093

Table 5: Average Travel Time.

Direction	Red phase offset (second)	Scenario 1 (second)	Scenario 2 (second)	Scenario 3 (second)	Scenario 4 (second)
Downhill	10	25.6	24.1	24.2	24.1
	15	29.9	28.3	26.8	26.6
	20	36.7	35.3	33.0	32.6
	25	42.3	41.1	39.4	38.9
Uphill	10	26.1	24.7	24.1	24.7
	15	30.2	29.1	27.4	26.4
	20	36.9	35.8	33.4	32.8
	25	42.7	41.5	39.7	39.1

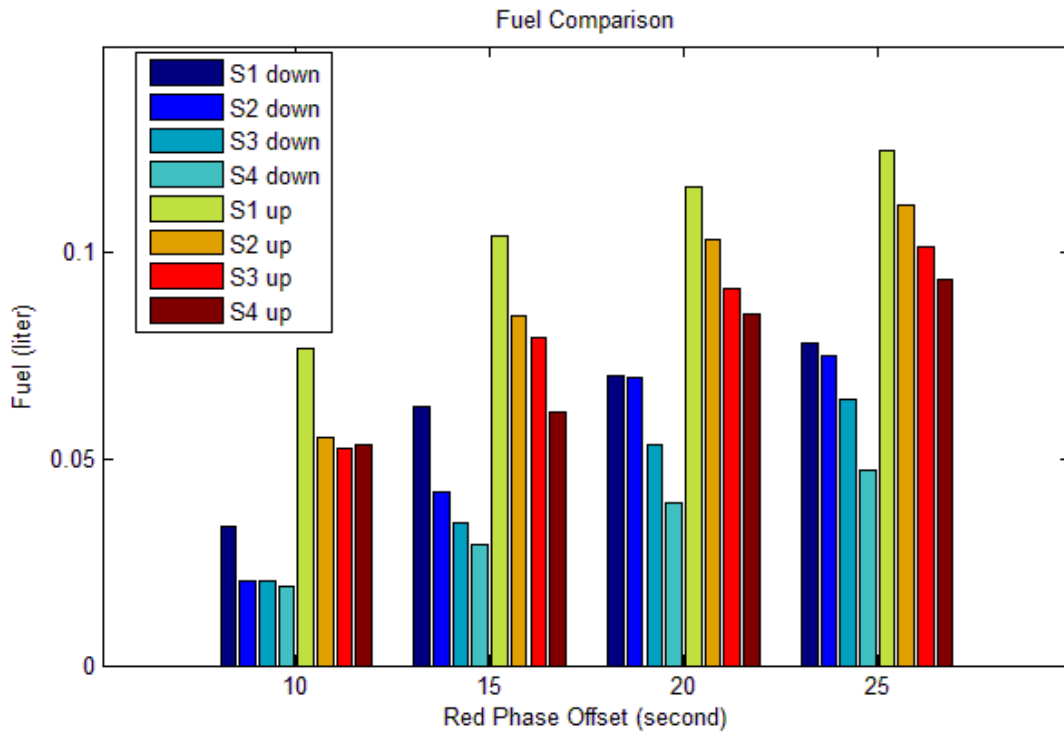


Figure 38: Average fuel consumption.

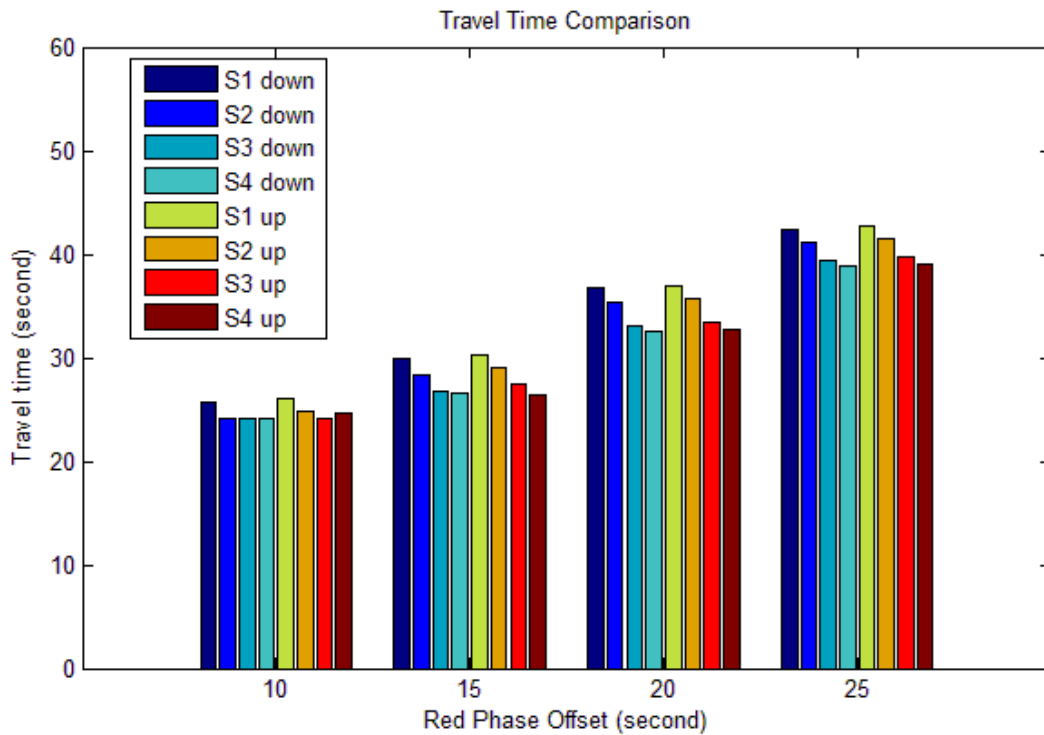


Figure 39: Average travel time.

We consider scenario 1 as the base scenario, and then calculate the difference of fuel consumption and travel time in scenario 2, 3 and 4 by compared to the base scenario. Table 6 presents the comparison of fuel consumption under different scenarios. The comparison results indicate that the average fuel consumption levels in all the other three scenarios are lower than the fuel levels in scenario 1, which means all the other scenarios are helpful to reduce fuel consumption compared to the uninformed drive. Compared to the base scenario, the average savings of fuel are 18.3%, 27.7% and 37.8% by scenario 2, 3 and 4, respectively. It's interesting to see that the 15 seconds red phase offset always corresponds to the maximum fuel saving for both downhill and uphill directions, when we compare the fuel consumption between scenario 1 and scenario 4. This may be explained by the fact that the vehicle with Eco-CACC has the maximum speed difference compared to the case that vehicle without Eco-CACC, under 15 seconds red light value. The same findings and trends can also be found in Table 7 by the comparison of travel time under different scenarios.

Table 6: Comparison of Fuel Consumption for Different Scenarios.

Direction	Red phase offset (second)	Difference between S2 and S1 (%)	Difference between S3 and S1 (%)	Difference between S4 and S1 (%)
Downhill	10	-39.8	-39.4	-42.8
	15	-32.6	-45.0	-53.2
	20	-0.7	-23.9	-43.6
	25	-4.4	-17.5	-39.8
Uphill	10	-28.5	-31.7	-30.5
	15	-18.5	-23.9	-40.9
	20	-10.9	-21.5	-26.7
	25	-10.5	-18.7	-25.0
Average		-18.3	-27.7	-37.8

Table 7: Comparison of Travel Time for Different Scenarios.

Direction	Red phase offset (second)	Difference between S2 and S1 (%)	Difference between S3 and S1 (%)	Difference between S4 and S1 (%)
Downhill	10	-5.9	-5.7	-5.9
	15	-5.4	-10.4	-11.3
	20	-3.9	-10.1	-11.3
	25	-3.0	-7.0	-8.1
Uphill	10	-5.3	-7.8	-5.4
	15	-3.6	-9.3	-12.7
	20	-3.0	-9.5	-11.1
	25	-2.8	-7.0	-8.4
Average		-4.1	-8.3	-9.3

The findings and trends by comparing four scenarios can be easily observed in the following figures. The comparison of fuel consumption for different scenarios for downhill and uphill directions are presented in Figure 40 and Figure 41. The comparison of travel times for different scenarios for downhill and uphill directions are presented in Figure 42 and Figure 43. Compared to other three scenarios, scenario 4 always corresponds to the lowest fuel consumption and travel time with the same combination of red phase offset and drive direction. The average results indicate the automated drive of scenario 4 saves 37.4% in fuel consumption and 8.6% of travel times, respectively.

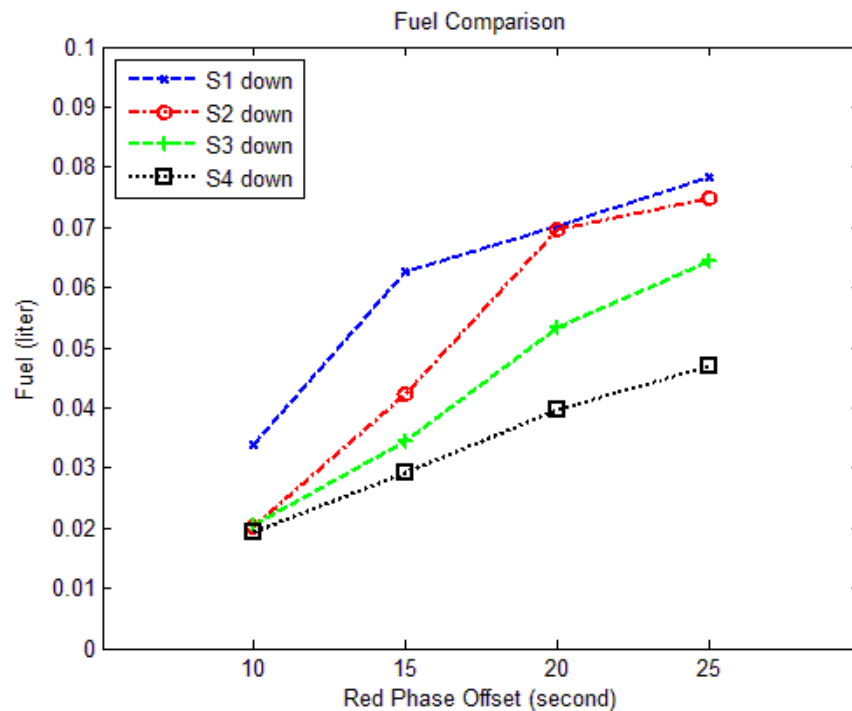


Figure 40: Comparison of fuel consumption for different scenarios for downhill direction.

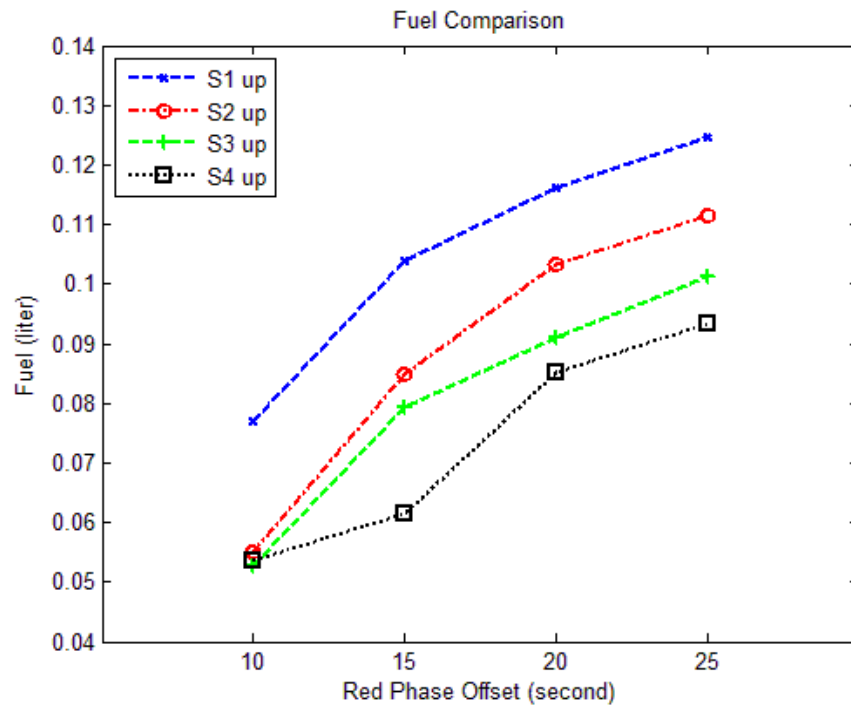


Figure 41: Comparison of fuel consumption for different scenarios for uphill direction.

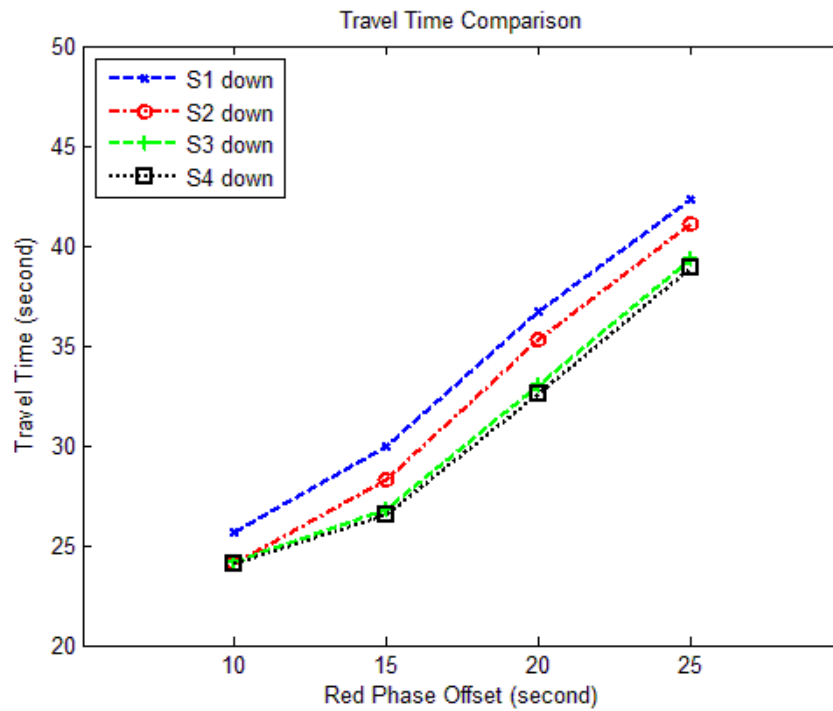


Figure 42: Comparison of travel time for different scenarios for downhill direction.

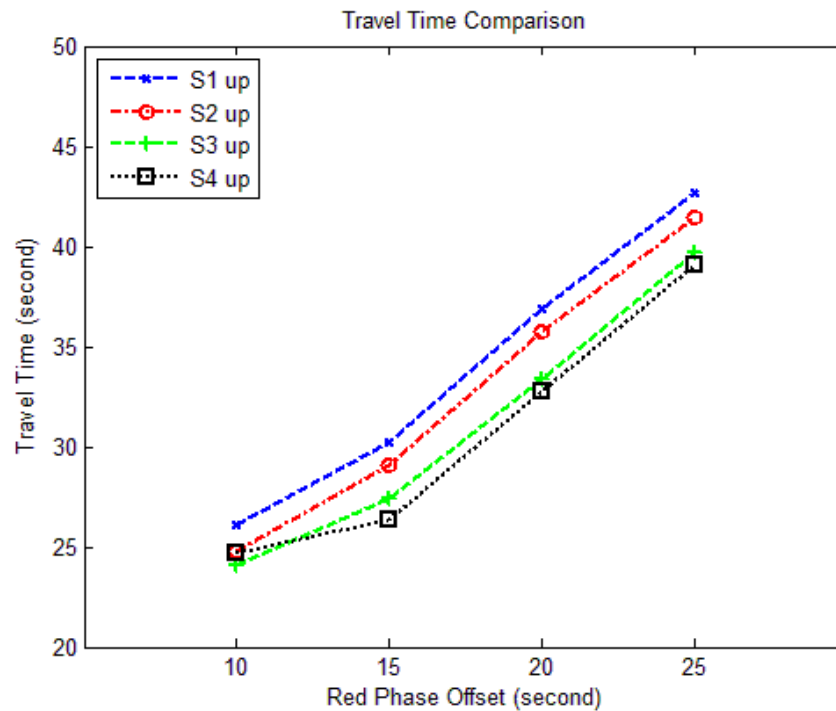


Figure 43: Comparison of travel time for different scenarios for uphill direction.

To investigate the driver behavior and vehicle's trajectories for different scenarios, the examples for each combination of red phase offset, drive direction and scenario are presented in the following figures. It should be noted that the automated vehicle cannot perfectly follow the advisory speed calculated from the Eco-CACC system. For instance, the advisory speed in scenario 4 for 10 seconds of red light offset is a constant value of 40 mph. When vehicle drives on the downhill direction in Figure 44, vehicle speed increases from 40 mph to 41.6 mph because of the positive gravity force and the automated control system doesn't engage the break for such small discrepancy. When vehicle drives on the downhill direction in Figure 45, vehicle speed initially drops from 40 mph to 37.2 mph because of the negative gravity force on the uphill direction, and then the automated control system starts to accelerate to reach 40 mph.

Figure 49 is a good example to explain the differences of driver behavior and vehicle trajectories under four scenarios. In scenario 1, the vehicle reduces speed to a completely stop on the intersection because of the red signal. In scenario 2, the countdown information help the driver to slowly decelerate to a completely stop with a moderate deceleration rate compared to scenario 1. In scenario 3, the driver tried to follow target speed by reducing vehicle speed initially and then increasing speed to pass the intersection. In scenario 4, the vehicle speed reduced from 40 to 20 mph, and then maintained the speed around 20 mph to approach the intersection. The speed curves indicate the vehicle didn't stop during scenario 3 and 4, and the average speeds of scenario 3 and 4 are much higher than other two scenarios. In fact, Eco-CACC helps the test vehicle to follow a smoothed speed profile with much less acceleration or deceleration maneuvers, and thus the test vehicle drives at a higher average speed to pass intersection. The sample trips demonstrate the benefits of the Eco-CACC

system in assisting drivers to drive smoothly in the vicinity of intersections and therefore reduce the fuel consumption levels.

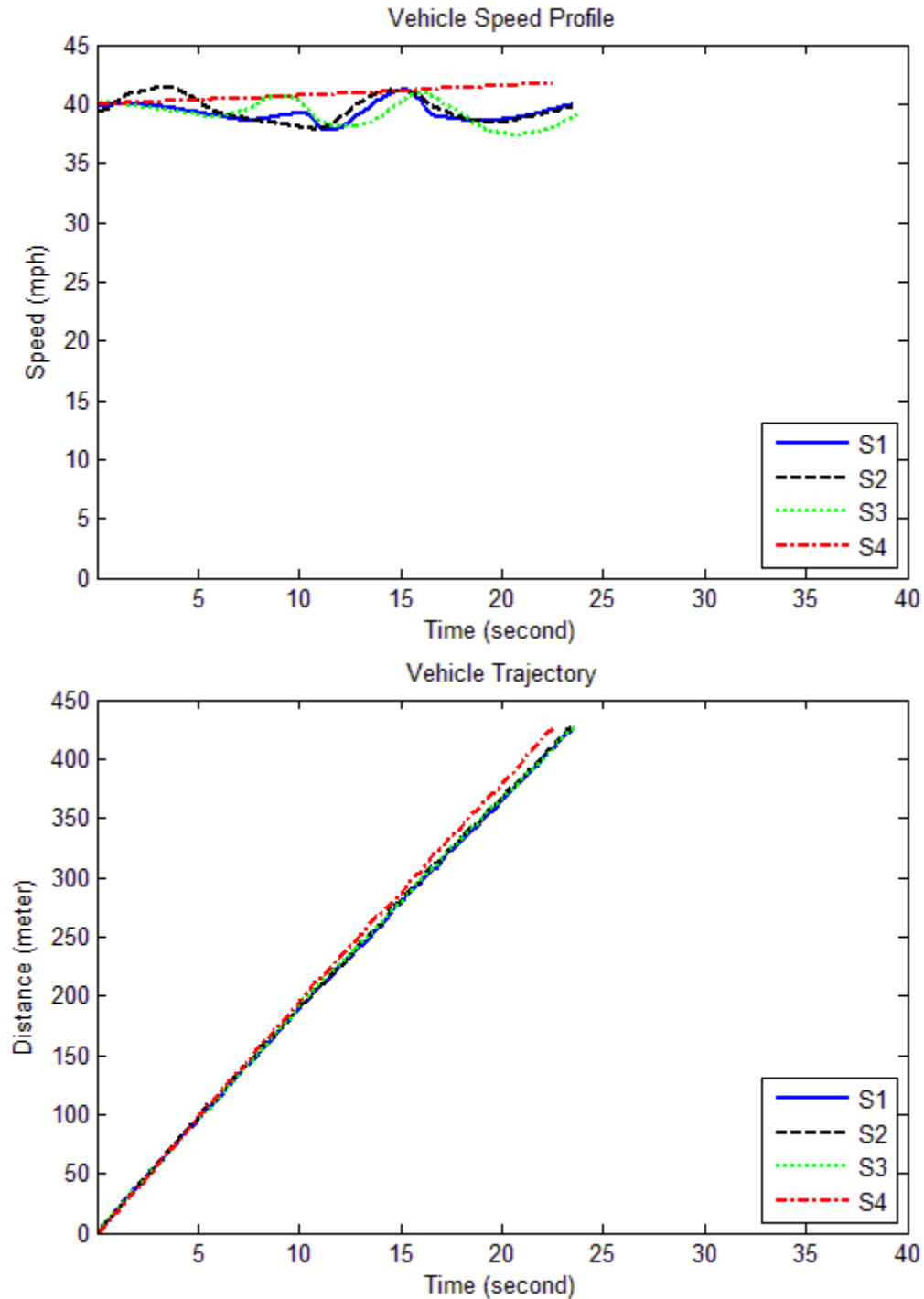


Figure 44: Example of vehicle speed profile and trajectory under red phase offset 10 seconds, downhill direction.

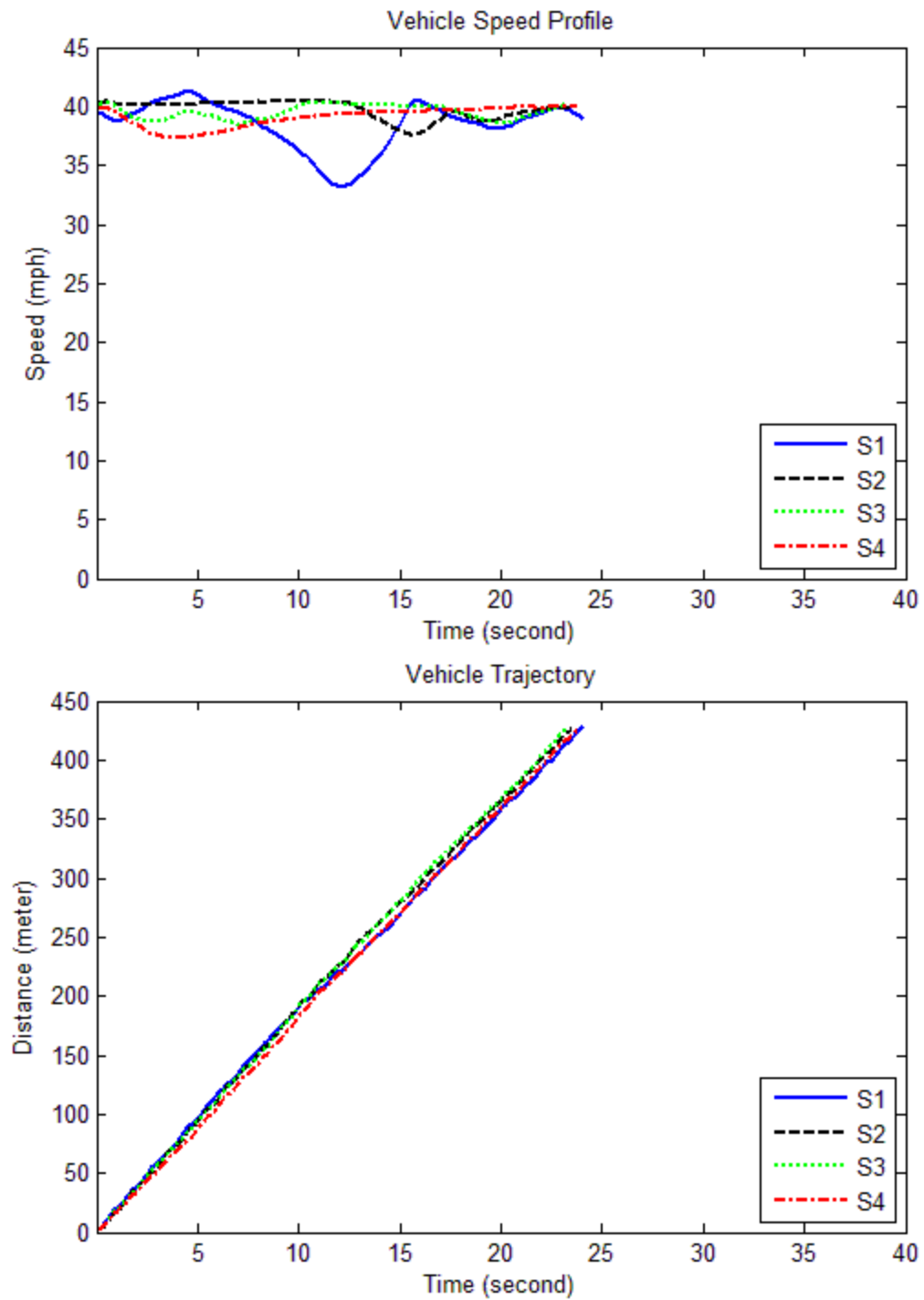


Figure 45: Example of vehicle speed profile and trajectory under red phase offset 10 seconds, uphill direction.

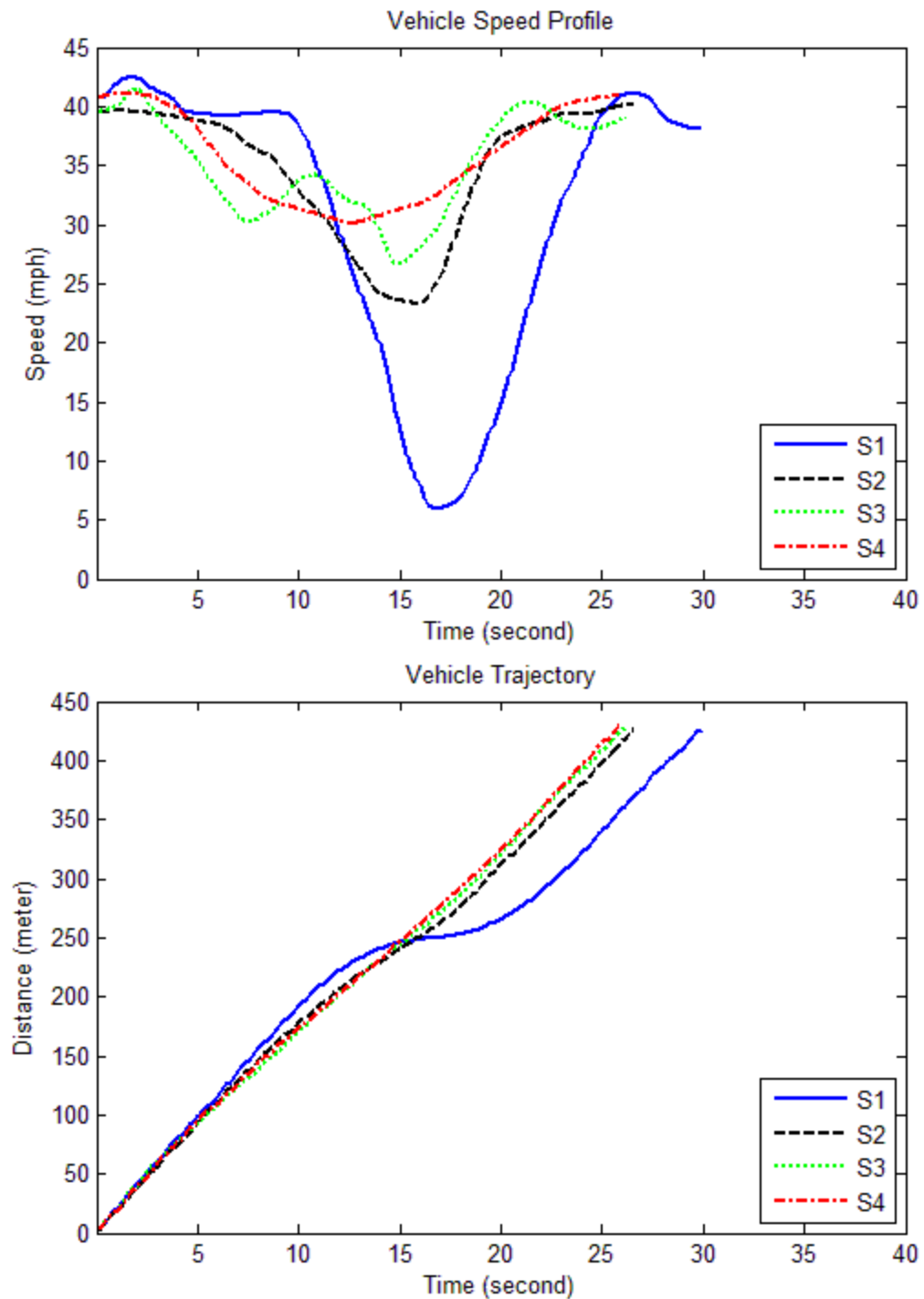


Figure 46: Example of vehicle speed profile and trajectory under red phase offset 15 seconds, downhill direction.

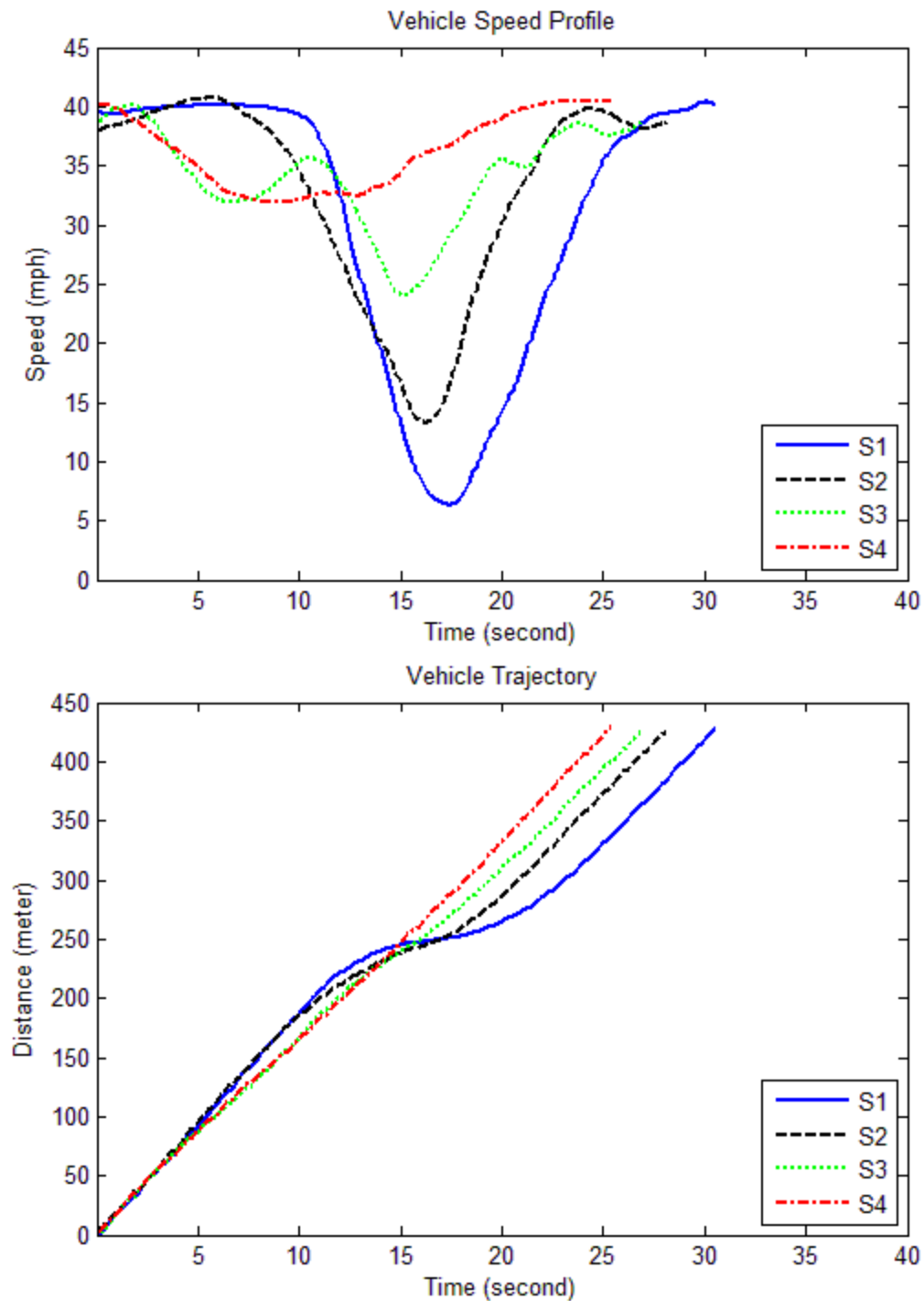


Figure 47: Example of vehicle speed profile and trajectory under red phase offset 15 seconds, uphill direction.

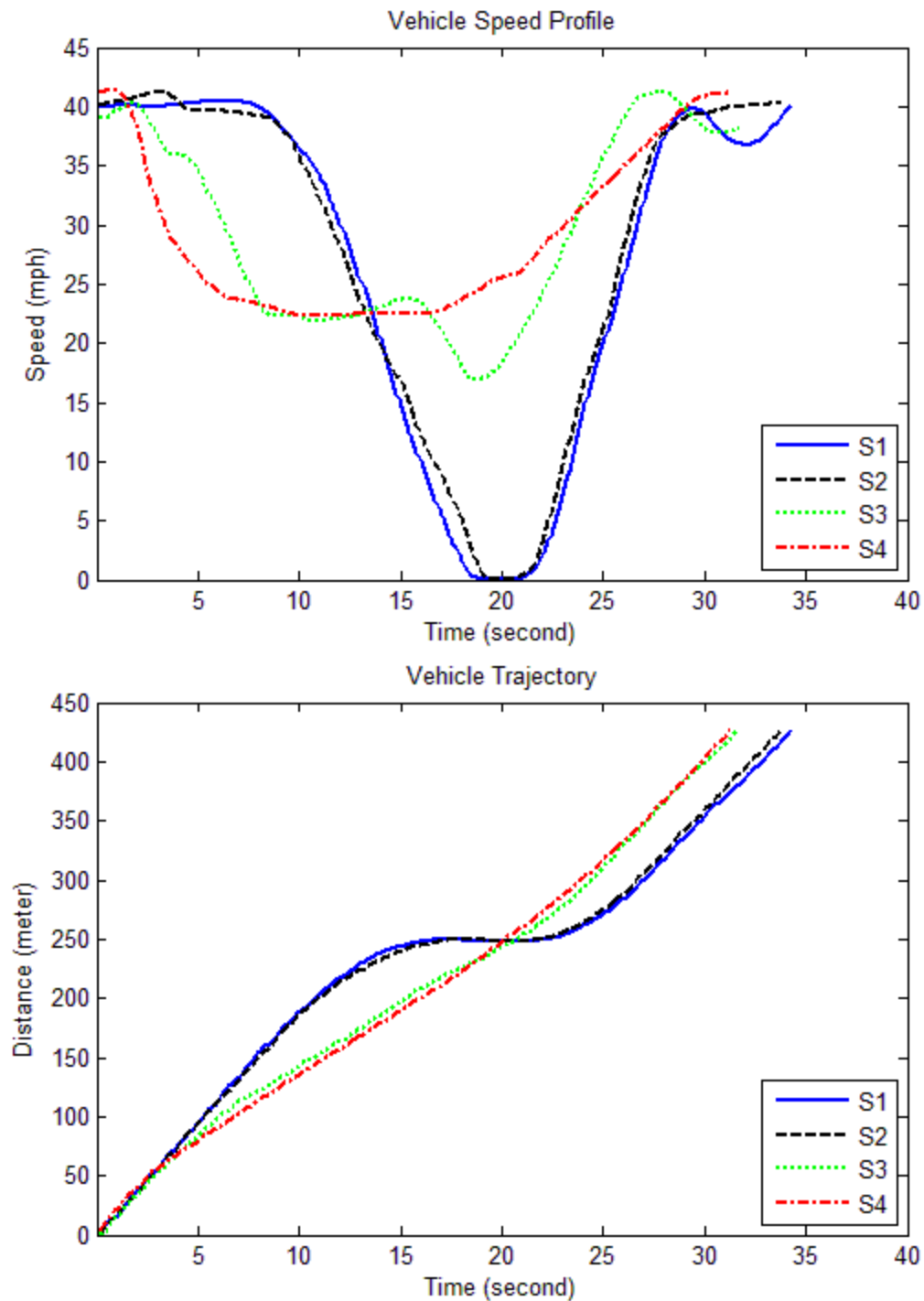


Figure 48: Example of vehicle speed profile and trajectory under red phase offset 20 seconds, downhill direction.

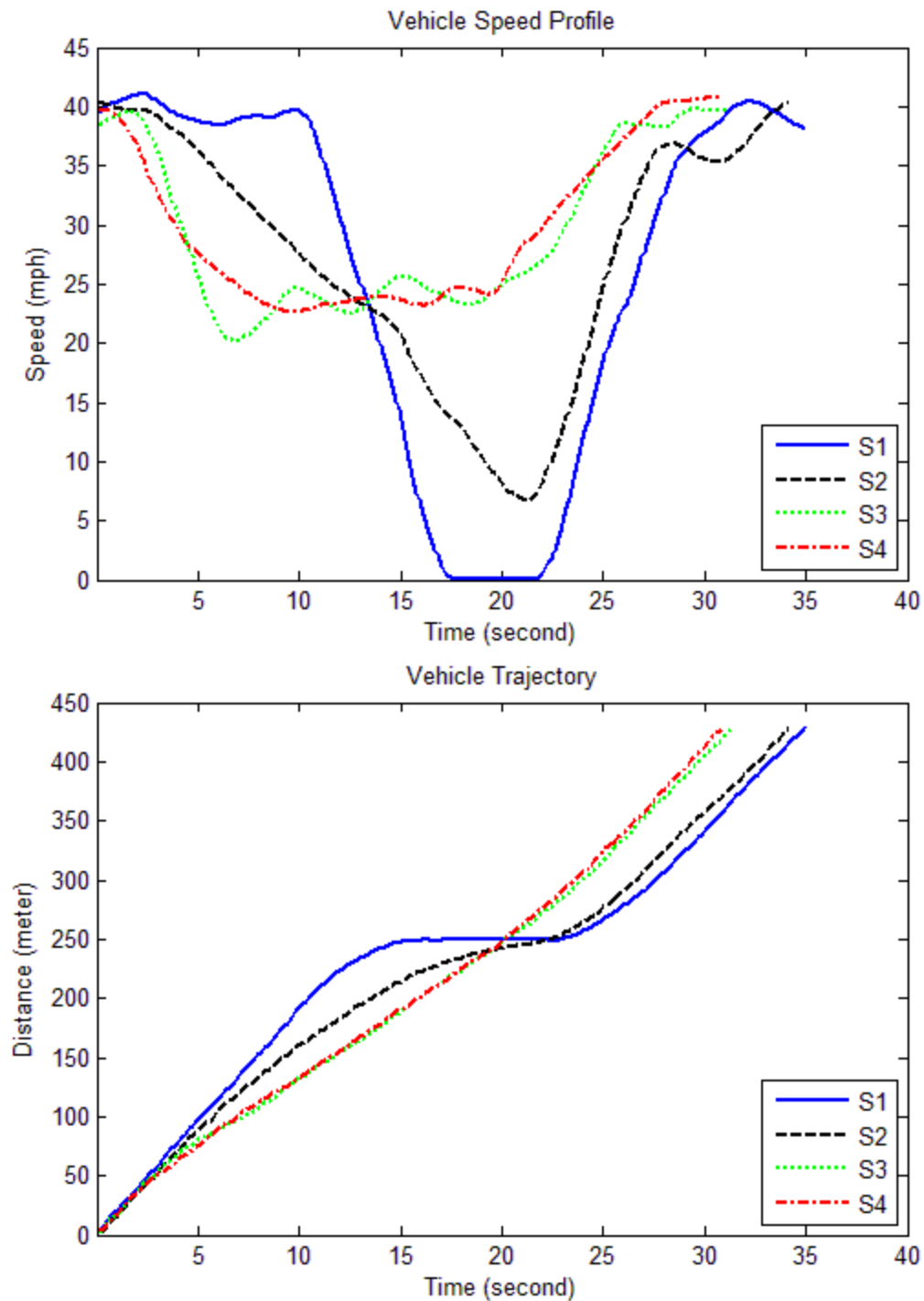


Figure 49: Example of vehicle speed profile and trajectory under red phase offset 20 seconds, uphill direction.

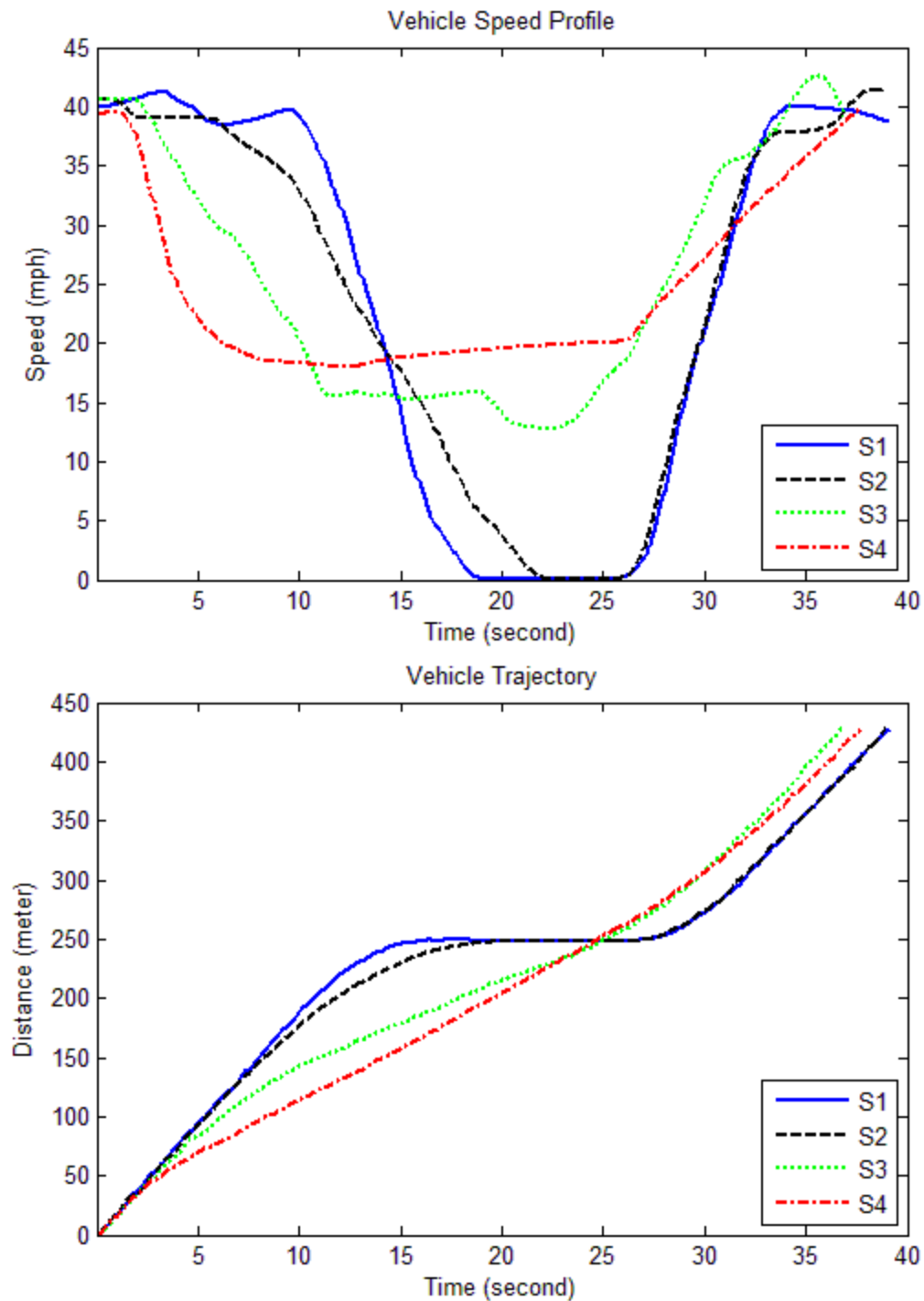


Figure 50: Example of vehicle speed profile and trajectory under red phase offset 25 seconds, downhill direction.

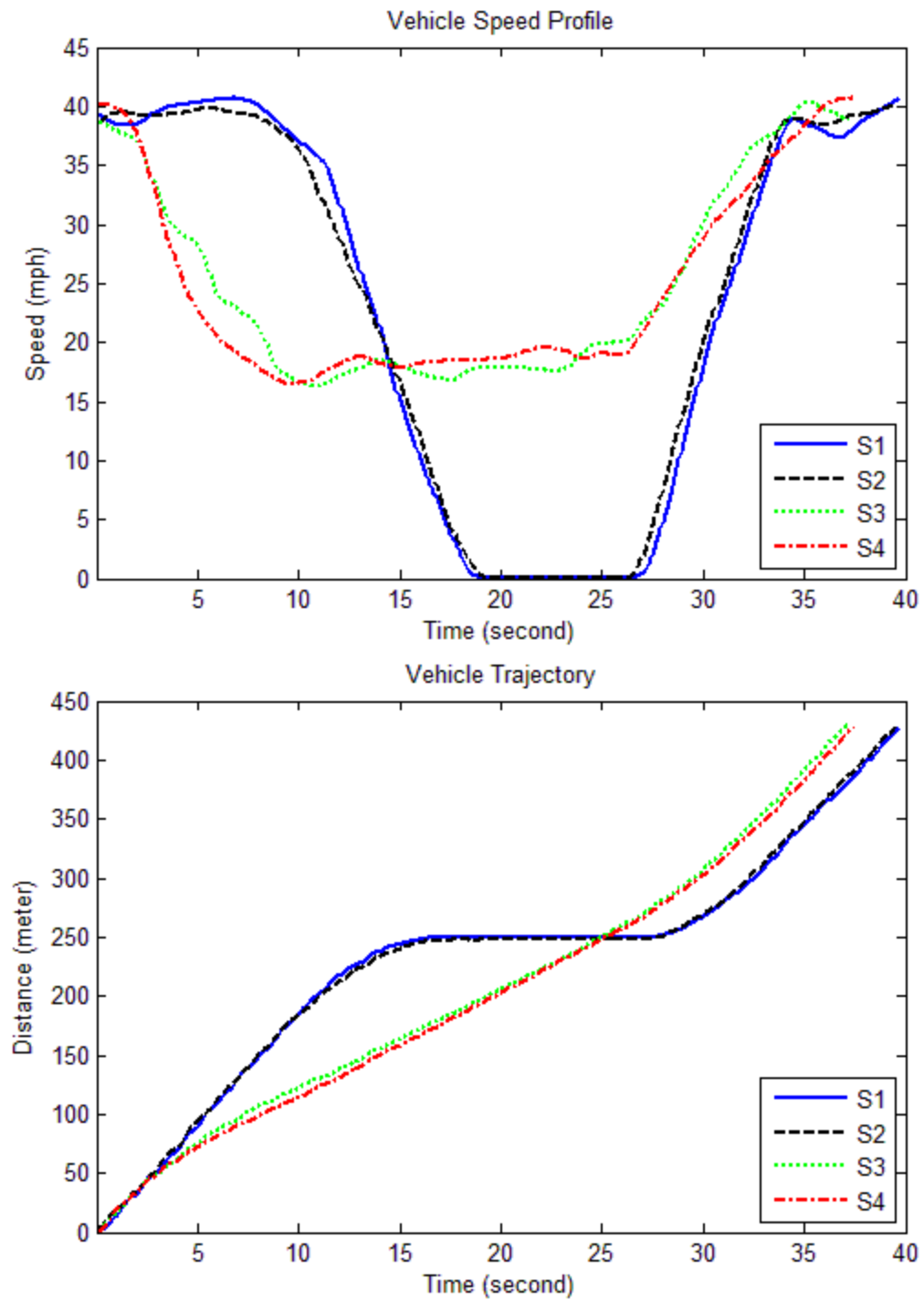


Figure 51: Example of vehicle speed profile and trajectory under red phase offset 25 seconds, uphill direction.

Post-Run Questionnaire Survey

After running the field test on the Virginia Smart Road Connected Vehicle Test Bed, each participant was asked to conduct a post-run questionnaire survey. The survey results according to the answers by 32 participants are provided in the section. The first two questions are related to the driver’s decision. Given that the automated control of scenario 4 doesn’t need driver’s decision once the system is activated, scenario 4 is not included in the first two questions. According to the results in Figure 52, 72% of participants selected scenario 2 instead of scenario 3 as the top choice regarding to improving driver’s ability to make decision on how to proceed through intersection, since most of participants feel that the current signal timing information is easy to understand and make adjustment for driving the car but the target speed in scenario 3 is very difficult to follow. According to Figure 53, 58% of participants selected scenario 2 as the top choice to help them to avoid completely stop at intersection. According to Figure 54, Figure 55 and Figure 56, the top choice regarding to “save fuel consumption”, “make driving more comfortable” and “enhance safety to drive through intersection” is the automated Eco-CACC in scenario 4, and the manual Eco-CACC is the last choice regarding to those questions. Most participants feel that the manual Eco-CACC distracts their attention to watch road environment since driver needs to focus on the odometer to adjust vehicle speed according to the advisory speed. It’s very interesting that although 84% of participants thought scenario 3 is the worst case to save fuel consumption, but the data analysis result indicates scenario 3 provides 27.7% save of fuel compared to the uninformed drive in scenario 1. According to Figure 57, there are equal percentage of participants (around 43%) selected scenario 1 and 4 as the top choice regarding to “you would like to have in your car”. At last, Figure 58 indicates 91% of participants would like to have the Eco-CACC system in the car.

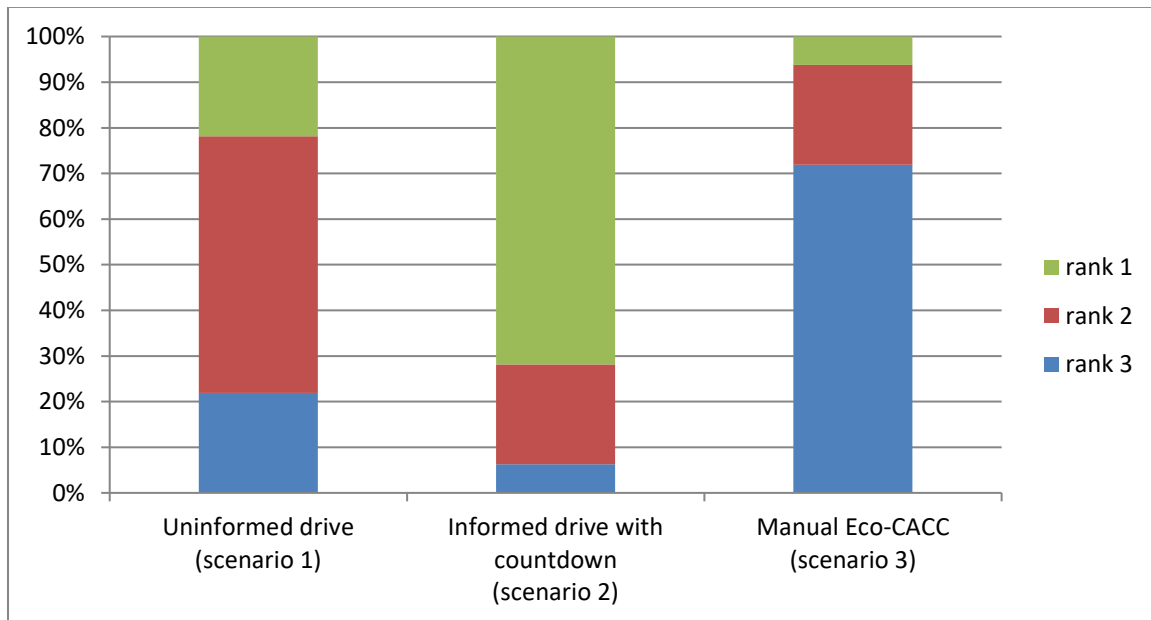


Figure 52: Ranking scenarios by “improve your ability to make decision on how to proceed through intersection”.

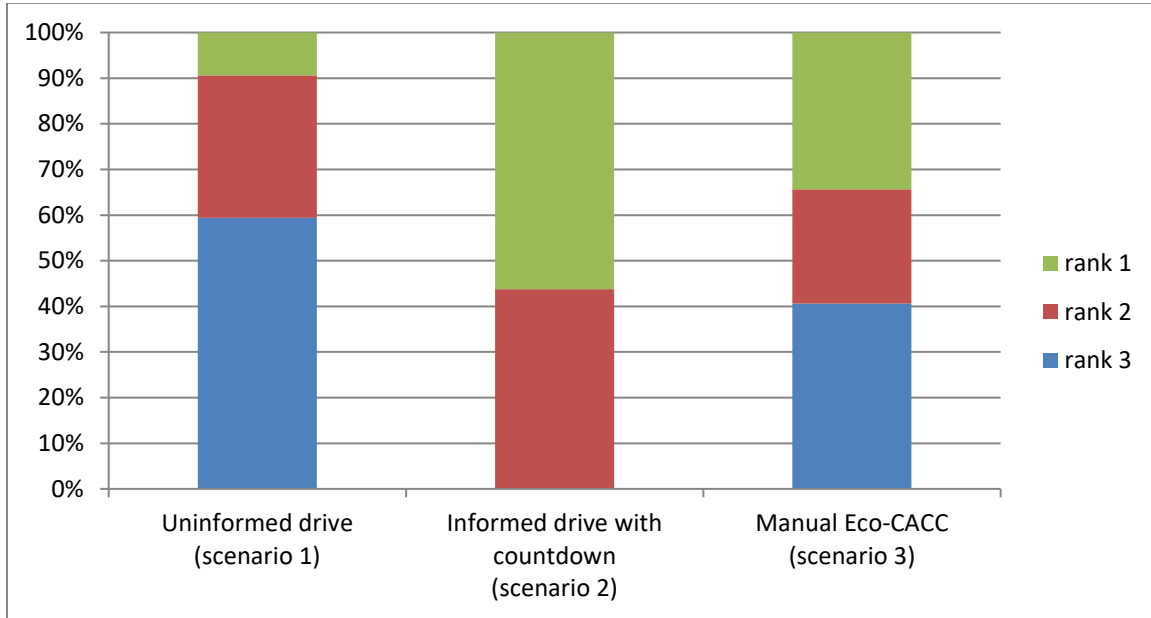


Figure 53: Ranking scenarios by “avoid completely stop at intersection”.

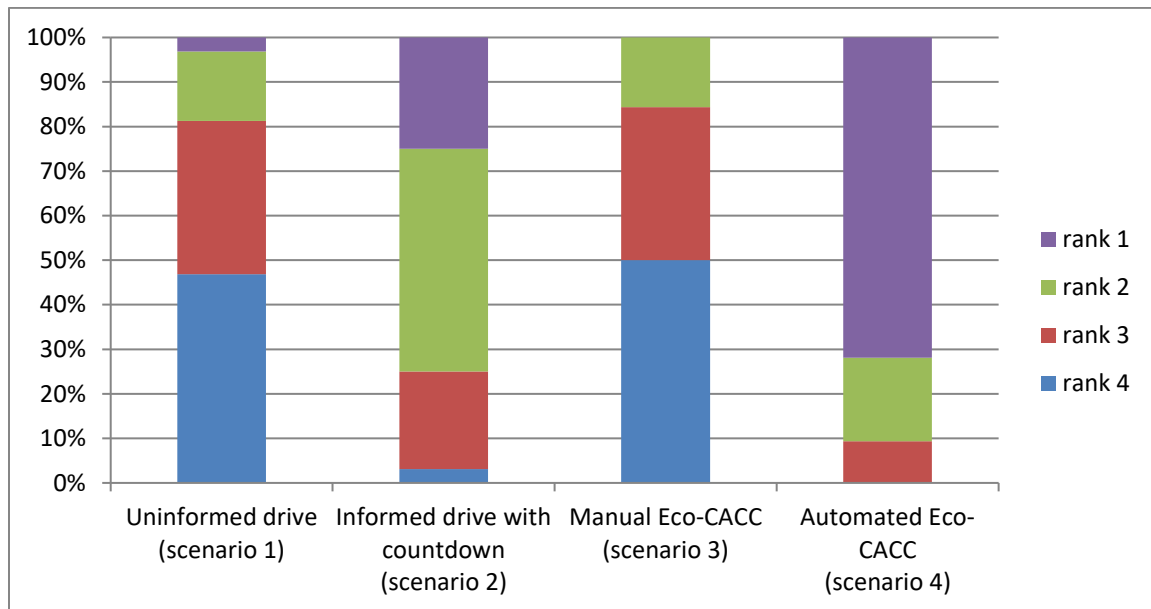


Figure 54: Ranking scenarios by “save fuel consumption”.

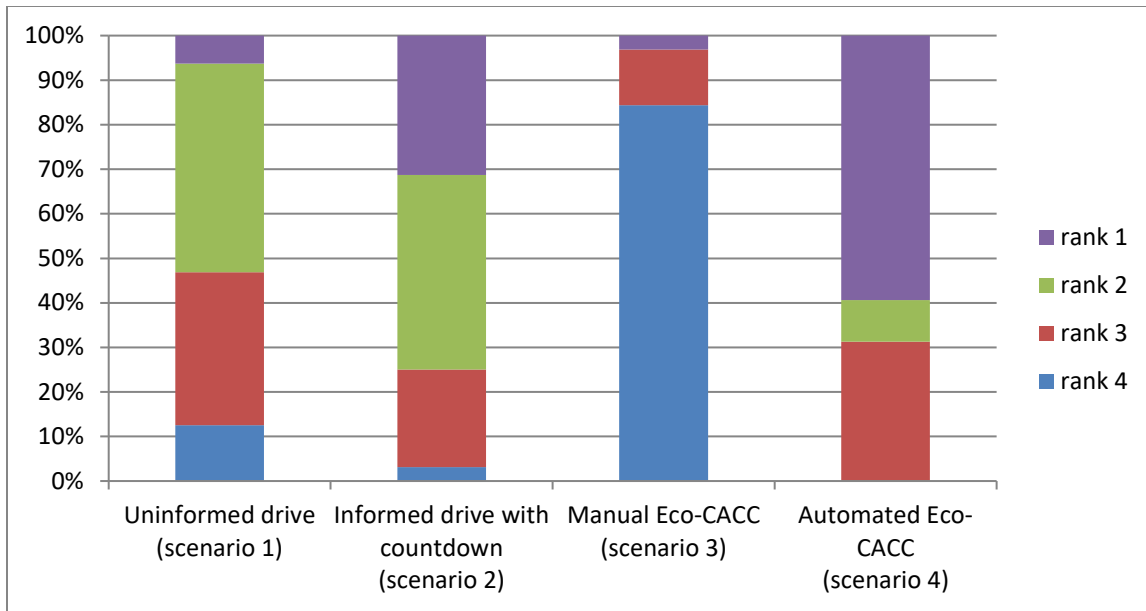


Figure 55: Ranking scenarios by “make driving more comfortable”.

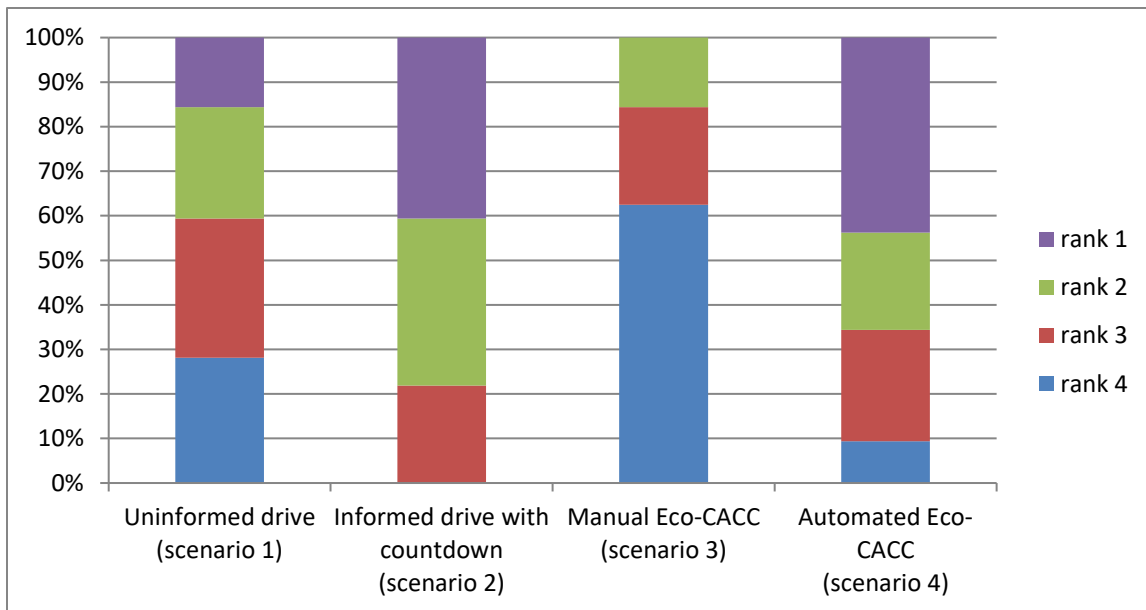


Figure 56: Ranking scenarios by “enhance safety to drive through intersection”.

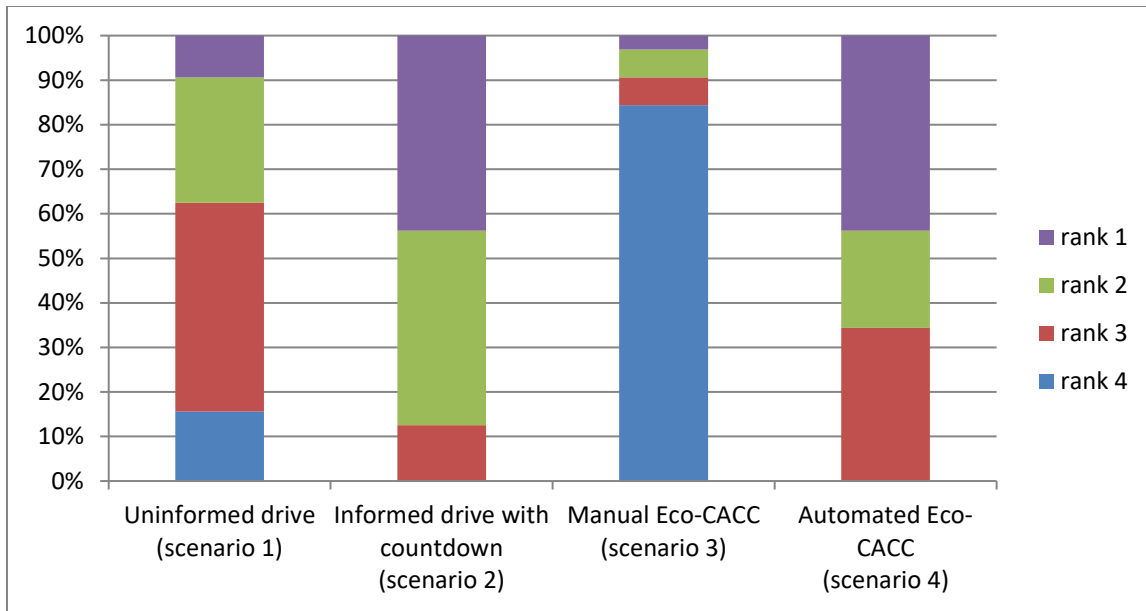


Figure 57: Ranking scenarios by “you would like to have in your car”.

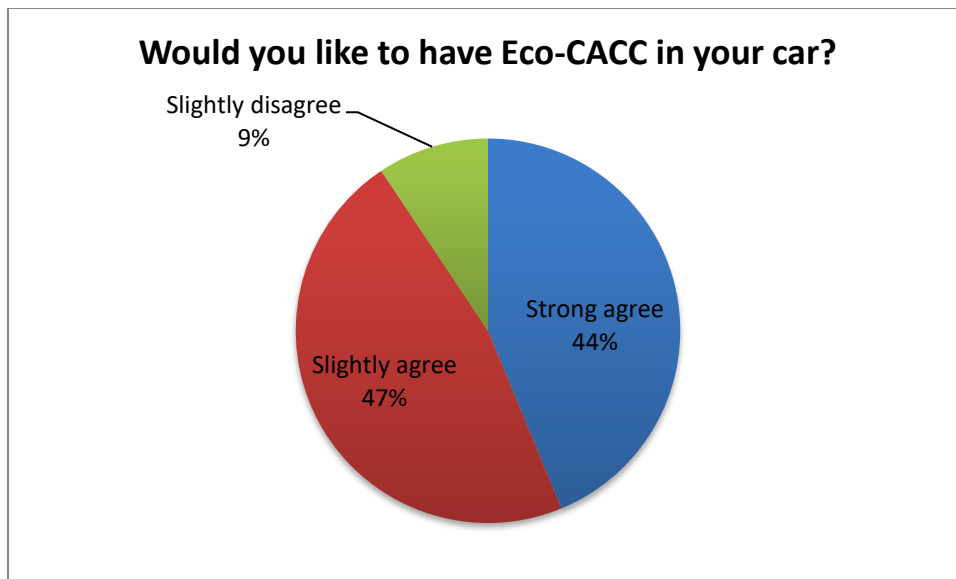


Figure 58: Vote to use Eco-CACC technology in the car.

Conclusions

The research develops Eco-CACC algorithms by considering a single intersection, multiple intersections, and field implementation for human drivers and automated vehicles. The Eco-CACC algorithms for isolated and multiple intersections are evaluated in simulated environment using INTERGRATION software, and the developed algorithms are also

implemented into the automated vehicle and the Eco-CACC systems are evaluated by the field test.

In this research, the INTEGRATION microscopic traffic assignment and simulation software is used to evaluate the performance of a proposed Eco-CACC algorithm by considering isolated intersection to assess its network-wide energy and environmental impacts. A simulation sensitivity analysis demonstrates that as the CACC-equipped vehicle market penetrate rate increases the energy and environmental benefits also increase, and that the overall savings in fuel consumption are as high as 19% when the market penetration rate is 100%. On multi-lane roads, the algorithm may produce network-wide increases in the fuel consumption level when the market penetrate rate is less than 30%. The analysis also demonstrates that the length of control segments, the SPaT plan, and the traffic demand levels significantly affect the algorithm performance. The study further demonstrates that the algorithm may produce increases in fuel consumption levels when the network is over-saturated and thus further work is needed to enhance the algorithm for these conditions.

This research also develops Eco-CACC-MS algorithms to minimize fuel consumption for vehicles to pass multiple intersections. The algorithm accelerated or decelerated the equipped vehicles to a constant speed to cruise to the intersections so as to reduce their fuel consumption levels. In addition, the Eco-CACC-MS algorithm was evaluated with the INTEGRATION microscopic simulator. The simulation of the single-lane intersections proved that fuel consumption savings were greater at higher MPRs. The reductions in fuel consumption reached 7% for Eco-CACC-MS-Q and 4.2% for Eco-CACC-Q at 100% MPR. And, taking the vehicle queue into consideration, the Eco-CACC-MS-Q algorithm always performed better than Eco-CACC-O. In the two-lane intersection, due to lane-changing and passing behaviors, the proposed algorithm increased the total fuel consumption levels when the MPRs were less than 30%. Once the MPRs were larger than 30%, positive savings could be observed. In addition, the Eco-CACC-MS algorithm was implemented in a network with four consecutive intersections, and the fuel consumption savings were also observed to be as high as 7.7% for single-lane roads, and 4.8% for two-lane roads. The study also included a comprehensive sensitivity analysis of traffic demands, phase splits, offsets, and the distances between intersections. The analysis indicated that under the given offset of 75 seconds, the phase split of 50%, and the 1000-meter segment between the two intersections, loading vehicles at 700 vphpl resulted in the highest fuel consumption savings, at 13.5%. And, given the offset, the demand and the distance between intersections, with a larger percentage of the phase split, the savings from the proposed algorithm were smaller. In addition, when the offset was closer to the optimal offset, fuel consumption savings were smaller. Furthermore, the optimal distance between intersections exists to maximize the savings in fuel consumption.

The research develops an Eco-CACC system to compute the fuel-efficient speed profile in the vicinity of signalized intersections. The Eco-CACC algorithm is implemented into an Eco-CACC system in the VTTI automated vehicle. In the Eco-CACC system, the computed speed profile can either be broadcasted as audio alert to the driver to manually control the vehicle, or be implemented into the automated vehicle (AV) to automatically control the vehicle. From an algorithmic standpoint, the proposed algorithm addresses all possible scenarios that a driver may encounter while approaching a signalized intersection. Additionally, from an implementation standpoint the research addresses the challenges

associated with communication latency, data errors, real-time computation, and ride smoothness. The system was tested in the Virginia Smart Road Connected Vehicle Test Bed. Four scenarios were tested for each participant, including a base scenario of uninformed drive, a scenario that driver provided with a red indication countdown, a manual Eco-CACC scenario that driver follows an audio recommended speed profile, and finally an automated Eco-CACC scenario that vehicle uses longitudinally automated control to follow the speed profile. The field test includes 32 participants, and each participant conducted 64 trips to pass through a signalized intersection under different combination of signal timing and road grade. The analyzed results demonstrate the benefits of the Eco-CACC system in assisting vehicle to drive smoothly in the vicinity of intersections and therefore reduce the fuel consumption levels. Compared to the uninformed drive, the longitudinally automated Eco-CACC system controlled vehicle resulted in savings in fuel consumption levels and travel times in the range of 37.8 and 9.3 percent, respectively.

REFERENCES

- [1] R. K. Kamalanathsharma, "Eco-Driving in the Vicinity of Roadway Intersections - Algorithmic Development, Modeling, and Testing," Doctor of Philosophy, Virginia Polytechnic Institute and State University, 2014.
- [2] USDOT. (2015). *Connected Vehicle Technology*. Available: http://www.its.dot.gov/connected_vehicle/connected_vehicle_tech.htm
- [3] M. Barth and K. Boriboonsomsin, "Real-world carbon dioxide impacts of traffic congestion," *Transportation Research Record: Journal of the Transportation Research Board*, pp. 163-171, 2008.
- [4] H. Rakha, K. Ahn, and A. Trani, "Comparison of MOBILE5a, MOBILE6, VT-MICRO, and CMEM models for estimating hot-stabilized light-duty gasoline vehicle emissions," *Canadian Journal of Civil Engineering*, vol. 30, pp. 1010-1021, 2003.
- [5] X. Li, G. Li, S.-S. Pang, X. Yang, and J. Tian, "Signal timing of intersections using integrated optimization of traffic quality, emissions and fuel consumption: a note," *Transportation Research Part D: Transport and Environment*, vol. 9, pp. 401-407, 2004.
- [6] A. Stevanovic, J. Stevanovic, K. Zhang, and S. Batterman, "Optimizing traffic control to reduce fuel consumption and vehicular emissions: Integrated approach with VISSIM, CMEM, and VISGAOST," *Transportation Research Record: Journal of the transportation research board*, pp. 105-113, 2009.
- [7] Y. Saboohi and H. Farzaneh, "Model for optimizing energy efficiency through controlling speed and gear ratio," *Energy Efficiency*, vol. 1, pp. 65-76, 2008.
- [8] Y. Saboohi and H. Farzaneh, "Model for developing an eco-driving strategy of a passenger vehicle based on the least fuel consumption," *Applied Energy*, vol. 86, pp. 1925-1932, 2009.
- [9] M. Barth and K. Boriboonsomsin, "Energy and emissions impacts of a freeway-based dynamic eco-driving system," *Transportation Research Part D: Transport and Environment*, vol. 14, pp. 400-410, 2009.
- [10] H. A. Rakha, R. K. Kamalanathsharma, and K. Ahn, "AERIS: Eco-vehicle speed control at signalized intersections using I2V communication," 2012.
- [11] K. J. Malakorn and B. Park, "Assessment of mobility, energy, and environment impacts of IntelliDrive-based Cooperative Adaptive Cruise Control and Intelligent Traffic Signal control," in *Sustainable Systems and Technology (ISSST), 2010 IEEE International Symposium on*, 2010, pp. 1-6.
- [12] R. Kamalanathsharma and H. Rakha, "Agent-Based Simulation of Ecospeed-Controlled Vehicles at Signalized Intersections," *Transportation Research Record: Journal of the Transportation Research Board*, pp. 1-12, 2014.
- [13] B. Asadi and A. Vahidi, "Predictive cruise control: Utilizing upcoming traffic signal information for improving fuel economy and reducing trip time," *Control Systems Technology, IEEE Transactions on*, vol. 19, pp. 707-714, 2011.
- [14] T. Guan and C. W. Frey, "Predictive fuel efficiency optimization using traffic light timings and fuel consumption model," in *Intelligent Transportation Systems-(ITSC), 2013 16th International IEEE Conference on*, 2013, pp. 1553-1558.

-
- [15] H. Xia, "Eco-Approach and Departure Techniques for Connected Vehicles at Signalized Traffic Intersections," 2014.
- [16] H. Xia, K. Boriboonsomsin, and M. Barth, "Dynamic eco-driving for signalized arterial corridors and its indirect network-wide energy/emissions benefits," *Journal of Intelligent Transportation Systems*, vol. 17, pp. 31-41, 2013.
- [17] M. Barth, S. Mandava, K. Boriboonsomsin, and H. Xia, "Dynamic ECO-driving for arterial corridors," in *Integrated and Sustainable Transportation System (FISTS), 2011 IEEE Forum on*, 2011, pp. 182-188.
- [18] M. Munoz-Organero and V. C. Magana, "Validating the impact on reducing fuel consumption by using an ecodriving assistant based on traffic sign detection and optimal deceleration patterns," *Intelligent Transportation Systems, IEEE Transactions on*, vol. 14, pp. 1023-1028, 2013.
- [19] M. V. Aerde and S. Yagar, "Dynamic Integrated Freeway/Traffic Signal Networks: Problems and Proposed Solutions," *Transportation Research*, vol. 22A(6), pp. 435-443, 1988.
- [20] M. V. Aerde and S. Yagar, "Dynamic Integrated Freeway/Traffic Signal Networks: A Routeing-Based Modelling Approach," *Transportation Research*, vol. 22A(6), pp. 445-453, 1988.
- [21] M. V. Aerde and H. Rakha, *INTEGRATION © Release 2.30 for Windows: User's Guide –Volume II: Advanced Model Features*. Blacksburg, 2007.
- [22] M. V. Aerde and H. Rakha, *INTEGRATION © Release 2.30 for Windows: User's Guide –Volume I: Fundamental Model Features*. Blacksburg: M. Van Aerde & Assoc., Ltd., 2007.
- [23] H. Rakha, K. Ahn, and A. Trani, "Development of VT-Micro model for estimating hot stabilized light duty vehicle and truck emissions," *Transportation Research Part D: Transport and Environment*, vol. 9, pp. 49-74, 2004.
- [24] J. Sangster and H. Rakha, "Enhancing and calibrating the Rakha-Pasumarthy-Adjerid car-following model using naturalistic driving data," *International Journal of Transportation Science and Technology*, vol. 3, pp. 229-248, 2014.
- [25] H. Rakha, "Validation of Van Aerde's simplified steadystate car-following and traffic stream model," *Transportation Letters*, 2013.
- [26] H. Rakha, P. Pasumarthy, and S. Adjerid, "A simplified behavioral vehicle longitudinal motion model," *Transportation letters*, vol. 1, pp. 95-110, 2009.
- [27] M. Van Aerde, "Single regime speed-flow-density relationship for congested and uncongested highways," in *74th Annual Meeting of the Transportation Research Board, Washington, DC*, 1995.
- [28] H. Rakha and B. Crowther, "Comparison of Greenshields, Pipes, and Van Aerde Car-Following and Traffic Stream Models," *Transportation Research Record*, vol. 1802, 2002.
- [29] R. K. Kamalanathsharma, H. A. Rakha, and H. Yang, "Network-wide impacts of vehicle eco-speed control in the vicinity of traffic signalized intersections," in *Transportation Research Board 94th Annual Meeting*, 2015.
- [30] H. A. Rakha, K. Ahn, K. Moran, B. Saerens, and E. Van den Bulck, "Virginia tech comprehensive power-based fuel consumption model: model development and

-
- testing," *Transportation Research Part D: Transport and Environment*, vol. 16, pp. 492-503, 2011.
- [31] R. K. Kamalanathsharma and H. A. Rakha, "Fuel-Optimal Vehicle Throttle Control: Model Logic and Preliminary Testing," 2014.
- [32] R. K. Kamalanathsharma and H. A. Rakha, "Leveraging Connected Vehicle Technology and Telematics to Enhance Vehicle Fuel Efficiency in the Vicinity of Signalized Intersections," *Journal of Intelligent Transportation Systems: Technology, Planning, and Operations*, 2014.
- [33] R. K. Kamalanathsharma, H. A. Rakha, and B. Badillo, "Simulation Testing of Connected Vehicle Applications in a Cloud-Based Traffic Simulation Environment," presented at the Transportation Research Board Annual Meeting, Washington DC, 2014.
- [34] H. Rakha and I. Lucic, "Variable power vehicle dynamics model for estimating truck accelerations," *Journal of transportation engineering*, vol. 128, pp. 412-419, 2002.
- [35] H. Chen, H. A. Rakha, A. Loulizi, I. El-Shawarby, and M. H. Almannaa, "Development and Preliminary Field Testing of an In-Vehicle Eco-Speed Control System in the Vicinity of Signalized Intersections," *IFAC-PapersOnLine*, vol. 49, pp. 249-254, 2016.
- [36] H. Rakha, H. Chen, M. Almannaa, R. K. Kamalanathsharma, I. El-Shawarby, and A. Loulizi, "Field Testing of Eco-Speed Control Using V2I Communication," 2016.
- [37] H. Chen, H. A. Rakha, M. Almannaa, A. Loulizi, and I. El-Shawarby, "Field Implementation of an Eco-cooperative Adaptive Cruise System at Signalized Intersections," presented at the 94th Annual Meeting Transportation Research Board, Washington D.C., 2017.
- [38] Y. J. Li, "An overview of the DSRC/WAVE technology," in *International Conference on Heterogeneous Networking for Quality, Reliability, Security and Robustness*, 2010, pp. 544-558.
- [39] K. L. Young and M. G. Lenné, "Driver engagement in distracting activities and the strategies used to minimise risk," *Safety Science*, vol. 48, pp. 326-332, 2010.
- [40] J. Stutts, J. Feaganes, D. Reinfurt, E. Rodgman, C. Hamlett, K. Gish, *et al.*, "Driver's exposure to distractions in their natural driving environment," *Accident Analysis & Prevention*, vol. 37, pp. 1093-1101, 2005.